5-1-2011

From growth to extinction : explored by life history and metabolic theory

Zuo Wenyun

Follow this and additional works at: https://digitalrepository.unm.edu/biol_etds
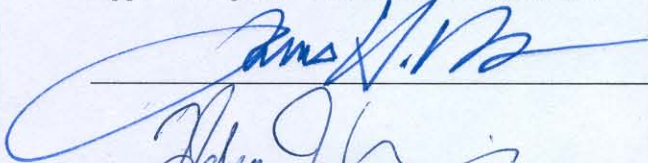
Wenyun Zuo

Candidate
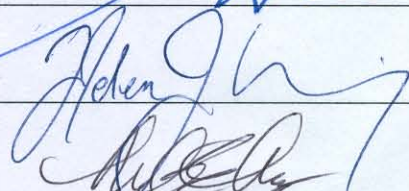
Biology
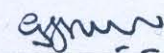
Department

This dissertation is approved, and it is acceptable in quality
and form for publication on microfilm:
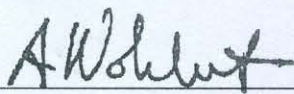
Approved by the Dissertation Committee:

_____ , Chairperson

Accepted:

_____

Dean, Graduate School

APR 1 9 2011

Date

FROM GROWTH TO EXTINCTION: EXPLORED BY LIFE HISTORY AND METABOLIC THEORY

by

Wenyun Zuo

B.S., Peking University, 2003

M.S., Institute of Botany, Chinese Academy of Sciences, 2006

DISSERTATION

Submitted in Partial Fulfillment of the

Requirements for the Degree of

Doctor of Philosophy

Biology

The University of New Mexico

Albuquerque, New Mexico

March, 2011

Dedication

To my parents, Kexuan Zuo and Rongfen Wen.

Acknowledgments

I may never have gotten into the field of Ecology without my father's inspiration. I certainly would never have gotten a chance to finish my study without my mother's finest care for last 12 years. She is a strong woman who taught me to be independent and optimistic in life. I would not have been able to overcome my English barriers and study in the U.S. without the tremendous help and encouragement from my best friend, Ni Lao. I thank my wonderful family, friends and colleagues for their love, support and encouragement.

My advisor, Dr. James H. Brown, has been providing generous support and care for the last five years. He is not only my mentor but also a great friend. I acknowledge my committee members, Dr. Geoffrey B. West, Dr. Melanie E. Moses and Dr. Helen Wearing, for teaching, mentoring, and supporting me throughout the dissertation process. I specially thank Dr. Eric L. Charnov who is a mentor, an ex-committee member, a coauthor, a summer funding sponsor, and a friend. I also thank all my collaborators, especially Dr. Chen Hou, Dr. Richard Sibly, and Dr. Astrid Kodric-Brown, my cohorts at the Program in Interdisciplinary Biological and Biomedical Sciences (PIBBS), and everyone in Brown and Smith labs.

I thank my friends at UNM, and particularly Arnab Saha and Dr. Amitabh Trehan, for providing five years of friendship, inspiration and distractions.

I thank HHMI-NIBIB Interfaces grant and Scholarships from the Biology Department at UNM for their five years support on this work.

I thank you all.

FROM GROWTH TO EXTINCTION: EXPLORED BY LIFE HISTORY AND METABOLIC THEORY

by

Wenyun Zuo

ABSTRACT OF DISSERTATION

Submitted in Partial Fulfillment of the
Requirements for the Degree of

Doctor of Philosophy
Biology

The University of New Mexico

Albuquerque, New Mexico

March, 2011

FROM GROWTH TO EXTINCTION: EXPLORED BY LIFE HISTORY AND METABOLIC THEORY

by

Wenyun Zuo

B.S., Peking University, 2003

M.S., Institute of Botany, Chinese Academy of Sciences, 2006

Ph.D., Biology, University of New Mexico, 2011

Abstract

The laws of energy and material conservation are fundamental principles across various scales and systems. Based on the conservation laws, I derive several theoretical models to understand mechanisms behind the energy budget of ontogenetic growth and the pattern of the late Pleistocene extinction of megafauna in the Americas. First, I present a model, empirically grounded in data from birds and mammals, that correctly predicts how growing animals allocate food energy between synthesis of new biomass and maintenance of existing biomass. Previous energy budget models have typically been based on rates of either food consumption or metabolic energy expenditure. The model provides a framework that reconciles these two approaches and highlights the fundamental principles that determine rates of food assimilation and rates of energy allocation to maintenance, biosynthesis, activity, and storage.

The model predicts that growth and assimilation rates for all animals should cluster closely around two canonical curves.

Second, the previous model, which focuses on endotherms, has been extended to understand effects of temperature on the energy budget of ontogenetic growth of ectotherms. A tendency for ectotherms to develop faster but mature at smaller body sizes in warmer environments has been studied for decades, and is called the temperature size rule (TSR). It can be explained by a simple model in which the rate of growth or biomass accumulation and the rate of development or differentiation have different temperature dependence. The model accounts for both TSR and the less frequently observed reverse-TSR, predicts the fraction of energy allocated to maintenance and synthesis over the course of development, and the temperature independent growth efficiency. It also predicts that less total energy is expended when developing at warmer temperatures for TSR and vice versa for reverse-TSR. It has important implications for effects of climate change on ectothermic animals and also provides how selection may lead to the evolution of both TSR and reverse-TSR.

Finally, based on mammalian life history and life history scaling relationships, an exploitation-extinction theory has been developed for the rate of human harvest in the disappearance of the Pleistocene megafauna in the Americas. The theory demonstrates that the added mortality of human harvest on populations need not be selective to produce a size-biased extinction. The variation in the adult natural instantaneous mortality rate and/or the maximum recruitment compensation at any body mass are main components determining the probability of extinction. The theory successfully predicts the shapes of the extinction probability curves for the late Pleistocene extinction in the Americas. It provides a theoretical basis to challenge a major criticism of the "overkill" theory that early Paleoindian hunters had to be extremely selective to have produced the highly size-biased pattern characteristic to the late Pleistocene extinction of megafauna in the Americas.

Contents

Contents

Contents

Contents

List of Figures

List of Tables

List of Tables

Glossary

A The energy flux of assimilated food or the rate of intake of metabolizable energy.

B_0 Metabolic constant for a given taxon.

$B_{0,rest}$ Resting metabolic constant for a given taxon.

B_{act} The rate of energy expenditure for locomotion, feeding, and other activities.

B_{basal} Basal metabolic rate.

B_{field} Field metabolic rate.

B_g Resting metabolic rate of the growing organism.

B_m The mass-specific maintenance metabolic rate.

B_{maint} The rate of energy expenditure to maintain the existing biomass.

B_{rest} Resting metabolic rate.

$B_{rest,adult}$ Resting metabolic rate at the adult size.

B_{syn} The rate to synthesize the new biomass.

B_{tot} Total metabolic rate.

Glossary

C	The maximum recruitment compensation.
E_a	Activation energy for overall metabolic rate.
E_c	Combustion energy content of a unit biomass.
E_d	Activation energy for development rate.
E_g	Activation energy for growth rate.
E_m	Energy required to synthesize a unit of biomass.
F	An additional source of instantaneous mortality due to human harvest.
H	The human population density at Late Pleistocene.
I	The coefficient of the adult instantaneous mortality scaling.
I_1	The coefficient of the harvest mortality scaling.
K	Peak normalized metabolic rate.
M	Adult body size or body size at age of first breeding, α.
N	The population size.
N_0	The number of individuals who survive till age of first breeding, α.
N_α	The number of cohorts born.
P	The extinction probability.
P_{LR}	The extinction probability from empirical data via logistical regression.
P_{TH}	The extinction probability from the theory.

Glossary

Q_{10}	The temperature quotient which compares the rate of a process to its rate at a temperature ten degrees less
Q_{maint}	Energy expended on maintenance.
Q_{sto}	Energy stored in new biomass.
Q_{syn}	Energy expended to synthesize the new biomass.
Q_{tot}	Total quantity of energy expended.
R_0	The net reproductive rate which is the average number of daughters surviving to age α produced over the adult life span.
$R_{0,max}$	The maximum net reproductive rate.
T	Absolute temperature.
S	Energy stored as biomass.
b	The number of daughters produced per mother per unit time.
f	The activity scope, is a dimensionless parameter.
$g(x)$	The probability distribution of the extinction threshold.
k	Boltzmann's constant, 8.62×10^{-5} eV/K.
m	Body size at given time, t.
m_{adult}	Near-asymptotic adult size.
n	Sample size.
t	Time.
t_{dev}	Development time.

Glossary

q The exploitation efficiency or the catchibility coefficient.

t_m Time to reach some near-asymptotic adult size.

x The extinction index.

α Age of first breeding or reproductive age.

μ Relative mass, $\mu \equiv \frac{m}{M}$.

μ' Relative development stage, $\mu' \equiv \frac{t}{t_{dev}}$.

γ The dimensionless storage coefficient $\gamma = E_c/E_m$.

μ_d Relative mass at which A starts decreasing.

η Production efficiency.

γ_m $\gamma_m = \left(\frac{m_{adult}}{M}\right)^{1/4}$.

θ The adult instantaneous mortality rate.

ζ_α The probability of surviving to reproductive age α.

β The recruitment response.

β_{max} The maximum recruitment response.

κ The coefficient of approximated analytical solution, $\kappa \propto (\alpha \cdot \theta)^{-0.42}$.

Chapter 1

Introduction: A theoretical approach towards understanding mechanisms

Ecology studies exchanges of energy and material between biotic and abiotic systems, and interactions and dynamics within biotic systems. Grounded in the laws of energy and material conservation, mechanistic models can be built to explore a complex system through multiple scales, to characterize the fundamental units and behaviors of the system, to generate new questions, and to guide experiment designs. Here, based on the conservation laws, I analyze two different biological processes—ontogenetic growth and population extinction—at two different scales using the conceptual frameworks of life history theory and metabolic theory of ecology.

Ontogenetic growth is one of the most fundamental processes in biology. The process of growth entails the allocation of energy and materials to production of new biomass and maintenance of existing biomass. Energy budgets of growing animals have been analyzed since pioneering work of von Bertalanffy, Kleiber, and Brody in

the 1940s [1–6]. These investigators set up the empirical and conceptual framework for understanding the changes in body size and energy metabolism during ontogeny. Subsequently many mathematical models have been used to characterize growth (e.g., [7, 8]), but most of these provide only statistical descriptions of growth trajectories rather than mechanistic treatments of the mass-energy balance of the growth process. For example, Ricklefs [7] lists a family of "Pütter" growth models, which are purely descriptive growth models, and have the general form of $dm/dt = y_1 m^y - z_1 m^z$ (where y_1 and z_1 are coefficients and y and z are exponents), but differ in the values of the exponents y and z. Ricklefs [7] argues that using different exponents gives better fits to the growth curves of different species, due to variation in resource provisioning and tissue maintenance. For example, growth curves of most altricial birds are best fit by the logistic equation ($y = 1, z = 2$), whereas many precocial species conform more closely to the Gompertz function ($y \to 1, z \to 1$), and a small number of slowly growing pelagic seabirds and raptors are better fit by the von Bertalanffy function ($y = 2/3, z = 1$).

However, is the goodness of fits to empirical growth curves informative if the goal is to understand the mechanisms of allocation of energy and mass [9]? Descriptive growth models make few implicit or explicit assumptions about the biological processes that regulate growth and development. Coefficients and exponents obtained by curve fitting might be useful for specific system prediction within narrow scale range, but they are not insightful for understanding mechanisms. Conspicuous exceptions are von Bertalanffy's model [1], which characterized growth as the difference between rates of anabolism and catabolism, and the dynamic energy budget (DEB) models of Kooijman [10] which provide a more complete treatment, relating growth to the underlying biochemistry of metabolism. More recently, West, Brown and Enquist [11] considered the allometry of mass and energy balance during ontogeny in developing a general mechanistic Ontogenetic Growth Model (OGM). The OGM is a mechanistic model that uses parameters from fundamental cellular properties which

control growth and can be derived quantitatively from metabolic measurements that are not directly related to growth. It predicts a canonical sigmoidal growth curve that accurately describes the empirical growth trajectories for diverse kinds of animals when normalized by adult mass and time to maturity.

My first two chapters focus on understanding the energy budget of ontogenetic growth starting from food intake for both endotherms and ectotherms. In Chapter 1, "A General Model of Energy Budget During Ontogeny", we present a model that correctly predicts how growing animals allocate food energy between synthesis of new biomass and maintenance of existing biomass. The combustion of food supplies the energy that fuels growth, maintenance, and activity, which is fundamental to animal survival [6]. A large body of previous work used energy budget models to understand ontogenetic growth [6, 7, 11–15]. They typically have their bases in rates of either food consumption or metabolic energy expenditure. Our model provides a framework that reconciles these two approaches and highlights the fundamental principles that determine rates of food assimilation and rates of energy allocation to maintenance, biosynthesis, activity, and storage. The model predicts that growth and assimilation rates for all animals should cluster closely around two universal curves. Data for mammals and birds of diverse body sizes and taxa support these predictions.

In Chapter 2, "A general model for effects of temperature on ectotherm ontogenetic growth and development", we extend the mechanistic model, which is derived in Chapter 1 and mainly supported by endotherm data, to understand the energy budgets of ontogenetic growth of ectotherms. Rates of nearly all biochemical reactions and biological processes increase approximately exponentially with temperature. Body temperatures of ectotherms fluctuate with environmental temperatures, so that changing temperature literally changes the pace of life of ectotherms. The rate of ontogenetic growth and development is no exception. Ectothermic animals

develop faster at warmer temperatures [16], and they usually mature at smaller body sizes – as much as 20% smaller for a 10^oC temperature increase. This phenomenon has been called the "temperature size rule" (TSR) [17]. Like most biological "rules", however, there are exceptions, including well documented cases of a reverse-TSR, where the mature body sizes are larger at higher temperatures. Here we develop a simple model for the effects of temperature on ontogenetic development of ectothermic animals. The model extends an earlier model for allocation of energy and biomass to growth [18] by explicitly incorporating the temperature dependence of the rate of development and the rate of somatic growth. Any imbalance in these two rates results in either the TSR or reverse-TSR, depending on which process is more sensitive to temperature. The model predicts the fraction of energy allocated to maintenance and biomass synthesis at a given development stage, including the total quantity of energy expended during development. We first model explicitly the case of post-hatching development, where an animal consumes food to fuel its metabolism. Later we consider the case of embryonic development, where the organism fuels its metabolism from energy reserves stored in the egg.

My third chapter analyzes the mechanism behind the body size biased extinction pattern in the late Pleistocene megafauna extinction. Numerous species of large-bodied mammalian herbivores such as mammoth and mastodons, horses and their allies, camelids, oxen and bison, glyptodonts, giant sloths and other taxa were widespread across the Americas [19–22] around 13,400 years ago when they disappeared within a relatively short time. Some 80% of the large-bodied species went extinct, including all mammals over 600 kg [23]. Determining the mechanism underlying the geologically abrupt [24] late Pleistocene extinction of megafauna in the Americas has been difficult and fraught with controversy because it overlaps in timing with both the initial arrival of humans into the Americas and a major transition from glacial to interglacial climate. The controversial "blitzkrieg" or "overkill" theory [19], which attributes the extinction to overharvest by early Paleoindian hunter-gatherer

population, has slowly gained traction as the most parsimous explanation of the event (e.g., [22]); indeed, even formerly staunch advocates of climate change have recently concluded "human impacts probably figured prominently in the extinctions" [25]. However, a continuing criticism of the "overkill" theory has been the seeming implausibility of a relatively small number of humans killing off millions of animals, and the lack of direct archaeological evidence that early Paleoindian hunters preyed on all large-bodied mammal species that went extinct (e.g., [26, 27], but see [28, 29]). Moreover, opponents have argued that early Paleoindian hunters would have had to be extremely selective to have produced the highly size-biased extinction, and that the economics of foraging theory suggest that such a size-specialized diet would have been energetically unfeasible [30]. In Chapter 3, we demonstrate theoretically that additional mortality caused by human harvest, even if not size selective, was sufficient to cause a size-biased extinction. Our results clearly indicate how animal populations may be driven to extinction by human exploitation even in the absence of other forms of habitat degradation. It simply requires that the added harvest mortality overpowers the increased density dependent recruitment that is normally present as population size approaches zero. Of course harvest mortality could fall more heavily on large-bodied species, but invoking it is unnecessary in order to explain the resulting size bias. Our simple and quite transparent theory allows us to account for the gradual rise in extinction risk with body mass [23, 31] as well as to predict the special characteristics of species at any fixed body mass that are relatively more/less at risk of extinction.

These models: 1) highlight the fundamental principles that determine rates of food assimilation and rates of energy allocation to maintenance, biosynthesis, activity, and storage and predict that growth and assimilation rates for all animals should cluster closely around two canonical curves; 2) predict that the fraction of energy allocated to maintenance and synthesis over the course of development, that growth efficiency is independent of temperature, and that less total energy is expended when

developing at warmer temperatures for TSR and vice versa for reverse-TSR. It has important implications for effects of climate change on ectothermic animals and the role of natural selection in the evolution of both TSR and reverse-TSR; 3) indicate that variation in the adult natural instantaneous mortality rate and/or the maximum recruitment compensation at any body mass are the main components determining extinction probability, which provides a theoretical basis to challenge a major criticism of the "overkill" theory that early Paleoindian hunters had to be extremely selective to have produced the highly size-biased pattern unique to the late Pleistocene extinction of megafauna in the Americas. The goal of all three theoretical models is to understand the mechanisms underlying the system. They are derived from first principles and simplifying assumptions, which allow us to capture the big picture instead of specific details. These models provide not only first-order explanations for important phenomena but also quantitative baselines that can be used as a starting point to incorporate more detail and explain deviations from predictions.

Chapter 2

A General Model of Energy Budget During Ontogeny

Collaborated with Chen Hou, Melanie E. Moses, William H. Woodruff, James H. Brown, and Geoffrey B. West[1]

Abstract

All organisms face the problem of how to fuel ontogenetic growth. We present a model, empirically grounded in data from birds and mammals, that correctly predicts how growing animals allocate food energy between synthesis of new biomass and maintenance of existing biomass. Previous energy budget models have typically had their bases in rates of either food consumption or metabolic energy expenditure. Our model provides a framework that reconciles these two approaches and highlights the fundamental principles that determine rates of food assimilation and rates of energy allocation to maintenance, biosynthesis, activity, and storage. The model predicts

---

that growth and assimilation rates for all animals should cluster closely around two universal curves. Data for mammals and birds of diverse body sizes and taxa support these predictions.

The "food of life" and the "fire of life" – the combustion of food to supply the energy that fuels growth, maintenance, and activity – is fundamental to animal survival [6]. A large body of previous work used energy budget models to understand ontogenetic growth [6,7,11–15]. These models have contributed importantly to many conceptual and applied problems, including life history theory, animal husbandry, and biomedicine. Still largely missing, however, is a complete quantitative framework that specifies how food is transformed into metabolic energy and stored biomass. Here, we present such a framework, which quantifies explicitly how assimilated food is transformed into biomass and metabolic energy during ontogeny.

When an animal is growing, some fraction of the assimilated food is oxidized to fuel the total metabolic rate, B_{tot}, whereas the remaining fraction is synthesized and stored as biomass, S (Fig.2.1). Thus, the energy flux of assimilated food, A, sometimes called the rate of intake of metabolizable energy [6,12], is expressed as

$$A = B_{tot} + S = B_{tot} + E_c \frac{dm}{dt} \tag{2.1}$$

where A is defined as the combustion energy content of ingested food per unit time minus the combustion energy content of excreta per unit time, E_c is the combustion energy content of a unit biomass, and dm/dt is the rate of change in biomass, m, at time, t.
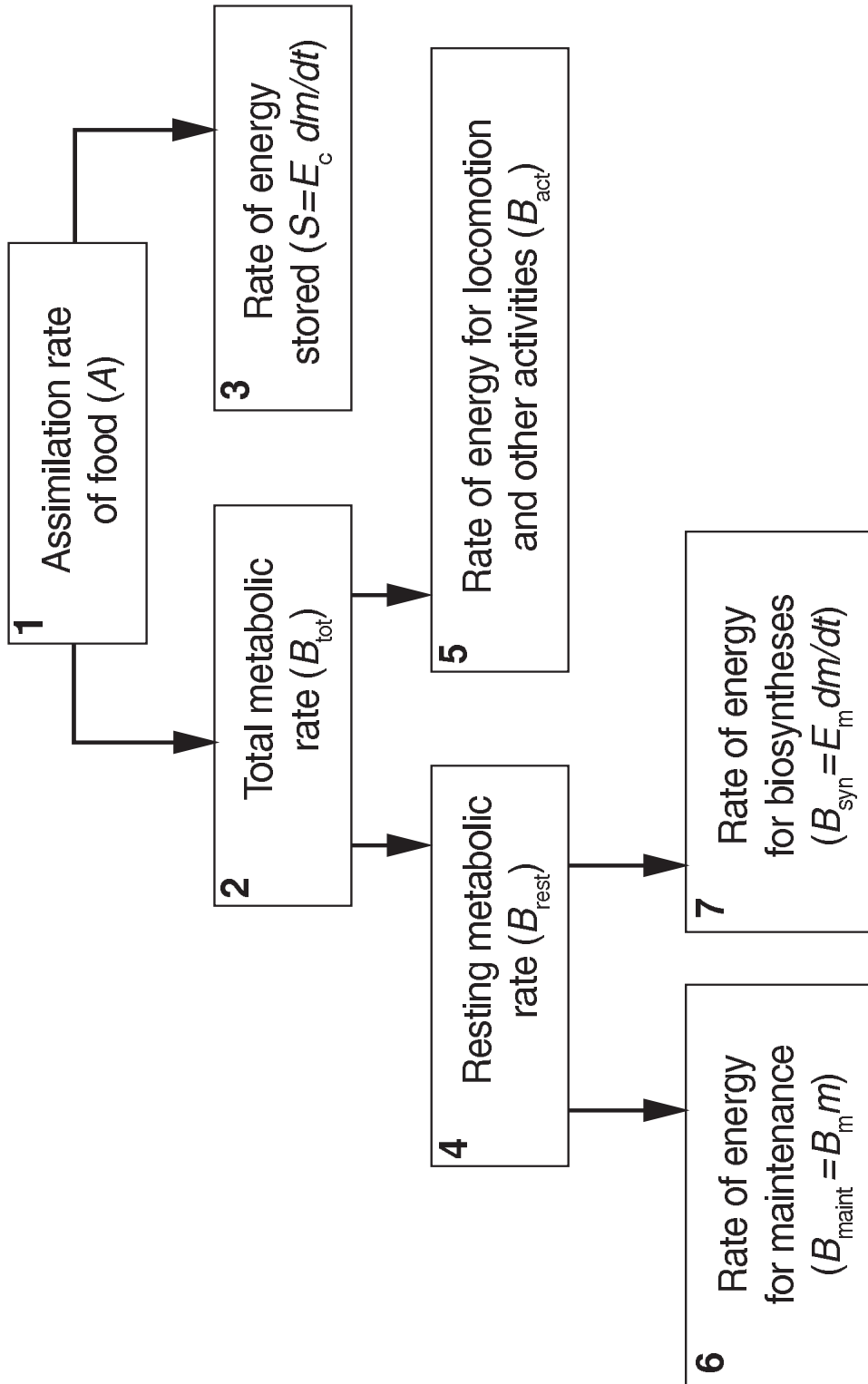
Figure 2.1: Partitioning of assimilated energy during ontogeny. Partitioning between boxes 2 and 3 represents Eq.2.1, and partitioning between boxes 6 and 7 represents Eq.2.2.

Chapter 2. A General Model of Energy Budget During Ontogeny

We build on an ontogenetic growth model(OGM), which specifies the allocation of metabolic energy between growth and maintenance and views the scaling of metabolic rate with body size as the primary constraint on growth [11]. It partitions the basal metabolic rate, B_{basal}, between the rate of energy expenditure to maintain the existing biomass, B_{maint}, and the rate to synthesize the new biomass, B_{syn} (Fig. 2.1): so, $B_{basal} = B_{maint} + B_{syn} = B_m m + E_m dm/dt$, where $B_m \sim M^{-1/4}$ is the mass-specific maintenance metabolic rate, M is the adult body mass, and E_m is the energy required to synthesize a unit of biomass.

It is difficult to measure B_{basal} over ontogeny because animals grow even while resting. Therefore, for growing animals a more operational and realistic parameter is resting metabolic rate, B_{rest}, which is the sum of B_{basal} and specific dynamic action (SDA), the increment resulting from digestion. SDA is the energy expended for intestinal absorption, nutrient transport, amino acid oxidation, and protein synthesis [32, 33]. Because some fraction of metabolic rate is allocated to SDA during growth [32–35],we modify the OGM to obtain

$$B_{rest} = B_{maint} + B_{syn} = B_m m + E_m \frac{dm}{dt} \tag{2.2}$$

where B_m is larger here than in the OGM, which ignored SDA.

It is important to recognize the difference between the terms $S = E_c dm/dt$ in Eq.2.1 and $B_{syn} = E_m dm/dt$ in Eq.2.2 and, consequently, the difference between E_m and E_c. Energy expended during growth is partitioned between the energy content stored in the newly synthesized biomass and the energy expended in synthesizing this biomass from the constituent materials. So, S is the rate of accumulated energy content of new biomass, and E_c is its combustion energy content. On the other hand, B_{syn} is the metabolic power expended on biosynthesis, and E_m is the energy expended to synthesize a unit of biomass. The term B_{syn} corresponds to the organizational work of growth [12] and is completely dissipated as heat, not conserved in stored biomass. In the OGM, the energy expended on biosynthesis was incorrectly estimated

by using the empirical combustion energy [11].

For adult mammals and birds, the total metabolic rate is typically referred to as field metabolic rate, and the relationship between total and resting metabolic rates is expressed as $B_{tot}(M) = B_{act}(M) + B_{rest}(M) = fB_{rest}(M)$, where B_{act} is the rate of energy expenditure for locomotion, feeding, and other activities and f, the activity scope, is a dimensionless parameter. In adult endotherms, f is about 2 to 3 and independent of body mass [36, 37] (see *SI*). Assuming that a similar relationship holds during growth, we can write, using Eq.2.2, $B_{tot}(m) = fB_{maint}(m) + fB_{syn}(m)$. We define the dimensionless storage coefficient, $\gamma = S/B_{syn} = E_c/E_m$, as the ratio of the energy stored in a unit of biomass to the energy expended to synthesize this biomass. Substituting γ and B_{tot} into Eqs.2.1 and 2.2 gives

$$
\begin{aligned}
A(m) &= B_{maint}(m) + B_{act}(m) + B_{syn}(m) + S(m) \\
&= (f + \gamma)B_{rest}(m) - \gamma B_{maint}(m).
\end{aligned}
\tag{2.3}
$$

Equation 2.3 is quite general, independent of how B_{rest}, B_{maint}, or f scale with m. Empirical measurements of metabolic rate over ontogeny and theoretical evidence linking growth and metabolism show that resting metabolic rate $B_{rest}(m) \approx B_0 m^{3/4}$ over ontogeny, where B_0 is constant for a given taxon [38] (see *SI*). The mass-specific maintenance rate, taking into account SDA, is $B_m \approx B_0 M^{-1/4}$ [11]. The use of these scaling relations in Eq.2.3 yields

$$
\begin{aligned}
A(m) &= (f + \gamma)B_0 m^{3/4} - \gamma B_0 M^{-1/4}m \\
&= B_{rest,adult}[(f + \gamma)\mu^{3/4} - \gamma\mu]
\end{aligned}
\tag{2.4}
$$

where μ ($\equiv m/M$) is relative mass and $B_{rest,adult} \approx B_0 M^{3/4}$ is the resting metabolic rate at the adult size.

Note that Eq.2.4 predicts that during ontogeny the food assimilation rate, A, unlike metabolic rate, does not obey a simple power law as a function of body mass, m. This prediction is well supported (see *SI*). In Fig.2.2, we plot some examples of the

normalized assimilation rate ($A/B_{rest,adult}$) versus m for six different animals and fit the data with Eq.2.4. Values of f, γ, and R^2 from the nonlinear least squares regression for these and several other bird and mammal species are in Table 2.2 (in *SI*). The storage coefficient, $\gamma = E_c/E_m$, can in principle be determined independently from the energetics of biosynthesis. The energy content of biomass, E_c, averages about 24,000 J/g for dry mass [39], with fourfold variation across vertebrates of different taxa and ontogenetic stages [40]. In contrast to E_c, E_m, the energy expended to synthesize a unit of biomass, is difficult to determine empirically (but see *SI*). Theoretical considerations suggest that the average energy required for biosynthesis of macromolecules from monomers is about 2400 J/g (see *SI*). This theoretical value of E_m gives an upper bound of $\gamma \sim 10$, the precise value depending on the additional energy expended on biosynthesis, metabolism, and excretion [13]. For mammals and birds, γ averages about 3 and ranges from 1 to 9 depending on species, diet, and age [13, 38](see *SI*). This result is consistent with values ranging from 0.8 to 7 for fish, birds, and mammals estimated from the OGM [38](see *SI*). We estimated from food assimilation that γ ranges from 0.6 to 5.3 with an average of 2.71 ± 1.18 (Table 2.2), showing that, despite some variation, the empirical measurements are in agreement with the theoretical prediction. Values of f vary somewhat, depending on activity levels and behavior. The mean value of f estimated from food assimilation is 2.67 ± 0.61 (Table 2.2 in (SI)), also in agreement with data for adult mammal and bird species (see *SI*).
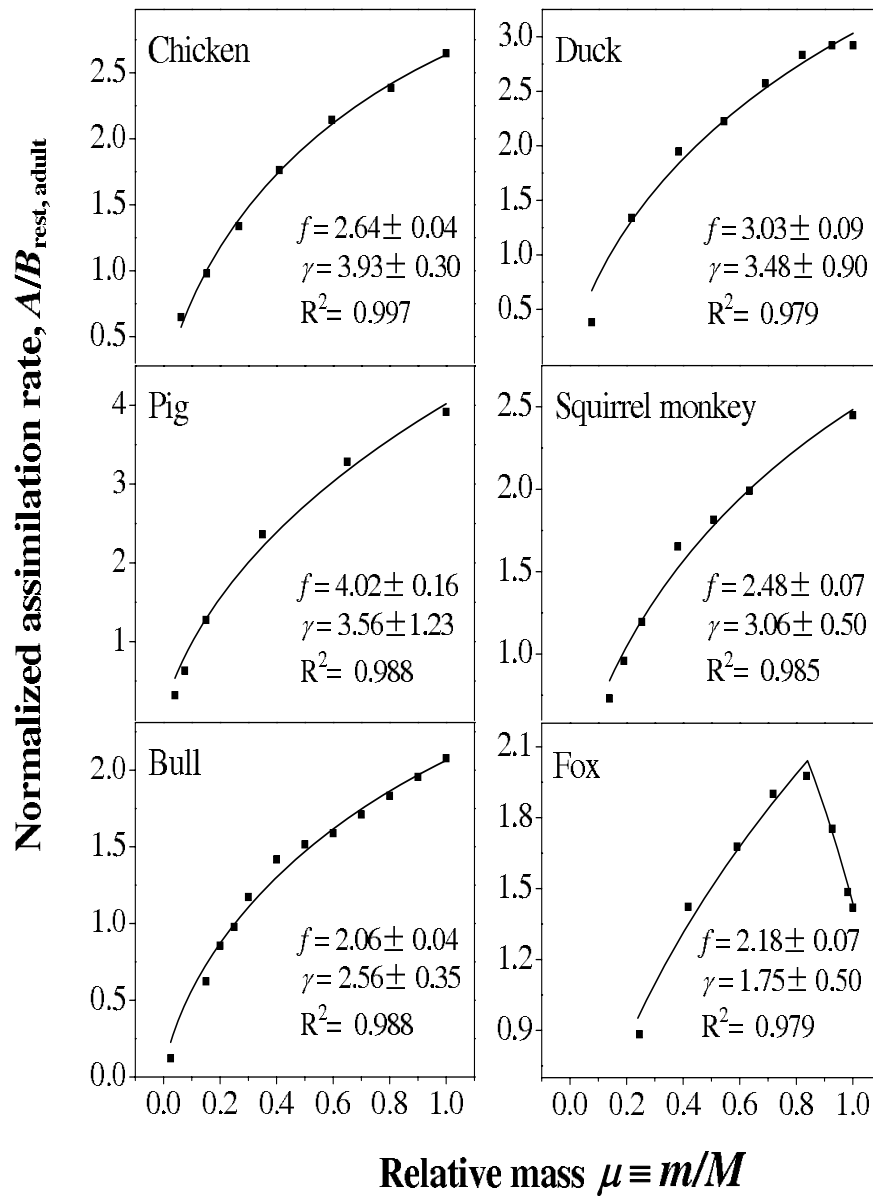
Figure 2.2: Examples of normalized assimilation rate as a function of relative body mass for six mammals and birds (■). The solid lines are fits of our model to these data with use of Eq.2.4. (Parameters f and γ were estimated by using a nonlinear least squares regression method based on the Levenberg-Marquardt algorithm.) The majority of assimilation rate curves reported in the literature are monotonic, but a few, including curves for furbearers such as fox, are peaked relationships (see *SI*).

When growth ceases, that is, $\mu = 1$ ($m = M$), Eq.2.4 predicts that the food assimilation rate equals the total metabolic rate, which scales with mass, M. So, A is equal to $fB_0M^{3/4}$ across adults of different species. Data for *ad libitum* energy intake from food of 120 species of zoo mammals with body masses ranging from 0.025 kg to 3000 kg show $A = 7.07M^{0.75}$, supporting the prediction [41,42](see *SI*). Taking the average value of B_0 for resting metabolic rates of mammals, 3.92W/kg$^{3/4}$(see *SI*), gives $f \approx 1.8$. This is somewhat less than that expected for wild animals, which may reflect lower activity levels in captivity.

Our model predicts that growth rates of diverse animals should exhibit universal properties. The fraction of energy assimilation rate allocated to growth is the sum of S and B_{syn}. With Eq.2.2 and the definition of γ, this fraction becomes $S+B_{syn} = (1+\gamma)B_{rest,adult}(\mu^{3/4} - \mu)$. If we normalize this quantity with respect to $(1+\gamma)B_{rest,adult}$, then all animal species, regardless of taxon or adult mass, should fall on the same parameterless universal curve, $\mu^{3/4} - \mu$. This further predicts that the maximum energy utilization rate for growth occurs when $d(\mu^{3/4} - \mu)/d\mu|_{\mu=\mu_0} = 0$, which gives $\mu_0 = (3/4)^4 = 0.316$. Equation 2.3 suggests a way to test these predictions. If we subtract the rate of metabolism for activity, B_{act}, and maintenance, B_{maint}, from the assimilation rate, A, the difference gives the rate of energy assimilation allocated to growth, $S + B_{syn}$. This quantity, normalized as above, is plotted as a function of the relative mass mu in Fig.2.3A.

The normalized assimilation rates for mammals and birds of widely varying body sizes and taxa show such universal properties, clustering closely around the predicted parameterless curve with a peak at ~ 0.316.
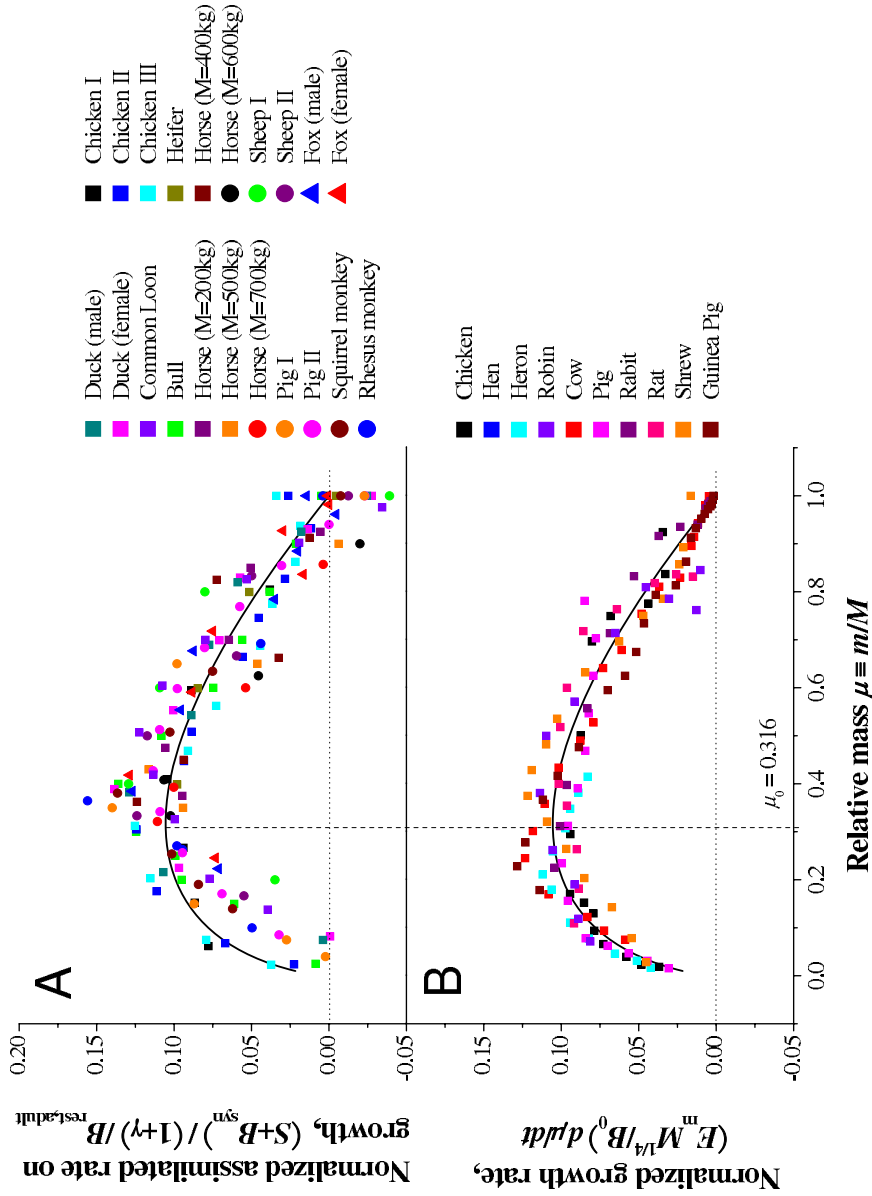
Figure 2.3: Two growth curves that are universal in the sense that they have their bases in principles of energy allocation and are predicted to be independent of taxon and body size: (**A**) universal rate of assimilation of food for growth and (**B**) universal rate of change in body mass. The empirical estimates (colored symbols for different organisms, with assimilation and growth rates measured independently in different studies, see *SI*) closely match the theoretical predictions (continuous curves that peak at 0.316).

Additionally, the rate of energy allocation to growth must be proportional to the growth rate, dm/dt, so the universal curve and the value of $\mu_0 = (3/4)^4 = 0.316$ can be derived independently from the growth rate equation, Eq.2.2, $dm/dt = (B_0/E_m)m^{3/4}[1 - (m/M)^{1/4}]$. This can be reexpressed as $(E_m M^{1/4}/B_0)d\mu/dt = \mu^{3/4} - \mu$. Data for normalized growth rates, $(E_m M^{1/4}/B_0)d\mu/dt$, for diverse mammals and birds measured independently from the above measurements of assimilation rate support this prediction (Fig.2.3B). So, estimations from the rate of food assimilation and the rate of change in body mass independently predicted analogous universal curves with a maximum at a relative body mass of ~ 0.316.

The predicted allometric scalings of metabolic energy allocation are summarized in Fig.2.4A, which shows the rates of food assimilation and total, resting, and maintenance metabolism for two individuals of different adult size depicted by different colors. The figure illustrates the complete energy budget during growth, $A = B_{maint} + B_{act} + B_{syn} + S$, and allocation of energy at any given size is shown by the colored vertical lines. The assimilation rate, A, of a growing individual does not scale as a power law with mass, whereas its rates of total and resting metabolism, B_{tot} and B_{rest}, both scale as $m^{3/4}$ and its maintenance rate, $B_{maint} = B_m m$, scales linearly. In contrast, for adults of different sizes, rates of assimilation and total (dashed line) and resting (maintenance, solid black line) metabolism all scale as $M^{3/4}$. Across species of different adult masses, growth ceases when all resting metabolism is allocated to maintenance [11], so that $B_{rest} = B_{maint}$, as indicated in Fig.2.4A (circles) representing two different adult masses, M_1 and M_2. Lastly, if otherwise identical individuals vary in energy allocated to activity, thereby having different values of B_{act} and B_{tot}, they must compensate by adjusting their assimilation rates, A, if they are to mature at the same adult mass, M.
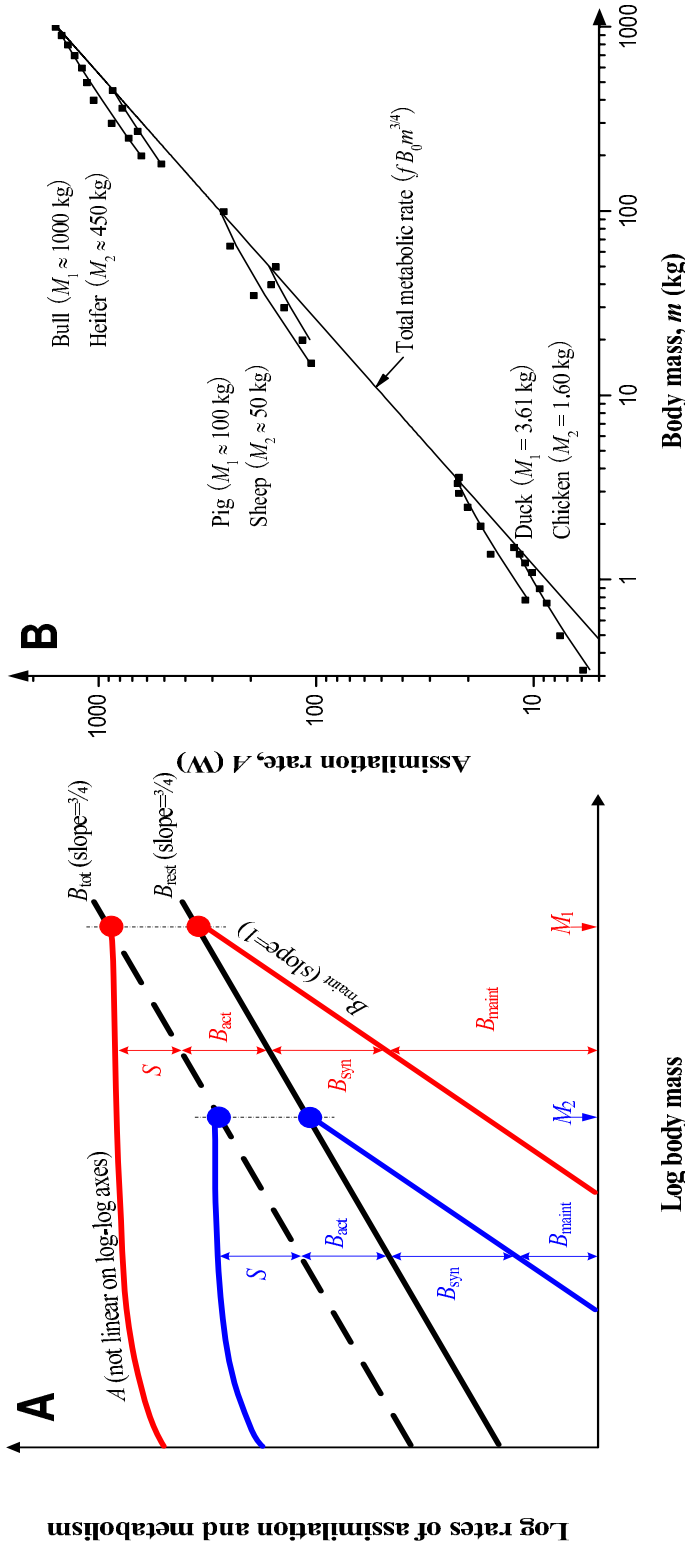
Figure 2.4: (**A**) Schematic illustrating the allometric scalings of energy allocation during growth for two individual organisms (shown with different colors) of different adult sizes, M_1 and M_2. For each individual, the colored vertical lines illustrate how, at any given body mass during ontogeny, the rates of energy allocated to maintenance (B_{maint}), biosynthesis (B_{syn}), activity (B_{act}), and storage (S) sum to equal the rate of assimilation, A. The scalings across individuals of two different body sizes are shown as dashed and solid black lines for total and resting metabolic rates, respectively, with the colored dots corresponding to these rates at the adult sizes, M_1 and M_2. (**B**) Assimilation rate as function of body mass for three pairs of mammals or birds. To facilitate comparison, we assumed that $f = 2.67$ for all animals.

One implication of the model is that when two individuals with the same B_0, f, and γ but different adult body masses, M_1 and M_2 ($M_1 > M_2$), have the same body mass, m, during growth, the assimilation rate of the one with the greater adult mass, M_1, must be larger than the one with the smaller adult mass, M_2, that is, $A(m, M_1) - A(m, M_2) \propto (M_2^{-1/4} - M_1^{-1/4})m > 0$. To test this prediction, we plotted the assimilation rates of three pairs of closely related animals assumed to have the same B_0, f, and γ as a function of body mass, m, during growth. As illustrated in Fig.2.4B, when members of each pair had the same body mass, m, during growth, the one with larger adult size (M) had a higher assimilation rate.

Our quantitative, predictive model for the energy budget of an individual during growth differs from phenomenological models that fit curves to data. It also differs from dynamic energy budget theory (DEB), which assumes a 2/3 power scaling of food assimilation rate during ontogeny, on the basis that energy uptake is limited by absorptive surface area, which scales like any simple geometric surface [14]. By contrast, our model predicts that food assimilation rate cannot have a simple power-law scaling relation with body mass during ontogeny. Furthermore, DEB assumes that food assimilation rate is supply limited, whereas our model views assimilation rate as arising from the developing organism matching food supply to metabolic energy demand. Our model provides a point of departure for addressing pathological cases of imbalance between supply and demand such as starvation or overeating. It captures the salient features of energy acquisition and allocation during ontogenetic development and quantitatively predicts universal assimilation and growth rate curves in agreement with data for mammals and birds. How well it captures the fundamental features of growth in other organisms, such as ectothermic vertebrates, insects, aquatic invertebrates, plants, and unicellular algae and protists, remains to be seen.

2.1 Response to Comments on "Energy Uptake and Allocation During Ontogeny"

abstract

Our extended ontogenetic growth model is a theoretical model based on conservation of energy and general biological mechanisms underlying ontogenetic growth. We do not believe that the comments of Makarieva *et al.* and Sousa *et al.* expose substantive problems with our model. Nevertheless, they raise interesting, still unresolved questions and point to philosophical differences about the role of theory and of simple, general models as opposed to complicated, specific models.

We presented a model for energy uptake and allocation over an organism's growth and development that reconciles rates of food assimilation with rates of allocation to maintenance, biosynthesis, activity, and storage [43]. Makarieva *et al.* [44] and Sousa *et al.* [45] raise concerns about our model, which we address here.

Makarieva *et al.* [44] take issue with the assumption of our extended ontogenetic growth model that resting metabolic rate scales as $M^{3/4}$ throughout postembryonic growth and development, similar to the scaling across adult animals of different species. They claim that young animals have elevated metabolic rates compared with what is predicted for their body mass from interspecific scaling. This further implies that metabolic rate as a function of mass throughout ontogeny cannot be a simple power function. So, instead of plotting as a straight line on logarithmic axes, the relationship must be biphasic or curvilinear, with the slope initially steeper and subsequently shallower than the interspecific $M^{3/4}$ scaling (as shown in Fig.1B

in [44]). The scaling of metabolic rate during ontogeny is ultimately an empirical issue, albeit one with important conceptual and methodological implications.

So what do the data say? In their Fig.1A, Makarieva *et al.* present data for metabolic rates "measured at rest in the postabsorptive state" for eight species of birds and mammals during postembryonic growth (data from [46]). Makarieva *et al.* selected the "eight largest values of metabolic rates in early ontogeny," which would tend to bias their results in the direction of their claim, and show that the metabolic rate early in ontogeny is relatively higher than predicted by our model [43]. We have compiled and plotted in Fig.2.5 all the data from [46], including a ninth species, quail, which deviates from predictions in Makarieva *et al.* [44] and was not included in their analysis. Our analysis (see also Table 2.1) offers some support for Makarieva *et al.*s claim that metabolic rates, relative to the predicted mass to the 3/4 power, are consistently and substantially higher during early ontogeny than at adulthood. Although the data for the individual species are well described by a power law (see Table 2.1 and Fig.2.5), in most species there are times during early ontogeny when metabolic rates are higher than what would be predicted for an adult of the same size. Makarieva *et al.*, following the model proposed by Wieser [47], claim that the peak metabolic rate occurs at approximately 10% of adult mass, but this is true for only four of the nine species. The other five species have peak values at relative sizes that range from 1% to 48% of adult mass (see data and Fig.3 in [46]), and the rabbit has two distinct peaks.

Table 2.1: The scaling exponent over ontogeny, peak normalized metabolic rate $[K \equiv B_g(m)/(B_0 m^{0.75})]$ where B_g is resting metabolic rate of the growing organism [44], and the relative body mass ($\mu \equiv m/M$) of this peak for each species, from [46].

Species	Slope	R^2	K	μ
Rat	0.71	0.9631**	1.41	0.36
Guinea Pig	0.75	0.9901**	1.12	0.23
Hen	0.60	0.9643**	1.68	0.07
Rabbit†	0.77	0.905	1.55	0.05
Goose	0.86	0.9517*	1.71	0.13
Sheep	0.46	0.9185**	1.71	0.11
Pig	0.66	0.9777**	1.49	0.01
Cow	0.59	0.9452**	1.57	0.13
Japanese Quail	0.96	0.9858**	2.29	0.48
Mean	0.71		1.61	0.17

** $p < 0.0001$

* $p < 0.001$

† Rabbit shows another peak at $\mu = 0.25$.
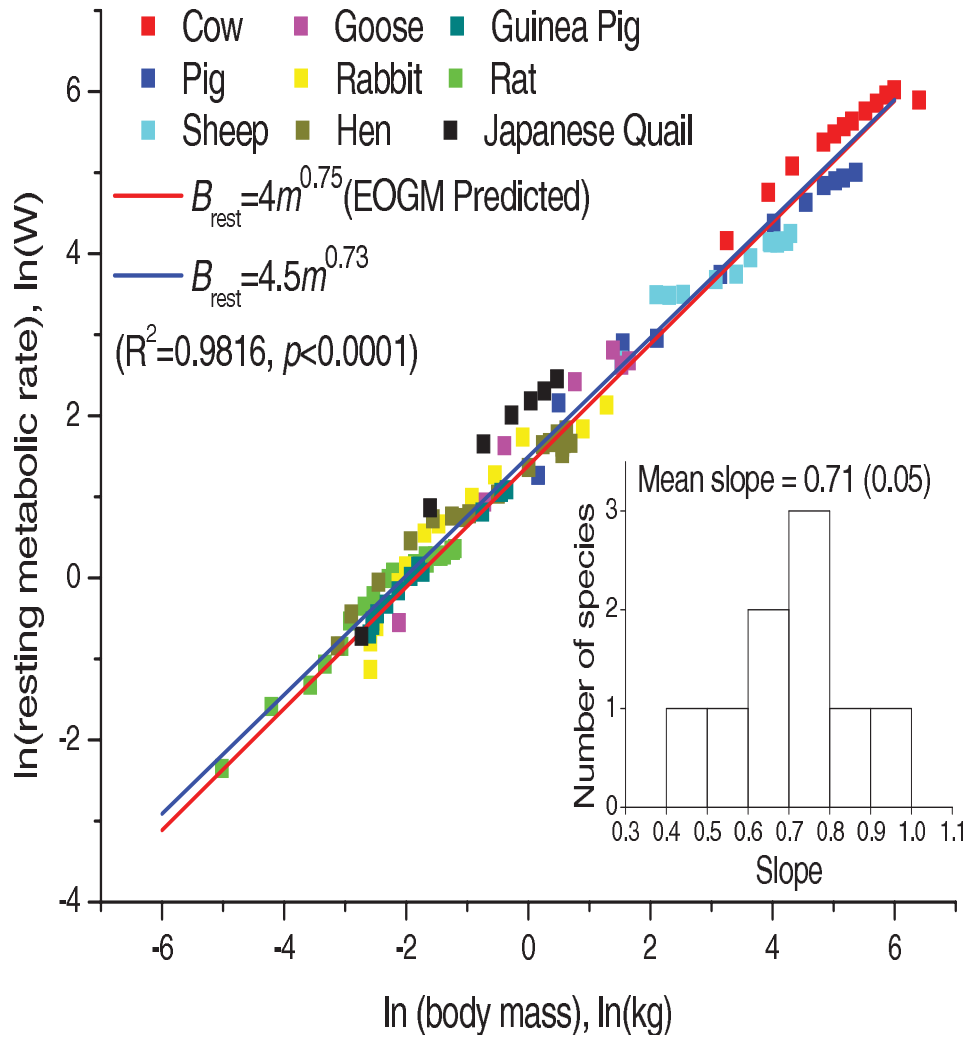
Figure 2.5: Scaling of resting metabolic rate with body mass over ontogeny for nine species from [46]. The red line is predicted by our extended ontogenetic growth model. The blue line is fitted to the data. The histogram shows the frequency distribution of the scaling exponents for these nine species.

Chapter 2. A General Model of Energy Budget During Ontogeny

Our analysis highlights two important points. First, there are necessarily deviations between detailed observations of individual growth curves and the predictions of a parsimonious model such as ours, and it is valuable for such deviations to be recognized in the literature. Second, the value of our model is that it provides a baseline to which data can be compared, so that the causes of any observed deviations can be revealed. Makarieva *et al.* point out such a systematic deviation from the model. However, they provide only a statistical description of these deviations, and one that does not capture the measurements for the majority of the species. Moreover, they do not provide any mechanistic explanation for these deviations. We suggest that these periods of peak metabolism may correspond with growth spurts that have been observed in a number of species and are also deviations from predictions of our model.

More generally, the comment of Makarieva *et al.* raises important, still unanswered questions about the energetics of growth and development. Our model was intended primarily to focus on the consumption of food and the allocation of the assimilated energy between maintenance of existing biomass and synthesis of new biomass. It does indeed imply that the total metabolic rate of a growing animal should be the same as that of an adult of the same mass. In doing so, it assumes that a constant fraction of this total metabolic rate is due to resting metabolism, B_{rest}, and a constant fraction to activity, B_{act}, so that $B_{tot} = B_{rest} + B_{act} = B_{rest} + fB_{rest}$, where B_{rest}, B_{act}, and B_{tot} all scale as $M^{3/4}$, and f is the activity scope. In adult animals, the total metabolic rate is the field metabolic rate, where $f \approx 3$. To apply our model to the metabolic rate measured early in ontogeny clearly depends on how activity is defined. At present, however, it is not clear even whether rest and activity represent comparable states for very young animals and adults. Most crucial for the realism of our model is not how the total metabolic rate is partitioned between rest and activity, but whether B_{tot} scales as $\sim M^{3/4}$ throughout postembryonic ontogeny, the same as across adult animals of different size. This appears to be true across a

wide variety of species [38].

Sousa *et al.* [45] make several specific criticisms to support their claim that only the dynamic energy budget (DEB) theory of Kooijman [14] provides a complete theoretical and mechanistic treatment of growth. We respond by emphasizing that our model is much simpler and more parsimonious than DEB. DEB requires three state variables (reserve, structure, maturity) and 12 primary parameters to be measured for every species [48], whereas our model contains only two variables (m and t) and five parameters (M, B_0, f, E_m, and E_c). There is nothing inherently wrong with the DEB approach, but for many theoretical and practical purposes it is desirable to have models that are as simple as possible as long as they still capture the essence of the phenomenon and give reasonably accurate predictions. As a particular case in point, Sousa *et al.* correctly point out that our model does not contain an explicit chemical description of metabolism. From this they correctly conclude that the model we proposed cannot explain the variable chemical composition of organisms growing with variable food. We note, however, that they present no data on how the chemical composition of the diet affects body composition or growth trajectory. In fact, as long as diets are relatively standard, the effects of such variable food are minor [12]. Sousa *et al.* also claim that because our model does not explicitly incorporate the chemistry of metabolism, it cannot be applied to the growth of anaerobic organisms. This is incorrect. The fact that it deliberately ignores the details of biochemistry allows our model to provide a general quantitative accounting for the allocation of energy and biomass during postembryonic growth of diverse animals with different diets and biochemical pathways.

A critical difference between our model [43] and DEB is whether assimilation rate scales as a power law of body mass as a growing animal increases in size. The original DEB assumes that rate of food assimilation, because it is proportional to gut surface area, scales as $M^{2/3}$ [14, 49]. We are unaware of any evidence supporting

this assumption. Indeed, our model would suggest that the highly elaborated fractal-like surface of the gut actually scales approximately as $M^{3/4}$ across adult animals of different species, so that the rate of energy uptake from food closely matches the rate of metabolic energy expenditure. Sousa *et al.* [45] suggest that DEB can account for changes in assimilation rate with increasing mass during growth "because the ratio of reserve to structure is not constant." Again, DEB introduces a level of detail and associated problems of defining and measuring "reserve" and "structure" that are peripheral to the central issue of how energy assimilation and allocation change with mass during ontogeny.

Sousa *et al.*'s characterization of our model as "demand" limited is misleading. DEB assumes that metabolic rate is limited by the availability and assimilation of food. Our model [43] is based on the original ontogenetic growth model of West *et al.* [11], which assumes that the scaling of metabolic rate with body mass is due to functional and geometric constraints on the capacity of the vascular network to supply energy to the body. So, like DEB, our model matches supply and demand, imposing mass and energy balance to require that uptake from food equals metabolic expenditure plus biomass storage.

Finally, we note that the comments of both Makarieva *et al.* [44] and Sousa *et al.* [45] expose fundamental philosophical differences about the role of models in biology. DEB is a single, very detailed model. It can potentially describe nearly all aspects of the metabolic basis of growth and account for variation within and across species due to variation in such factors as food supply, diet composition, and environmental conditions; to do so, however, requires measuring all 3 variables and 12 parameters. Our model, by contrast, is a very simple one that aims to quantify only the most essential features of energy acquisition and allocation. It is indeed similar to the model of Bertalanffy [5], as the comment authors and we ourselves have emphasized. Our model differs from Bertalanffy's model chiefly in its more

explicit treatment of rates of assimilation and metabolism, including whether the latter scales as $M^{3/4}$ or $M^{2/3}$. Such simple models can provide a point of departure for incorporating complexity due to factors such as food restriction, temperature, or biochemical pathways of metabolism and for exploring additional phenomena such as energy allocation during embryonic development and tradeoffs between growth and reproduction in animals with indeterminate growth. We suggest that the complexity of DEB is the primary reason that, although the theory is frequently cited, the complete model is rarely implemented and applied to particular organisms. In most cases, the details and complexity of DEB are not required and a much simpler model, such as Bertalanffy's model or our model [43], will suffice.

Both Makarieva *et al.* and Sousa *et al.* imply that models such as ours and Bertalanffy's are flawed because the small number of variables and parameters do not include an explicit treatment of the chemistry of the diet and metabolic pathways. We emphatically disagree that more general models cannot "shed new light on the fundamentals of ontogenetic growth." Two parameters in our model, f and E_m, are difficult to assess quantitatively with data currently available. f, the "activity scope", is discussed above. E_m, the quantity of energy used to synthesize a quantity of biomass, is a fundamental biological parameter. We find it surprising that even today there are few data that can be used to estimate the value of E_m, let alone to assess how it may vary with diet, type of tissue being synthesized, taxon of organism, and environmental conditions. Indeed, most of the data used to inspire and evaluate our models of growth and by Makarieva *et al.* in their critique come from studies conducted decades ago. Without models that call attention to fundamental features of biological energetics, additional decades likely will pass before biologists are motivated to make the relevant measurements.

2.2 Supporting Information (*SI*)

2.2.1 Theoretical estimates of the activity scope factor (f) and storage coefficient (γ)

The values of activity scope factor, f, and storage coefficient, γ, estimated from the food assimilation rate for mammals and birds of diverse body size and taxa are given in Table 2.2. For most species, the food assimilation rate, A, increases with the body mass monotonically over ontogeny. For these species, we assume a constant f over ontogeny. However, in fox and mink, A increases and then after attaining approximately 80% of adult mass, decreases. Since $A = B_{tot} + S$, and S of these three species increase monotonically, we hypothesized that the reason for the decrease in A is due to reduced activity, which is reflected in varying values of f. For these species, we assumed a simple function for f:

$$f(\mu) = \begin{cases} f_0 & \mu \leq \mu_d \\ f_0 - a(\mu - \mu_d) & \mu > \mu_d \end{cases} \tag{2.5}$$

where μ_d is the relative mass at which A starts decreasing and a and f_0 are two constants. The values of these parameters are given in Table A.1. We also calculate an effective value of f, the harmonic mean value over ontogeny, $\bar{f} = \int_0^1 f(\mu)d\mu$, for these species. The values of $\bar{f}$ are close to the average value of f of other species.

Our model did not fit the data for the female mink, which is the only case exhibiting two distinct peaks in normalized assimilation rate at different stages (value of μ) of ontogeny. We suspect that the data are in error, and have not included them in subsequent analysis.

All original data from literatures are in Table A.5.

Table 2.2: Values of f and γ for various organisms (estimated using nonlinear least squares regression method based on the Levenberg-Marquardt algorithm).

Species	f	γ	Value of R^2
Heifer	2.14	2.17	0.998
Pig I	4.02	3.56	0.988
Pig II	3.29	3.41	0.990
Bull	2.06	2.56	0.988
Sheep I	2.92	3.16	0.939
Sheep II	2.77	5.29	0.947
Horse ($M = 700$ kg)	2.96	1.45	0.974
Horse ($M = 600$ kg)	2.91	0.69	0.981
Horse ($M = 500$ kg)	2.70	1.35	0.973
Horse ($M = 400$ kg)	2.52	2.37	0.951
Horse ($M = 200$ kg)	2.24	3.08	0.980
Duck (male)	3.03	3.48	0.979
Duck (female)	3.16	3.44	0.975
Chicken I	2.64	3.93	0.997
Chicken II	1.57	3.97	0.976
Chicken III	1.61	3.41	0.973
Common Loon	2.41	1.94	0.976
Squirrel Monkey	2.48	3.06	0.985
Rhesus Monkey	2.25	3.38	0.958
Fox (female) ($f = \bar{f}$)	2.18	1.75	0.979
Fox (male) ($f = \bar{f}$)	2.17	1.88	0.977
Mink (male) ($f = \bar{f}$)	3.50	0.57	0.876
Mink (female) ($f = \bar{f}$)	7.87	-6.19	0.923
Mean	2.67	2.71	
SD	0.61	1.18	

2.2.2 The theoretical and empirical estimations of E_m and γ

Empirical values of production efficiency, η, storage coefficient, γ, and quantity of energy to synthesize a gram of biomass, E_m, are listed in Table A.2. Details of the calculation are the following.

The physiological production efficiency, η, is a quantity closely related to γ. It is a measure of the efficiency of the physiological processes responsible for egg and milk production and tissue growth. It is defined as the energy content of production relative to the energy content of the biomass produced plus the fraction of the metabolic energy expended to synthesize that biomass [12, 13, 50], $\eta = E_c/(E_c + E_m) \times 100\%$. With the definition $\gamma = E_c/E_m$, we express γ in terms of η as $\gamma = \eta/(1 - \eta)$.

E_m is defined as the quantity of energy expended to synthesize a unit of biomass. Theoretical considerations suggest the minimum value of E_m would be the energy required for biosynthesis of tissue macromolecules from monomers [13, 51]. The value of "one dry gram of average metazoan biomass contains approximately 0.01 moles of polymeric linkages [52, 53]. On average, three phosphate bonds are hydrolyzed in the synthesis of each polymeric linkage and the free energy ($\triangle G$) in going from 3 ATP to 3 ADP is approximately 86 kJ/mol. Hence $0.01 \times 86\text{kJ} = 860\text{J}$ are required to synthesize 1 gram of biomass" [52]. By assuming an aerobic system with tissue respiration operating at 65% efficiency, $860/0.65 = 1323\text{J}$ was calculated to be required to generate the necessary ATP to synthesize 1 gram of dry biomass [52]. Taking the heat of combustion (E_c) of 23.1 kJ [39] gives $\gamma \sim 17$. The value of free energy ($\triangle G$), 86 kJ/mole, in going from 3ATP to 3ADP, is based on the standard free energy change of hydrolysis of ATP. Since the concentrations of ATP, ADP, and P_i in the cell are much lower than the standard concentrations, and the pH inside cells differ from the standard pH of 7.0, the actual free energy of hydrolysis of ATP under intracellular conditions differs from the standard free-energy change [54]. On

29

the basis of the concentrations of ATP, ADP, and P_i in rat hepatocyte, myocyte, neuron, human erythrocyte and *E. coli* cells, we found that the actual free-energy change of ATP hydrolysis under intracellular conditions in these cells ranges from 46.7 to 52.7 kJ/mol averaging about 49 kJ/mol, which is higher than the standard value. Taking the average value, the free energy in going from 3 ATP to 3 ADP is $49 \times 3 = 147$ kJ/mol, and the energy to synthesize one gram of dry biomass is $E_m = 2262$ J/g, so $\gamma = E_c/E_m \sim 10.2$.

The theoretical value of E_m should be considered the lower bound, therefore the value of γ obtained this way is an upper bound, because other energy requirements for biosynthesis, including the cost of transport of molecules into and within cells, the cost of mechanical separation of nucleic acid strands and daughter cells during mitosis [52], need to be taken into account. However, it is difficult to separate the energy used for growth from that used for maintenance in these energy requirement. Recently, on the basis of the theoretical ontogenetic growth model, which theoretically disentangled the allocation of energy to growth and maintenance, the value of E_m for embryos and juveniles of birds, fish and mammals, was estimated with data from growth curves and growth time [38]. We also used direct measurements of metabolism and growth of dry biomass to estimate E_m for chick embryos. These results span an order of magnitude. For embryos of birds and fishes, E_m was calculated to be about 800 to 2800 J/g; for mammalian embryos, it ranges from 2700 to 7100 J/g; for juvenile birds, it ranges from 1400 to 7500 J/g; and for juvenile mammals, it ranges from 1800 to 9500 J/g. These values are for wet mass. From these values we calculated the value of γ for post-birth organisms. Taking $E_c = 7000$ J/g(wet mass) [39,55], values of γ given by the data in [38] range from 0.74 to 5, which agree with ours obtained from food assimilation rate in this paper, $\gamma = 0.6 - 5.3$.

The values of production efficiency, and therefore the values of γ and E_m, vary with species, age, temperature, composition of diet and type of substance accumu-

lated [52]. For example, η in young chickens was 72% ($\gamma \sim 2.6$) at $38°C$ and decreased to 57% ($\gamma \sim 1.3$) at $21°C$ [56]. Production efficiencies range from 50% to 90% ($\gamma \sim$ 1 to 9) for mammals and chickens [13]. These values are consistent with the range of values reported in Table 2.2 (0.57 to 5.29). η also varies widely; as a representative value of $\eta = 75\%(\gamma = 3)$ was adopted [50]. This value has been adopted by other authors (for example, see [57]), and is very close to what we obtained here, $\gamma = 2.7$.

η for embryos of several birds, fish and worms was calculated in [12, 13]. For example, the energy of combustion of an average hens egg is about 364 kJ. Of this, 159 kJ is assimilated into the chick and 109 kJ remains as unused material. The remainder (96 kJ) is the energy lost through metabolism. So it was concluded that "the efficiency is about $100 \times 159/(159 + 96) = 62\%$" [12, 13]. With this value, we estimated a γ for chicken embryo of about 1.6. However, the energy lost through metabolism, 96 kJ, includes the energy used for maintenance and growth, and it is unclear how to separate these two. So, the production efficiency η calculated this way and the value of γ we obtained above is the lower bound of the real value. In the same way the values of η for embryos have been calculated for gastropods (62%$\sim$ 67%), silkworms (63%), frogs (51%), sea urchins (59%), green iguanas (48%) and herrings (70%). So the lower bounds of γ for these embryos range between 1 and 2.3.

Production efficiency for tissue gain is usually determined by the multiple regression method. This factorial approach partitions the metabolizable energy intake between the energy requirement for maintenance, which depends on body size, and the requirement for growth, which depends on the amount and composition of the added gain. If the metabolizable energy intake is plotted against tissue energy accumulation in a series of animals that grow by different amounts, then the slope given by the nonlinear multiple regression is the production efficiency [50, 58, 59]. A wide range of production efficiencies for different organisms post-born tissue gain were calculated in this manner (See Table A.2). A similar method has been used to es-

timate E_m for five avian embryos [60]. Instead of partitioning metabolizable energy intake rate, the metabolic rate was partitioned between the rates of maintenance and growth, and the nonlinear multiple regression method was used to fit the data [60]. When the metabolic rate was plotted against growth rate, the slope of the relation gives E_m.

2.2.3 Field and resting metabolic rate and the ratio of them for mammals and birds

Data from resting metabolic rates ($B_{rest} = B_{0,rest}M^{\psi}$) for mammals and birds are listed in Table A.3.

For mammals, data from resting metabolic rates with body masses ranging from 0.01kg to 650kg, show that $B_{rest} = 3.93M^{0.749}$ ($R^2 = 0.963$). The coefficient $B_0 = 3.93$ W/kg$^{0.75}$ is 20% larger than the one of the basal metabolic rate, 3.28 W/kg$^{0.75}$ [55], reflecting the fact that B_{rest} includes B_{basal} and Specific Dynamic Action (SDA).

For birds, the resting metabolic rate was measured during the daytime and night [61], resulting in scaling exponents of 0.729 (day) and 0.734 (night) for non-passerines and 0.704 (day) and 0.726 (night) for passerines. The coefficient B_0 of non-passerines at daytime was calculated to be 4.41 W/kg$^{0.75}$. This coefficient is about 10% larger than the one of the basal metabolic rate 4.06 W/kg$^{0.75}$ for non-passerines [55].

Data from field metabolic rate (B_{field}) of free-living and captive mammals and non passerine birds are listed in Table A.4.

For adult mammals and birds, the relationship between field and resting metabolic rates can be expressed as, $B_{field}(M) = fB_{rest}(M)$, where f is a unitless constant reflecting the addition energy expenditure required to support activities beyond maintenance [36, 62, 63]. We use the formula $f = \frac{B_{field}(M)}{B_{rest}(M)} = \frac{B_{0,field}M^{3/4}}{B_{0,rest}M^{3/4}} = \frac{B_{0,field}}{B_{0,rest}}$ to

calculate f for each data set. The parameter $B_{0,rest}$ is shown in Table A.3.

Doubly labeled water method was used to measure the field metabolic rates of free-living mammals [37]. For eutherians, which we study in this paper, the ratio between field and resting metabolic rate, f, is 2.57, which is very close to the value we obtained from the assimilated food data, $f = 2.61 \pm 0.61$. By measuring the daily metabolizable energy intake rate, several studies of captive adult mammals also show the 3/4 scaling power of the field metabolic rates. The values of f obtained in these studies are a little less than 2, reflecting the limited activities levels for animals in captivity.

A measurement of daily metabolizable energy intake of caged birds [64] found that for non passerines, $B_{field} = 4.8M^{0.755}$ ($N = 9$). These scaling exponents are close to the ones reported in [37] for both groups of birds, but the coefficients $B_{0,field}$ of the caged birds in this study are about twofold smaller than the values of the free-living birds in other studies [37].

2.2.4   The empirical evidence for 3/4 power during ontogeny

Numerous studies provide data on the scaling of metabolic rate with body mass for adult animals of different species. The preponderance of evidence supports an inter-specific scaling exponent of 3/4 [55, 65–68]. There are fewer studies that examine how metabolic rate scales with mass over ontogeny, but the preponderence of these also support an exponent of 3/4. Recently compiled data [69] from 497 studies of the allometric scaling of metabolic rate within species, including both cases where body size changes over ontogeny and where body size varies among adult individuals. Our reanalysis of Glazier's data shows that when the body mass range is sufficient (larger than 2 orders of magnitude), the empirical estimates are very close to 3/4 with small variation [38]. Data for metabolic rate over ontogeny from Fishbase [70]

was compiled and analyzed to accurately estimate the scaling exponent [38], and a similar result was obtained: the exponent is close to 3/4, and it is less variable when calculated for species with larger mass range. A similar distribution for intra-specific and inter-specific scaling exponents (mean intra-specific = 0.72, inter-specific = 0.76) was shown in ([55], Fig.4.7). Several other analyses support the 3/4 power scaling of metabolism over ontogeny in domesticated animals including steers, sheep and cattle [71–74]. Additional studies compared both ontogenetic scaling exponents and coefficients for domestic animals, and again found that they are close to the inter-specific values: exponents of 0.74 for rams and 0.76 for wethers [75] and exponent of 0.75 for beef cattle [76]. Finally, the data of biological time to some benchmark stage or body size, which can be measured more easily and reliably than metabolic rate, also supports the 3/4 power prediction by the OGM [38].

Chapter 3

A general model for effects of temperature on ectotherm ontogenetic growth and development

Collaborated with Melanie E. Moses, Geoffrey B. West, Chen Hou, and James H. Brown

3.1 Abstract

The temperature size rule (TSR) is the tendency for ectotherms to develop faster but mature at smaller body sizes in warmer environments. It can be explained by a simple model in which the rate of growth or biomass accumulation and the rate of development have different temperature dependence. The model accounts for both TSR and the less frequently observed reverse-TSR, predicts the fraction of energy

allocated to maintenance and synthesis over the course of development, and also predicts that less total energy is expended when developing at warmer temperatures for TSR and vice versa for reverse-TSR. It has important implications for effects of climate change on ectothermic animals.

keywords: development rate — ectotherm development — energy budget — growth rate — temperature size rule

3.2 Introduction

Changes in environmental temperature regimes pose potentially severe problems for ectothermic organisms. Their body temperatures fluctuate with environmental temperatures and the rates of nearly all biochemical reactions and biological processes increase approximately exponentially with temperature. So changing temperature literally changes the pace of life.

The rate of ontogenetic growth and development is no exception. Ectothermic animals develop faster at warmer temperatures [16], and they usually mature at smaller body sizes – as much as 20% smaller for a 10^oC temperature increase. This phenomenon has been called the "temperature size rule" (TSR) [17]. Like most biological "rules", however, there are exceptions, including well documented cases of a reverse-TSR, where the mature body sizes are larger at higher temperatures. Here we develop a simple model for the effects of temperature on ontogenetic development of ectothermic animals. The model extends an earlier model for allocation of energy and biomass to growth [18] by explicitly incorporating the temperature dependence of the rate of development and the rate of somatic growth. Any imbalance in these two rates results in either the TSR or reverse-TSR, depending on which process is more sensitive to temperature. The model predicts the fraction of energy allocated to maintenance and biomass synthesis at a given development stage, including the total

quantity of energy expended during development. We model explicitly the case of post-hatching development, where an animal consumes food to fuel its metabolism. Later we consider the case of embryonic development, where the organism fuels its metabolism from energy reserves stored in the egg.

3.3   The Model

Growth and development are fueled by metabolism. It is well known that within the normal temperature range metabolic rate increases approximately exponentially with temperature. This relationship can be described by the Boltzmann relation, $e^{-E_a/kT}$, where E_a is an "activation energy" that reflects the kinetics of the underlying biochemical reactions and quantifies the temperature dependence, k is Boltzmann's constant, and T is absolute temperature ([16, 18], but see [77]). For processes governed by aerobic respiration, such as growth and development of most ectothermic animals, E_a is typically ~ 0.65eV (corresponding to a Q_{10} of ~ 2.5 or a 2.5-fold increase in development rate for a $10^o C$ increase in temperature) [16].

The effect of temperature on body size at maturity, however, depends on how energy and materials are allocated during ontogeny. The body mass $m(t,T)$ at any time, t, during development depends on the magnitude of two different processes which can have different temperature dependence: 1) growth rate or rate of biomass accumulation, $\frac{\partial m}{\partial t}$, with temperature dependence $e^{-E_g/kT}$; and 2) development rate or rate of ontogenetic differentiation, $\frac{\partial \mu'}{\partial t}$, with temperature dependence $e^{-E_d/kT}$, where E_g and E_d are the respective "activation energies" (Fig.3.1). The relative developmental stage, $\mu' \equiv \frac{t}{t_{dev}}$, is defined in terms of the time to the current developmental stage, t, relative to the total development time, t_{dev}. Similarly, the relative body mass, $\mu \equiv \frac{m}{M}$, as the body size at any time, t, relative to adult body size [43]. Since $\frac{\partial \mu'}{\partial t} = \frac{1}{t_{dev}}$, the total time of development $t_{dev} \propto e^{E_d/kT}$. The

relative developmental stage is a simple way to standardize the overall ontogenetic trajectory on a $0-1$ scale, so $\mu' = 0.1$ means 10% of time to adulthood. The adult mass, $M = \int_0^1 \frac{\partial m}{\partial \mu'} \partial \mu'$, is proportional to $e^{-(E_g - E_d)/kT}$. It can also be calculated as $M = \int_0^{t_{dev}} \frac{\partial m}{\partial t} \partial t \propto e^{-(E_g - E_d)/kT}$. Unless these two processes, growth and development, have exactly the same temperature dependence ($E_g \equiv E_d$), size at maturity will vary with temperature (Fig.3.1).

The animal consumes food to fuel growth and development from hatchling to adult. We use extended ontogenetic growth model [43] to capture the energy allocation during growth. The rate of food assimilation, A, is the sum of the rates of energy consumption for maintenance and growth. So

$$A = B_{maint} + B_{syn} + S \tag{3.1}$$

and

$$B = B_{maint} + B_{syn} \tag{3.2}$$

where B_{maint} is the rate of energy expended on maintenance, B_{syn} is the rate of energy used to synthesize the new biomass, B is the total metabolic rate, S is the rate of energy allocation to or storage in new biomass, and $B_{syn} + S$ is the rate of energy expended on growth. Assuming that the energy content per unit of biomass remains constant over ontogeny and is independent of temperature, these equations reflect energy and mass balance at any time, t. The integrated form over the entire development period is

$$Q_{tot} = Q_{maint} + Q_{syn} + Q_{sto} \tag{3.3}$$

where Q_{tot} is the total quantity of energy expended, Q_{maint} is energy expended on maintenance, Q_{syn} is energy expended to synthesize new biomass, and Q_{sto} is energy stored in new biomass.
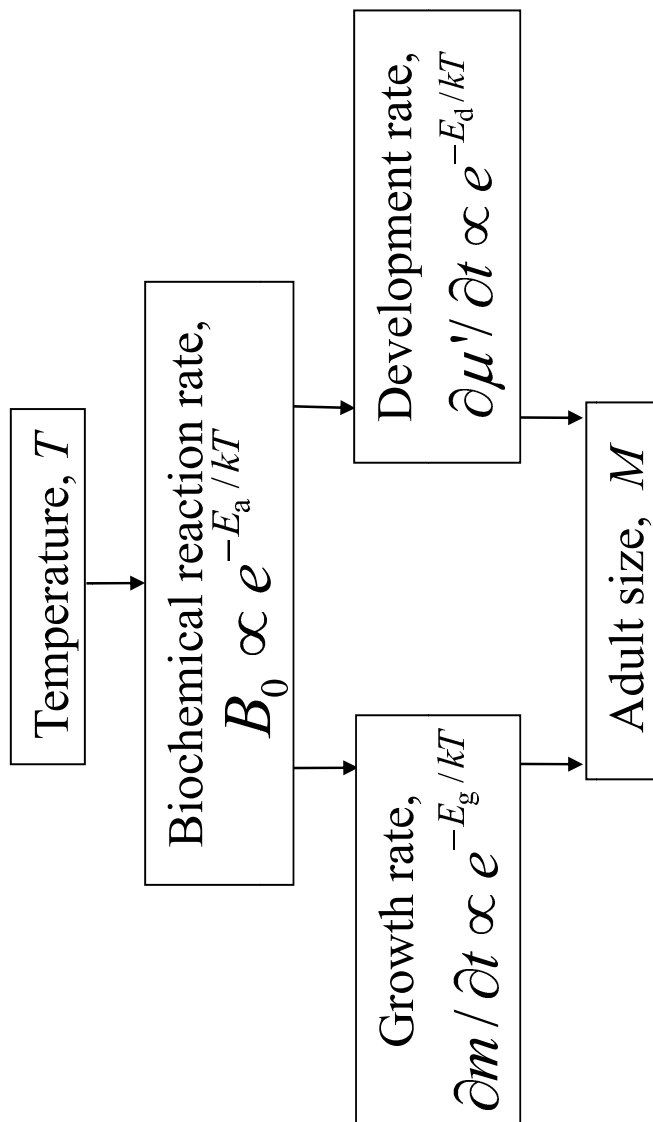
Figure 3.1: Flow chart showing effects of temperature on energy allocation during ontogenetic development. Metabolic rate, B, varies with body mass, m, and absolute temperature, T, as $B = B_0 m^{3/4}$, where B_0 is a temperature-dependent coefficient, $\propto e^{-E_a/kT}$, for a given species, E_a is the activation energy, and k is Boltzmann's constant. Other variables: t is time, E_g and E_d are the activation energies for biomass accumulation rate and development rate, respectively.

To incorporate effects of body size and temperature into Eq.3.1, we make two assumptions: 1) Throughout ontogeny, metabolic rate, B, scales with body mass as $B = B_0 m^{3/4}$, where B_0 is constant within and among individuals of the same species developing at the same temperature, but varies with temperature and species. The generality of $m^{3/4}$ scaling of metabolic rate has been questioned (but see [38, 43, 55]). It is straightforward to substitute a generic scaling exponent, ψ, or a different numerical value when there is compelling evidence for deviation from three-quarter-power scaling. 2) The temperature dependencies of the component processes can be characterized by Boltzmann relations as indicated above and below.

Rewriting Eq.3.2 to incorporate explicitly body mass dependence gives

$$B_0 m^{3/4} = \frac{B_0}{M^{1/4}} m + E_m \frac{\partial m}{\partial t}. \tag{3.4}$$

Additionally, $B_{maint} = B_m m$, where $B_m = B_0 M^{-1/4}$ is the mass-specific rate of energy expenditure for maintenance, M is the body mass at maturity, $B_{syn} = E_m \frac{\partial m}{\partial t}$, and E_m is the quantity of energy expended to synthesize a unit of biomass, assumed here to be independent of temperature. Dividing both sides of Eq.3.4 by $m^{3/4}$ gives

$$B_0 = (\frac{m}{M})^{1/4} B_0 + E_m \frac{1}{m^{3/4}} \frac{\partial m}{\partial t}. \tag{3.5}$$

Now incorporating the temperature dependencies in Fig.3.1 and $M \propto e^{-(E_g - E_d)/kT}$, Eq.3.5 gives

$$C_1 e^{-E_a/kT} = \mu^{1/4} C_1 e^{-E_a/kT} + E_m \mu^{-3/4} C_2 e^{3(E_g - E_d)/4kT} C_3 e^{-E_g/kT} \tag{3.6}$$

where $\mu \equiv \frac{m}{M}$ is the relative body mass at any time, t, which is temperature-independent; E_a, E_g, and E_d are the activation energies for the rates of overall metabolism, growth, and development, respectively; and C_1, C_2, and C_3, are temperature-independent coefficients. Therefore, Eq.3.6 gives the relationship among the temperature dependencies of rates of metabolism, growth, and development

$$E_a - \frac{1}{4} E_g - \frac{3}{4} E_d = 0. \tag{3.7}$$

Chapter 3. A general model for ectotherm growth and development

The model predicts the trajectories of biomass accumulation rate and development rate over ontogeny from hatching to maturity. Rewriting Eq.3.4 by normalizing with respect to M, the body mass at maturity, gives a normalized biomass accumulation rate (see *SI*)

$$\frac{E_m}{C_1 M^{3/4}} \frac{\partial m}{\partial t} = e^{-E_a/kT}(\mu^{3/4} - \mu), \tag{3.8}$$

where C_1 is a temperature-independent coefficient. By normalizing with respect to the effect of temperature, $e^{-E_a/kT}$, in Eq.3.8 predicts the biomass accumulation rate normalized to both temperature and body mass at maturity

$$\frac{E_m}{C_1 M^{3/4} e^{-E_a/kT}} \frac{\partial m}{\partial t} = \mu^{3/4} - \mu. \tag{3.9}$$

This model makes two additional predictions for the energy budgets of ectotherms during ontogeny. First, introducing effects of temperature into Eq.3.2 gives (see *SI*)

$$\frac{B_{syn}}{B_{maint}} = (\frac{1}{\mu})^{1/4} - 1. \tag{3.10}$$

This predicts that the same fraction of metabolic energy is allocated to maintenance and synthesis at any given relative body mass regardless of temperature and taxon. Second, integrating Eq.3.1 with respect to time gives Eq.3.3, and introducing effects of temperature gives

$$Q_{tot} = \int_0^{t_m} (B_{maint} + B_{syn} + S)\partial t = \{E_c - 4E_m[\frac{\gamma_m^3}{3} + \frac{\gamma_m^2}{2} + \gamma_m + \ln(1 - \gamma_m)]\} \tag{3.11}$$

where t_m is the time to reach some near-asymptotic adult size, $m_{adult} = (1 - \varepsilon)M$ with $\varepsilon \ll 1$ and $\gamma_m = (\frac{m_{adult}}{M})^{1/4}$ [11]. In Eq.3.11 E_c, E_m and γ_m are all independent of temperature, so the total quantity of energy consumed, Q_{tot}, during ontogeny varies predictably with temperature as $Q_{tot} \propto M \propto e^{-(E_g - E_d)/kT}$. The model predicts that TSR ectotherms should consume less energy and reverse-TSR ectotherms should consume more energy when developing at higher temperatures.

3.4 Empirical Evaluation

Experimental data for a variety of ectotherm taxa, such as nematodes, molluscs, crustaceans, insects, and amphibians (Table 3.1), support the model. The activation energy for metabolic rate, E_a, for each organism has been calculated based on Eq.3.7. The average of those calculated E_a is 0.62 ± 0.03eV. This average and most of the individual values are close to the predicted 0.65eV, but a few outliers in Table 3.1 and earlier studies [16, 78] encompass a total range from 0.15eV to 1.2eV. Equation 3.9 predicts that all organisms should exhibit identical "canonical" curves for normalized rates of biomass accumulation over ontogeny. Data for several organisms generally support this prediction. As predicted, the absolute rates, normalized only with respect to mass, increase with increasing temperature (Fig.3.2A), but when normalized with respect to both mass and temperature, these curves all converge on the same shape with a peak at $\mu \approx 0.3$ (Fig.3.2B). So, the highest rate of growth or biomass accumulation occurs at about 1/3 of adult mass, independent of temperature. This peak occurs at the same fraction of adult mass in ectotherms as it does in endotherms [43].

3.5 Discussions

It is well documented that in ectotherms rates of both somatic growth and ontogenetic development increase approximately exponentially with increasing temperature, so time to maturity is shorter at higher temperatures. Whether body size at maturity is smaller or larger, however, depends on the difference in the temperature dependence between these two rates: the TSR occurs when development rate is more temperature-sensitive, the reverse-TSR when biomass accumulation rate is more sensitive.

Table 3.1: Effects of temperature on rate of development, biomass accumulation, and metabolism and on body size at maturity. Experimental studies conducted at different temperatures provide data on development rate (E_d in $\frac{\partial \mu'}{\partial t} \propto e^{-E_d/kT}$) and body size ($E_g - E_d$ in $M \propto e^{-(E_g-E_d)/kT}$) of different species. Effects of temperature on growth rate (E_g in $\frac{\partial m}{\partial t} \propto e^{-E_g/kT}$) and metabolic rate ($E_a$ in $B \propto e^{-E_a/kT}$) are calculated by $E_a - \frac{1}{4}E_g - \frac{3}{4}E_d = 0$ (Eq.3.7) from the model (Original data in *SI*). The parameters are development rate t_{dev}^{-1}, adult size M, biomass accumulation rate $\frac{\partial m}{\partial t}$, and metabolic rate B

Taxa	Species	Sex	Development rate, t_{dev}^{-1} E_d (eV) empirical	Adult size, M $E_g - E_d$ (eV) empirical	Biomass accumulation rate, $\partial m/\partial t$ E_g (eV) calculated	Metabolic rate, B E_a (eV) calculated
Nematode	*Caenorhabditis elegans*	NA	0.61	-0.14	0.47	0.58
Mollusc	*Crepidula plana*	NA	0.45	-0.16	0.29	0.41
Crustacean	*Acanthocyclops*	F	0.66	-0.13	0.53	0.63
	viridis	M	0.73	-0.14	0.60	0.69
	Macrocyclops	F	0.78	-0.20	0.57	0.73

Continued on Next Page...

Table 3.1 – Continued

Taxa	Species	Sex	t_{dev}^{-1} E_d (eV) empirical	M $E_g - E_d$ (eV) empirical	$\partial m/\partial t$ E_g (eV) calculated	B E_a (eV) calculated
	albidus	M	0.77	-0.13	0.64	0.74
	Acanthocyclops	F	0.83	-0.14	0.69	0.80
	vernalis	M	0.86	-0.24	0.62	0.80
Insect	Drosophila	M	0.63	-0.26	0.37	0.57
	willistoni	F	0.63	-0.15	0.48	0.59
	Drosophila	M	0.70	-0.12	0.58	0.67
	equinoxialis	F	0.70	-0.16	0.54	0.66
	Drosophila	M	0.62	-0.3	0.32	0.55
	pseudoobscura	F	0.62	-0.3	0.32	0.55
	Drosophila	M	0.59	-0.19	0.4	0.54
	persimilis	F	0.59	-0.17	0.42	0.55
	Drosophila melanogaster	NA	0.81	-0.17	0.64	0.77
	Chaoborus	NA	0.53	-0.46	0.07	0.42

Continued on Next Page...

Table 3.1 – Continued

Taxa	Species	Sex	t_{dev}^{-1} E_d (eV) empirical	M $E_g - E_d$ (eV) empirical	$\partial m/\partial t$ E_g (eV) calculated	B E_a (eV) calculated
	flavicans					
	Lucilia illustris	NA	0.63	0.05	0.68	0.64
	Chorthippus brunneus	F	0.73	0.41	1.15	0.84
	Omocestus viridulus	F	0.11	0.18	0.29	0.15
	Myrmeleotettix maculatus	F	0.43	0.31	0.75	0.51
	Stenobothrus lineatus	F	0.57	0.33	0.90	0.66
Amphibian	Rana sylvatica	NA	1	-0.86	0.14	0.79
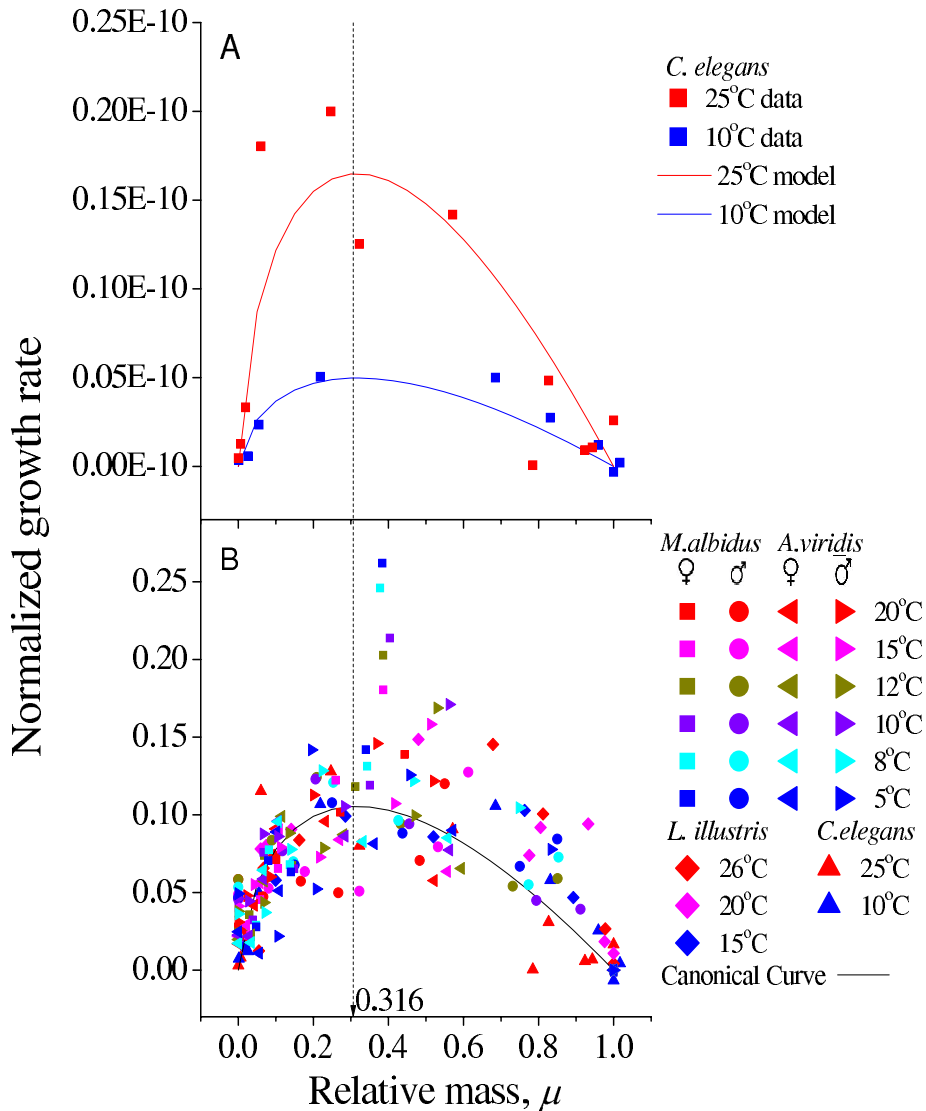
Figure 3.2: Different species of ectotherms developing at different temperatures follow the same canonical curve of biomass accumulation rate. (A) Normalized for differences in adult mass, rates of biomass accumulation are higher at higher temperatures, but the trajectories differ only in absolute rates (heights). (B) So, when also normalized with respect to temperature and mass, the rates for different species and temperatures all cluster closely around the theoretically predicted curve, which peaks at 31.6% of adult body mass. Species are *Macrocyclops albidus*, *Acanthocyclops viridis*, *Lucilia illustris*, and *Caenorhabditis elegans*. (Original data and calculations in *SI*)

The TSR and reverse-TSR are necessary consequences of differences in the temperature dependence of somatic growth rate and development rate. Many investigators have studied these processes (e.g., [17, 79–82]). It is now well documented that differences in size at maturity after developing at different temperatures can be due to differences in cell size, number of cells, or some combination of these. For example, *Caenorhabditis elegans*, other nematodes, rotifers, and some arthropods, have a determinate fixed number of cells at maturity, so variation in adult body size is due entirely to variation in cell size. In *Drosophila*, however, differences in adult body size after developing at different temperatures may be due primarily to differences in either cell size or cell number [83, 84].

This study appears to offer four important advances over previous theoretical and empirical treatments of the TSR. First, we present an analytical model that is both very simple and very general. It incorporates a minimum number of assumptions, parameters, and functions required to characterize the primary effect of temperature on the two critical processes: rate of biomass accumulation and rate of development. The parameters can all potentially be measured to evaluate the model, its assumptions, and its predictions empirically. Model predictions provide a quantitative baseline against which to compare data for different kinds of animals developing under different physiological and environmental conditions. The assumptions can be relaxed to generate more complicated models for animals where they may not apply. This level of simplicity and generality stands in contrast to studies using a Sharpe-Schoolfield model (see [82, 85]), which incorporates multiple parameters of enzyme kinetics that may be only indirectly relevant and are difficult to measure directly, and to studies on other aspects of development, such as hormonal regulation [80, 86, 87].

Second, our model easily accommodates cases where differences in adult body size after developing at different temperatures are due to any combination of variation

in cell size or cell number. In organisms with a fixed number of cells at maturity, such as *C. elegans*, variation in adult body size depends on the amount of somatic growth and hence the increase in cell size. This case can be analyzed quantitatively by modifying the model to define the relative developmental stage by relative number of cells rather than relative time.

Third, our model not only accounts for how temperature gives rise to both the TSR and reverse-TSR, it also predicts the effect of developmental temperature on three other important aspects of development. The first is the trajectory of biomass accumulation rate over ontogeny (Eqs.3.8 and 3.9; Fig.3.2). The model predicts that after normalizing for body mass at maturity, all ectotherms should exhibit quantitatively similar patterns of ontogenetic growth, with temperature affecting only the absolute growth rate. The second is the proportion of energy allocated to maintenance and biosynthesis at a given relative size is independent to temperature (Eq.3.10). The model predicts that organisms growing in different temperatures allocated the same proportion of its metabolic energy into maintenance and biosynthesis. The proportion only changes as the relative mass, μ, changes. The third novel prediction is how temperature affects the total quantity of energy used at each stage of development (Eq.3.11). We know of no other model that predicts these important unifying features of ontogeny. They are relevant to understanding effects of environmental temperature on the life history, ecology, and evolution of ectotherms. And again, when deviations from model predictions are observed empirically, these cases call attention to the importance of other factors left out of our deliberately very simple prediction.

Fourth, the model can be modified for the case of an embryo developing within an egg and fueled by energy reserves stored in yolk. In this case, the total quantity of energy available is fixed by egg size. The model predicts that when eggs of the same size are incubated at higher temperatures, a TSR ectotherm consumes less

energy during incubation and may hatch with unused yolk, whereas a reverse-TSR ectotherm uses more energy, consumes more yolk, and may hatch at a less developed stage. Actually, some TSR ectotherms appear to compensate by producing smaller eggs at higher temperatures [88, 89], supporting the prediction that they consume less total energy during development [90]. More complicated treatments may be required to incorporate other features of embryonic development, such as: i) cell size usually decreases over ontogeny with multiple cycles of cell division as a single-celled zygote develops into a multicellular hatchling; and ii) relative water content of the embryo may decrease and energy density of accumulated biomass may increase over ontogeny [91, 92].

It remains to explain why the majority of ectotherms follow the TSR, whereas only a minority exhibits the reverse-TSR. Several authors have proposed adaptive explanations (e.g., [93–103], and many other studies in the context of geographic variation in ectotherm body size in gradients of environmental temperature, especially in *Drosophila*). Our model is generally consistent with these hypotheses, but offers additional insights. Both growth rate and development rate vary approximately exponentially with temperature, and the magnitude of temperature dependence of each rate is subject to natural selection. In general, natural selection should tend to keep the temperature dependence of these rates very nearly equal, so that the developmental program buffers size at maturity against perturbations due to differences in temperature. However, Eq.3.7 shows that $E_g - E_d$ is very sensitive to E_a and E_d (e.g., $\triangle (E_g - E_d) = 4(\triangle E_a - \triangle E_d)$), and consequently body mass at maturity, M, is extremely sensitive to these temperature dependencies. Usually selection can be expected to minimize the time and the total energy consumed during ontogeny. Time can be minimized by behavioral temperature regulation, selecting higher temperatures for both incubation and post-hatching development. This tendency for "warmer to be better" [104] should translate into a TSR. Selection to incorporate a margin of safety so that embryos do not run out of yolk should also favor TSR.

A reverse-TSR should be expected only in rare cases when it is advantageous to develop at colder temperatures, such as to behaviorally select cold microclimates to avoid predators or to prolong development due to constraints of environmental seasonality [103]. The theory developed here should also apply to special cases, such as when temperature dependence of solubility and diffusion of oxygen in aqueous media limits egg size and development of aquatic organisms [105,106].

One interesting application of our theory is to organisms that have temperature-dependent sex determination, which occurs in many reptiles and amphibians, some fish, and at least one bird (e.g., [107–110]). Small differences in temperature during development should potentially affect not only the gender of the hatchling, but also the time of development and body size at hatching. It is known that warmer temperatures during development can produce either males or females, depending on taxon, for example, generally males in crocodilians and females in turtles. In the Australian brush turkey (*Alectura lathami*) higher temperatures during incubation of eggs result in proportionately more females with larger body mass at hatching [108], consistent with reverse-TSR. Temperature-induced sex-related differences in development time and body size at hatching should have potentially important consequences for subsequent life history and ecology.

The quantitative model developed here, and similar but more complicated analytical mathematical or computer simulation versions that could be developed for cases that do not meet the simplifying assumptions, provide a theoretical basis for assessing responses of ectothermic organisms to changes in environmental temperature regimes. The magnitude of recent anthropogenic global warming is already substantial and likely to increase for decades and perhaps centuries [111]. The impacts on ectothermic animals and their ecology will undoubtedly be profound. Many of these impacts can be understood in a general theoretical context that is based on the fundamental effect of temperature on metabolism, and the effects of metabolism on

many aspects of organism structure and function, population and ecosystem ecology, and biological evolution [67]. It will be impossible to conduct the detailed studies, on one species at a time, to predict effects of climate change on the abundance, distribution, and diversity of species. A practical alternative will be to start by developing general theory, like the model presented here, that is based on fundamental biological principles and can make testable quantitative predictions.

3.6   Acknowledgments

3.7   Supporting Information (*SI*)

3.7.1   Normalizing growth rate

Eq.3.4 could be rewritten as

$$B_0(\frac{m}{M})^{3/4} = B_0\frac{m}{M} + E_m\frac{1}{M^{3/4}}\frac{\partial m}{\partial t}, \tag{3.12}$$

where B_0 is constant within and among individuals of the same species developing at the same temperature, but varies with temperature and species [55]. Eq.3.12 gives an expression for growth rate $\frac{\partial m}{\partial t} = \frac{B_0 M^{3/4}}{E_m}(\mu^{3/4} - \mu)$, where $\mu \equiv \frac{m}{M}$, relative body size.

This can be expressed as $\frac{\partial m}{\partial t} = \frac{C_1 e^{-E_a/kT} M^{3/4}}{E_m}(\mu^{3/4} - \mu)$, which is called normalized growth rate.

The normalized growth rate predicts series growth curves for different temperatures (Figs.3.2 and 3.3).

3.7.2 Partition of energy allocation of maintenance and synthesis over ontogeny

Introducing temperature effects into Eq.3.2 gives,

$$B_{syn} = B_0 e^{-E_a/kT} m^{3/4} - \frac{B_0 e^{-E_a/kT}}{M(T)^{1/4}} m \tag{3.13}$$

$$B_{maint} = \frac{B_0 e^{-E_a/kT}}{M(T)^{1/4}} m \tag{3.14}$$

hence,

$$\frac{B_{syn}}{B_{maint}} = \frac{M^{1/4}}{m^{1/4}} - 1 = \frac{1}{\mu^{1/4}} - 1. \tag{3.15}$$

3.7.3 Calculation and original data for table 3.1

Because $M \propto e^{-(E_g - E_d)/kT}$, $t_{dev} \propto e^{-E_d/kT}$ and $E_a - \frac{1}{4}E_g - \frac{3}{4}E_d = 0$ (Eq.3.7), data in Table B.3 provide the estimated E_d, E_g, and E_a in Table 3.1.
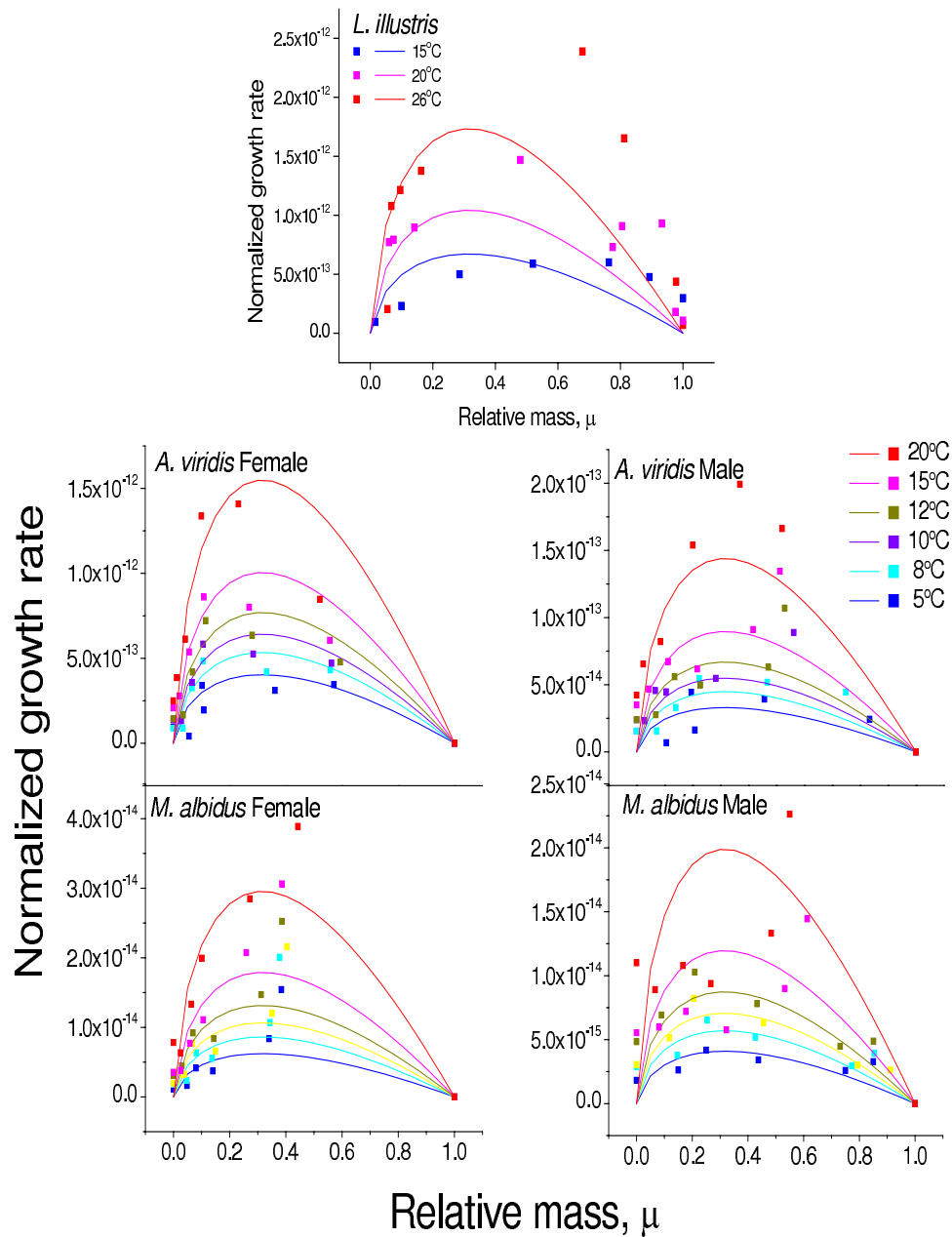
Figure 3.3: The illustration of temperature effects on growth rate $\left(\frac{\partial m}{\partial t} \propto e^{-E_g/kT}\right)$. According to OGM [11] and EOGM [43], growth rate peaks at 31.6% relative body size. Original data are available at Table B.1. Used parameters are available at Table B.2.

Chapter 4

A life history approach to the late Pleistocene megafaunal extinction

Collaborated with Eric L. Charnov and Felisa A. Smith

4.1 Abstract

A major criticism of the "overkill" theory for the late Pleistocene extinction of megafauna in the Americas has been the seeming implausibility of a relatively small number of humans selectively killing off millions of large-bodied mammals. Critics argue that early Paleoindian hunters had to be extremely selective to have produced the highly size-biased pattern unique to this event. Here, we develop an exploitation-extinction theory based on mammalian life history, which demonstrates the added mortality pressure of human harvest on populations need not be selective to produce a size-biased extinction. Moreover, our model indicates variation in the adult natural instantaneous mortality rate and/or the maximum recruitment compensation at any body mass are main components determining the shape of the extinction

probability curve. Our theory successfully predicts the shapes of the extinction probability curves for the late Pleistocene extinction in the Americas, although results are slightly different for North and South America taken individually. While we can recapture the pattern without invoking size-dependence for North America, a slight positive size-bias hunting is required for South America. This may reflect the dynamics of the human migration across the Americas. Early Paleoindian hunters may have had a higher encounter rate with megaherbivores in South America because of the tighter geographical configuration of the continent, or perhaps they began targeting cost-efficient prey once it was clear they were naïve to human hunting.

keywords: population dynamics — probability distribution — logistic regression — late Quaternary — mammalian extinctions — human harvest — North and South America — mortality rates

4.2 Introduction

The Americas of 13,400 years ago were vastly different than today. Numerous species of large-bodied mammalian herbivores such as mammoth and mastodons, horses and their allies, camelids, oxen and bison, glyptodonts, giant sloths and other taxa were widespread across both continents [19–22]. These megaherbivores were preyed upon by large-bodied carnivores such as sabertooth cats, short-faced bears and the dire wolf. Within a relatively short time, however, some 80% of these large-bodied species were extinct, including all mammals over 600 kg [23]. Determining the mechanism underlying the geological abrupt [24] late Pleistocene extinction of megafauna has been difficult and fraught with controversy because it overlaps in timing with both the initial arrival of humans into the Americas and a major climatic transition. Moreover, there are two major unique features of the extinction that must be explained. First is the rapidity with which it occurred. More than 150 species were extirpated

in the Americas within 1000 to 1500 years [24, 112]; recent work proposes an even tighter window, with an estimate of 400 years for North America [112]. The second is the strikingly size selective nature [19, 23, 113], which is completely unprecedented in the evolutionary history of Cenozoic mammals [20, 113]. These salient features lead to the development of the "blitzkrieg" or "overkill" theory [19], which attributes the extinction to overharvest by early Paleoindian hunter-gatherer population. This theory has been controversial, but variants have slowly gained traction as the most parsimous explanation of the event (e.g., [22]); indeed, even formerly staunch advocates of climate change as the driver have recently concluded "human impacts probably figured prominently in the extinctions" [25]. However, a continuing criticism of the "overkill" theory for the late Pleistocene extinction has been the seeming implausibility of a relatively small number of humans killing off millions of animals, and the lack of direct archaeological evidence that early Paleoindian hunters preyed on all large-bodied mammal species that went extinct (e.g., [26, 27], but see [28, 29]). Moreover, opponents have argued that early Paleoindian hunters would have had to be extremely selective to have produced the highly size biased extinction characteristic of the extinction, and that the economics of foraging theory suggest that such a size-specialized diet would have been energetically unfeasible [30]. Despite modeling efforts by Alroy [20], which suggested that a size bias in exploitation rate was not needed to explain the body mass bias of Pleistocene extinction of mammals, such an argument has not yet been laid to rest [114, 115].

Here, we demonstrate theoretically that a large enough extra mortality caused by human harvest, even if not size selective, was sufficient to cause a size-biased extinction. Our results clearly indicate how animal populations may be driven to extinction by human exploitation even in the absence of other forms of habitat degradation. This simply requires that the added harvest mortality overpowers the increased density dependent recruitment that is normally present as population size approaches zero. Of course harvest mortality could fall more heavily on large-bodied species,

but invoking it is unnecessary in order to explain the resulting size bias. Our simple and quite transparent theory allows us to account for the gradual rise in extinction risk with body mass [23,31] as well as to predict the special characteristics of species at any fixed body mass that are relatively more or less at risk of extinction.

4.3 Model Development

The model is based on basic population dynamics. A stable animal population has birth rates equal to death rates or, for continuous time, instantaneous mortality rates equal to recruitment rates: $\theta = \zeta_\alpha \cdot b$, where θ represents the adult instantaneous mortality rate, ζ_α the probability of surviving to reproductive age α, and b the number of daughters produced per mother per unit time. For simplicity, we assume daughters produced per mother per unit time and adult mortality rate are independent of adult age. However, considerable evidence [116–120] supports the operation of a density dependent response, so that if population declines, recruitment rate increases; which is reflected as $\beta \cdot \zeta_\alpha \cdot b$, where β, the recruitment response, is ≥ 1. The population grows since the recruitment rate now exceeds the adult mortality rate that is unaffected by population size. The reciprocal of adult mortality rate is the average adult life span. Thus, the average number of daughters surviving to age α produced over the adult life span, or the net reproductive rate, R_0, can be presented as $\frac{\beta \cdot \zeta_\alpha \cdot b}{\theta}$. For stable and unexploited populations $\beta = 1$ and hence $R_0 = 1$. When the population is exploited, β increases as the population declines until the maximum recruitment response (β_{max}) is reached.

To derive the extinction threshold, we start with a stable population and impose an additional source of instantaneous mortality due to human harvest (F). If the additional mortality is invariant with respect to age class, the overall adult mortality rate is simply increased to $\theta + F$, while survival to adult at age α is now

decreased by a factor of $e^{-F \cdot \alpha}$ (*SI text*). Since the net reproductive rate in the newly-exploited population decreases to $\frac{\zeta_\alpha \cdot b \cdot e^{-F \cdot \alpha}}{\theta + F}$, which is less than one, the recruitment rate increases, so that we obtain $\frac{\beta \cdot \zeta_\alpha \cdot b \cdot e^{-F \cdot \alpha}}{\theta + F}$. As the population approaches zero, the recruitment response approaches β_{max}, which gives the maximum net reproductive rate $R_{0max} = \frac{\beta_{max} \cdot \zeta_\alpha \cdot b \cdot e^{-F \cdot \alpha}}{\theta + F}$. If R_{0max} is less than one, the population will go extinct. Thus, we obtain (*SI text*):

$$\frac{e^{-\frac{F}{\theta} \cdot \alpha \theta}}{1 + \frac{F}{\theta}} < \frac{1}{\beta_{max}}. \tag{4.1}$$

Here, F/θ can be understood as the required recruitment compensation to avoid extinction for a population. The maximum recruitment compensation (C) of a given population can be calculated as:

$$\frac{e^{-C \cdot \alpha \theta}}{1 + C} = \frac{1}{\beta_{max}}. \tag{4.2}$$

If the maximum recruitment compensation is smaller than the required recruitment compensation to avoid extinction for a population (e.g., if $C < F/\theta$), the population is doomed to extinction. Clearly, species with the same $\alpha \cdot \theta$ and β_{max} values have the same maximum recruitment compensation.

We can determine the maximum recruitment compensation for mammals fairly readily. The average value of $\alpha \cdot \theta$ for mammals is close to 0.6 and independent of adult body mass [121]. Moreover, the maximum recruitment response, β_{max}, is about $2 \sim 3$ and is also independent of body mass [117–120]. Although Eq.4.2 has no analytical solution, it is well approximated as $C \approx \kappa \cdot \ln \beta_{max}$ for $\beta_{max} < 3.5$ with $\kappa \propto (\alpha \cdot \theta)^{-0.42}$ (for $\alpha \cdot \theta = 0.6$, $\kappa = 0.71$) (Fig.4.1). This approximation is used below for calculating the maximum recruitment compensation.
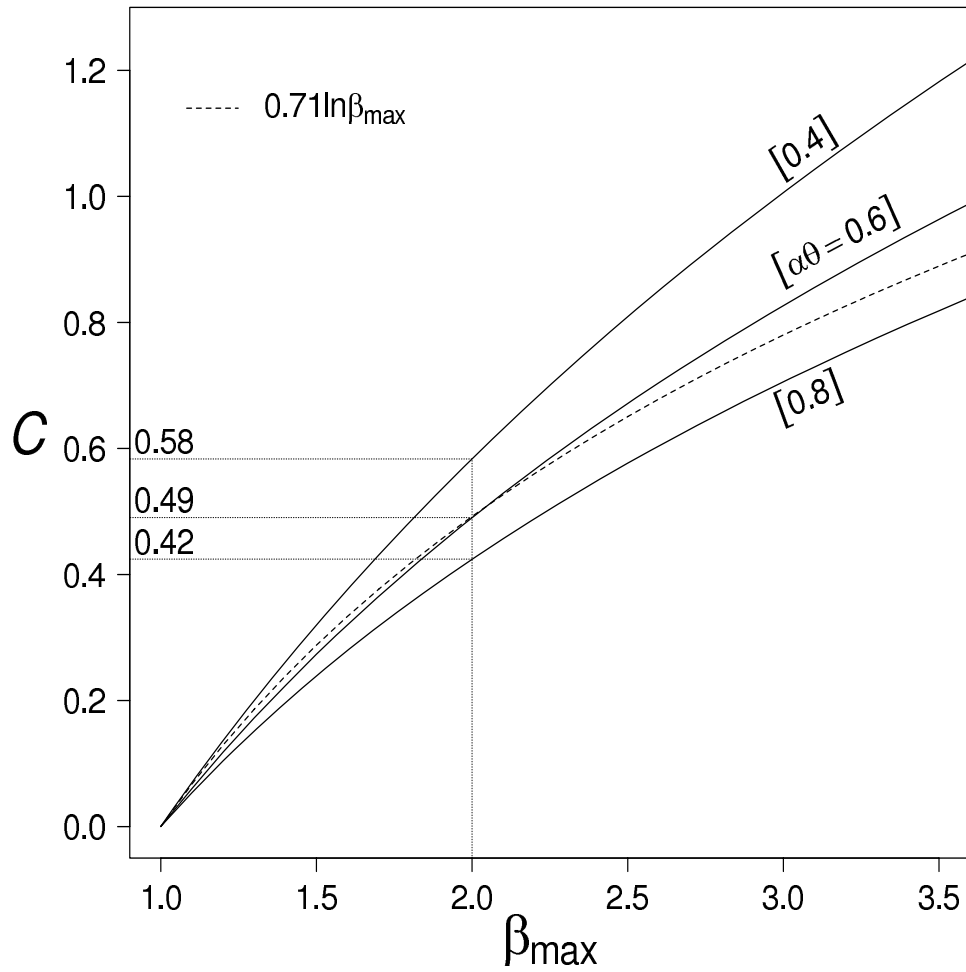
Figure 4.1: The numerical solution of the maximum recruitment compensation, C. The maximum recruitment compensation for various values of $\alpha \cdot \theta$ and β_{max}. At the average $\alpha \cdot \theta$ of 0.60, $C = 0.49$ if $\beta_{max} = 2$. C is well approximated by $C \approx \kappa \cdot \ln \beta_{max}$, where κ is an inverse function of $\alpha \cdot \theta$.

Implicit in the simple version of our model are the following assumptions. First, all species share the same maximum recruitment compensation and suffer the same human harvest mortality rate. Second, the scaling relationship of adult natural mortality rate, $\theta = IM^{-0.25}$ ([122]; where I is a mortality scaling coefficient), was the same in the Pleistocene as today. Third, across species of any given mass there is variability in adult natural mortality; this is confirmed by empirical data ([121], Fig.4.5A). The influence of these assumptions is illustrated in Fig.4.2. Since the population is doomed to extinction if $\theta < F/C$, at small body mass M_1 all species' adult mortality rates are above the deterministic extinction threshold (F/C) so none go extinct. As body mass increases, a progressively larger proportion of species are at risk as their adult mortality rates approach the threshold (e.g., $\theta < F/C$). At the largest body mass M_4, all species go extinct because their adult mortality rates are all below the threshold. Note that because the mortality rate scales as $\theta = IM^{-0.25}$, the average value of $\ln\theta$ decreases as body mass increases. Thus, the probability of extinction at any fixed body mass depends on both the mortality rate and the variation around that mortality rate. This variation, which is derived from the influence of life history or ecological differences among species (depicted as a series of values about each M in Fig.4.2), gives rise to a gradually rising extinction probability curve. Of course, the probability of extinction likely depends on more than simply variation around $\theta = IM^{-0.25}$. Variability in the maximum recruitment compensation (C), and/or the harvest mortality rate (F) also contribute to extinction probability increasing with body mass, as would any size selection harvest mortality rate. However, the principle would be the same: the proportion of species crossing the threshold gives the proportion going extinct at that body mass. Noticeably, the scaling relationship of $\theta \propto M^{-0.25}$ is crucial. It is the one factor changing consistently with body mass and it drives extinction probability from 0 to 1. A qualitative version of this argument is presented in Brooks and Bowman [123].
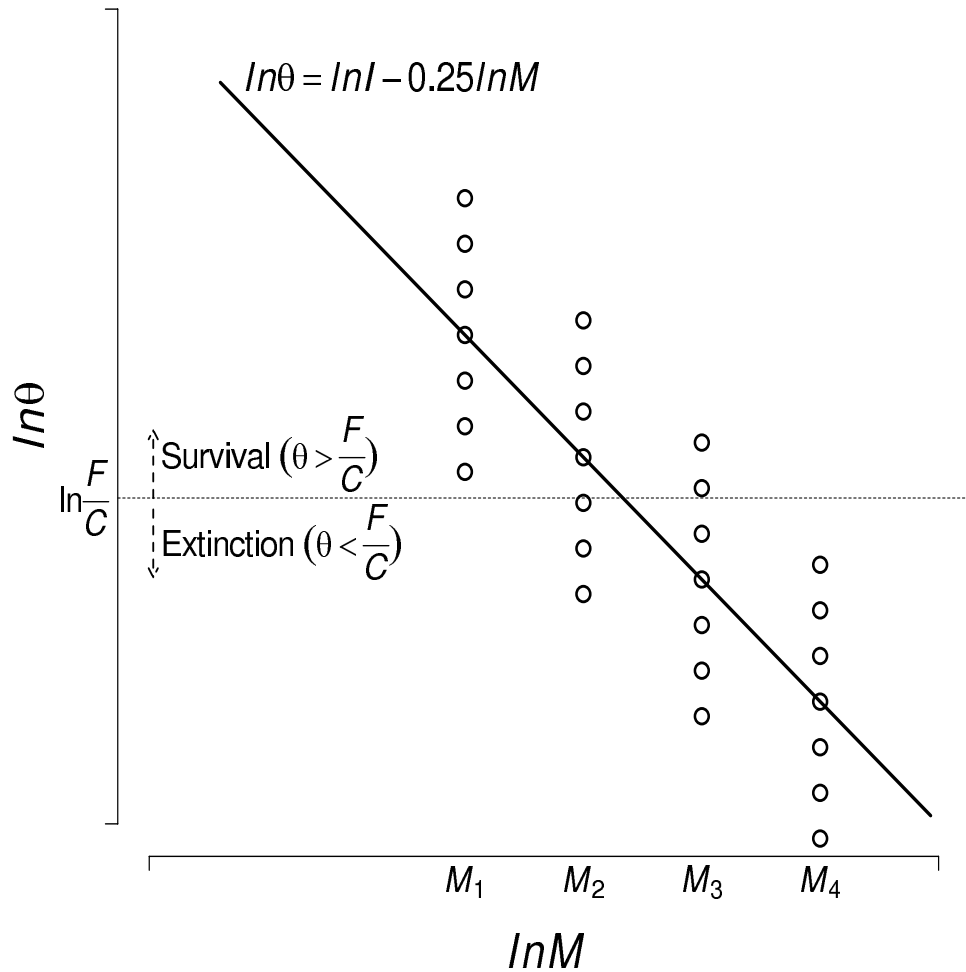
Figure 4.2: The extinction threshold combined with the adult mortality rate, θ, scaling generates size-biased extinction. The extinction threshold is the ratio of harvest mortality rate, F, and the maximum recruitment compensation, C, (go extinct if $F/C > \theta$). The variation in θ among species at any fixed body mass, M, means that the extinction probability will rise gradually with $\ln M$. At size M_1 no species crosses the threshold (F/C) and none go extinct; at size M_4 all go extinct. Three of seven go extinct at M_2, five of seven at M_3, and so forth. The θ scaling derives extinction probability from 0 to 1 with increasing M. The variation around the θ scaling turns a deterministic threshold into a gradually rising extinction probability curve.

A more comprehensive model can be derived by considering some of the important sources of variation in the threshold rule ($F/\theta > C$).

Assume a harvest mortality rate $F = I_1 \cdot M^\delta$, where δ is the body mass bias of harvest and I_1 is a harvest coefficient. When $\delta = 0$, there is no bias to the harvest; as $\delta > 0$ there is increasing preference for larger-bodied animals. Recall that $\theta = IM^{-0.25}$ and $C \approx \kappa \cdot \ln \beta_{max}$, thus the threshold rule ($F/\theta > C$) can be rewritten as

$$\ln M > \frac{\ln I + \ln \kappa + \ln (\ln \beta_{max}) - \ln I_1}{0.25 + \delta}, \tag{4.3}$$

where the extinction index, which is the right side of the inequality, is defined as

$$x \equiv \frac{\ln I + \ln \kappa + \ln (\ln \beta_{max}) - \ln I_1}{0.25 + \delta} \tag{4.4}$$

and is independent of body mass. The extinction index of each species is determined by I, κ, or β_{max}, and thus can be characterized by a probability distribution curve (i.e., $g(x)$ in Fig.4.3), which is also independent of body mass. For example, given a body mass of M_1, any species of this size with an extinction index above $\ln M_1$ will survive; those below it will go extinct. The overall extinction probability for species with body mass M_1 is a cumulative probability function of $g(x)$ from $-\infty$ to $\ln M_1$, such as:

$$P_{TH}(M_1) = \int_{-\infty}^{\ln M_1} g(x)dx \tag{4.5}$$

Thus, Eq.4.5 provides the gradually raised extinction probability curve. Note, our extinction rule (e.g., inequalities 4.1 and 4.3) is a deterministic threshold when parameters are constant. If species vary in parameter values, we obtain an extinction probability curve that gradually increases with body mass.
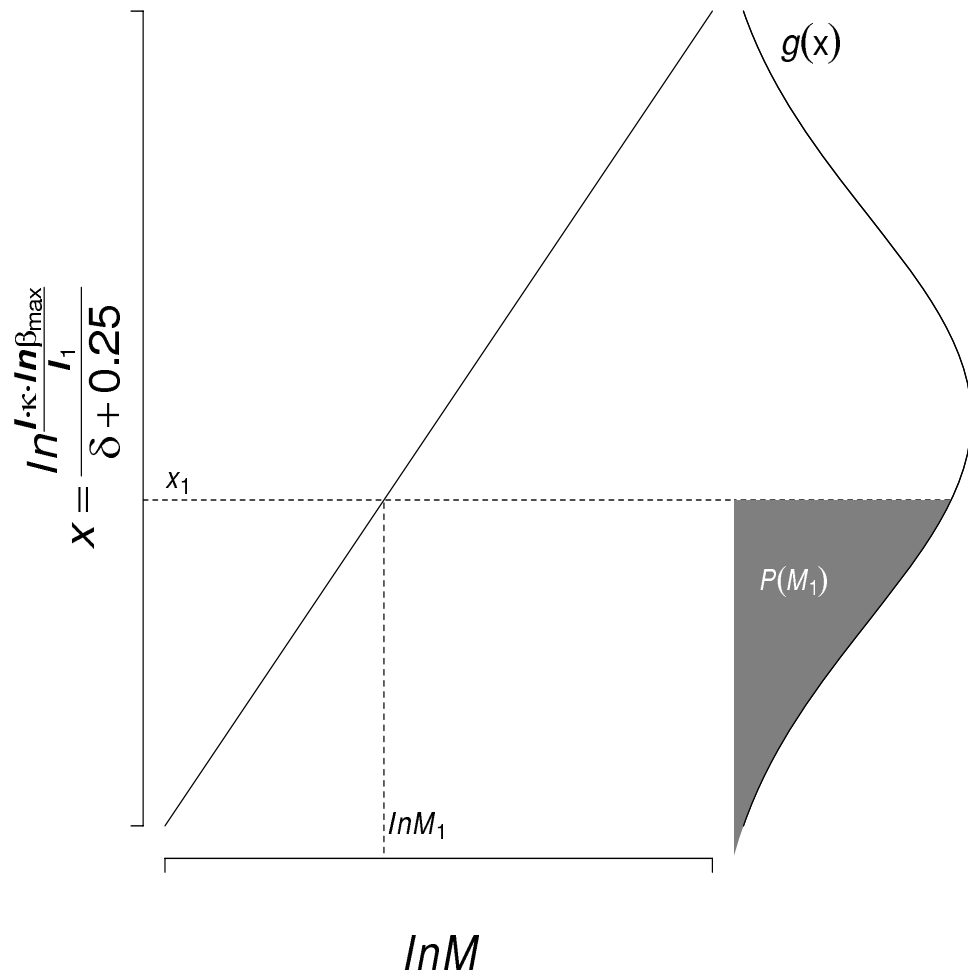
Figure 4.3: The probability of extinction at a given body mass. At any body mass (M_1), only some species' extinction indices may cross the extinction threshold ($\ln M_1$) if species at that size differ somewhat in θ, $\alpha \cdot \theta$, and/or β_{max}. The variable x aggregates I, κ, and β_{max} to produce a probability distribution $g(x)$. The area under $g(x)$ up to $x_1 = \ln M_1$ gives the proportion of species at M_1 that have indices smaller than the extinction threshold ($\ln M_1$), and thus go extinct. $P(M_1)$ is thus the probability of extinction at M_1.

4.4 Results

Our model suggests variation in the adult instantaneous mortality rate and/or the maximum recruitment compensation at any body mass is the main factor contributing to the shape of the extinction probability curve. The shape of the extinction probability curves for the late Pleistocene extinction in the Americas is successfully predicted by our model, although results differ somewhat for North and South America (Table 4.1 and Fig.4.4).

4.4.1 Estimation of Harvest Mortality Rate for a Mid-Size Mammal

We estimate the extinction probability curves for North and South America, and for the Americas together using logistic regression on a database of late Quaternary mammals [124]. Our analysis suggests that mammals of ~ 60kg had a 50% chance of extinction during the terminal Pleistocene (Fig.4.4). Previous work has suggested that in a stable population the adult mortality rate of 60kg mammal is about $\theta = 0.25$ yr^{-1} [121]. When $\beta_{max} = 2$ and $\alpha \cdot \theta = 0.6$, the maximum recruitment compensation (C) can be computed as 0.49 (Fig.4.1). Using these values, the human harvest mortality rate for a 60kg mammal should be $F|_{M=60} = 0.49 \times 0.25 = 0.12$ yr^{-1}.

4.4.2 Estimation of the Probability Distribution of the Extinction Threshold, $g(x)$

To estimate components of the $g(x)$ curve, we use data from Purvis and Harvey [121] on mortality rates and age of first breeding to generate a probability distribution of the variation in mortality rate and $\ln(\alpha \cdot \theta)$ (*SI text*). The extinction threshold

distribution is normal, with a standard deviation of $\sim$0.54. For the more realistic situation, allowing to vary β_{max} only slightly changes the standard deviation ($SD = 0.60$), but has a larger influence on the slope. Compare the general form of the slope $\frac{\pi(0.25+\delta)}{0.54\sqrt{3}}$ with fixed β_{max} versus $\frac{\pi(0.25+\delta)}{0.60\sqrt{3}}$ with varying β_{max} (see *Calculating the distribution of x* in Method and Eq.4.11).

4.4.3 Empirical Test of the Model

We use our theory to explore quantitatively the terminal Pleistocene extinction of large-bodied mammals in North and South America (see *Calibrating the Extinction Probability Curve, P Curve* in Methods). The predictions from our model are in good agreement with the empirical data (Fig.4.4). The predicted slope without invoking any size-selectivity (e.g., $\delta = 0$) is 0.76, well within the 95% confidence intervals for the empirical data from both the combined continents (Fig.4.4A; Table 4.1) and North America alone (Fig.4.4B). However, our predicted slope lies outside the 95% confidence intervals for South America unless we set $\delta = 0.15$. This implies some small degree of size-biased hunting is required to recover the actual pattern from the model (Table 4.1; Fig.4.4C).

Table 4.1: Parameters from data and the model.

	Slope for logistic regression	Standard deviation of $g(x)$ or P curve
Data (NA and SA, $n = 1323$)	0.85 (95%CI: 0.73~0.97)	2.13 (95%CI: 1.87~2.47)
Data (NA, $n = 572$)	0.66 (95%CI: 0.54~0.79)	2.73 (95%CI: 2.29~3.37)
Data (SA, $n = 775$)	1.23 (95%CI: 0.95~1.51)	1.47 (95%CI: 1.20~1.90)
Model ($\delta = 0$)	0.76	2.38 ($= 0.60/(\delta + 0.25)$)
Model ($\delta = 0.15$)	1.22	1.45 ($= 0.60/(\delta + 0.25)$)
Model ($\beta_{max} = 2$ and $\delta = 0$)	0.85	2.14 ($= 0.54/(\delta + 0.25)$)

*There are 24 species shared by both North America (NA) and South America (SA). n is the sample size.
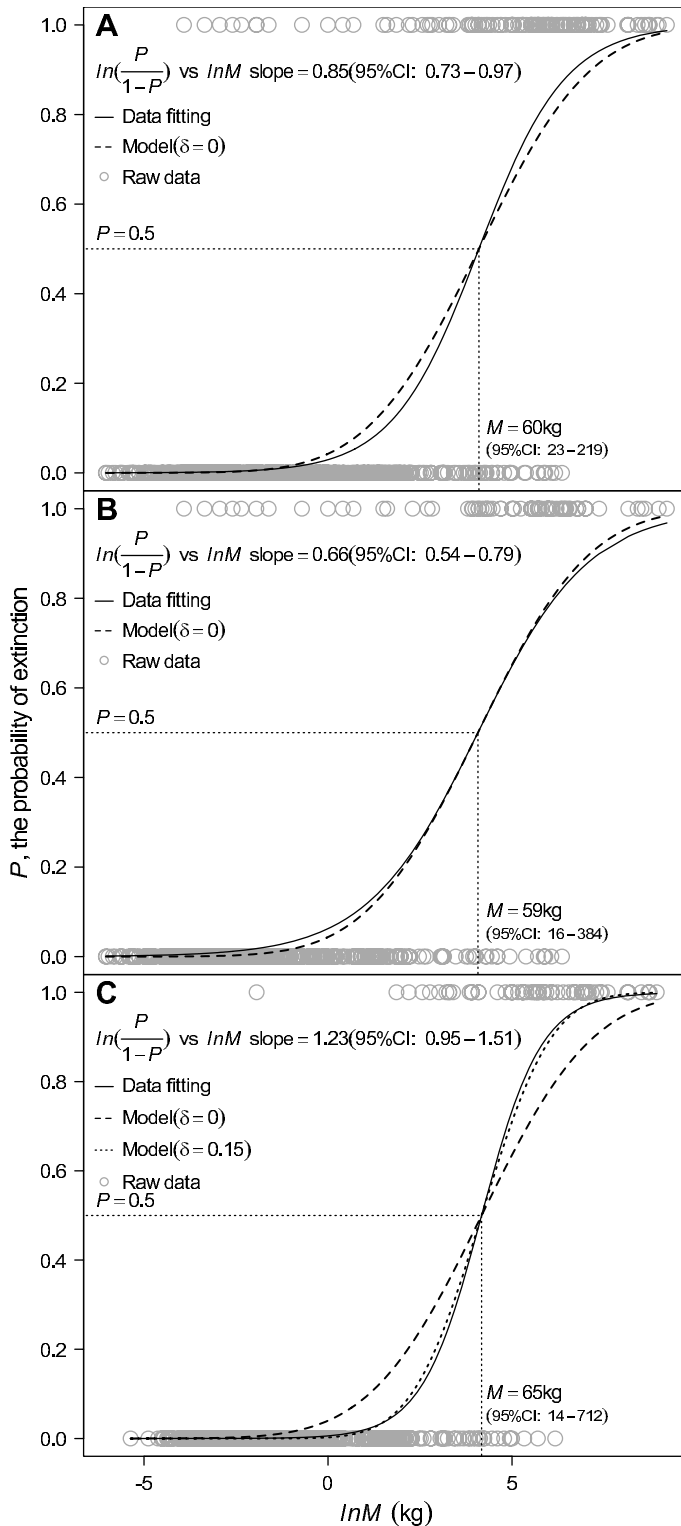
Figure 4.4: Extinction probability (P) versus $\ln M$ for Pleistocene mammals. Data (late Quaternary mammal database MOM (v 3.6) from Smith et al. [124]) are fitted by logistic regression using the statistical program R [125]. **(A)** In both Americas, slope of fitted extinction probability curve is 0.85. Our theory matches this distribution without size-dependent harvest mortality, F, ($\delta = 0$). **(B)** In North America, fitted slope $= 0.66$ and our theory matches this distribution with no size-dependence ($\delta = 0$). **(C)** In South America, fitted slope $= 1.23$ and size-dependence ($\delta = 0.15$) is required for the theory to match. See text and Table 1 for further discussion.

Regardless of the data employed, some variation in β_{max} seems necessary. Without the variation in β_{max}, the predicted slope (0.85) is larger than the estimated slope for NA alone (Table 4.1), which implies that humans preferentially hunted small mammals over larger ones, an unlikely situation. None of these quantitative results of $g(x)$ would alter if β_{max} were centered at 3, since the actual value of β_{max} is not used in the calculation. Of course, this all assumes that it is appropriate to use demographic data from living mammals (Fig.4.5).

4.5 Discussion

Our theory quantitatively illustrates that the additional but not size-selective mortality imposed by human harvest was sufficient to have resulted in the strongly size biased extinction found in the Americas, if we assume $F \approx 0.12$ for a ~ 60kg mammal. It is not necessary to invoke size bias by early Paleoindian hunters to have produced the highly size-biased pattern unique to this event. Rather, it simply requires that the added harvest mortality overpower the increased recruitment that is normally present as population size approaches zero. Our model almost perfectly recapitulates the empirical data (Fig.4.4).

Fishery scientists have studied overfishing, theoretically and empirically, for nearly half a century [116,126–131]. Here we have built upon, and extended these deterministic extinction ideas to a mammal-like life history. However, unlike fishery science, our estimation of the instantaneous harvest mortality rate $F = 0.12$ yr^{-1} for 60 kg mammals in the Pleistocene is based on indirect evidence. To directly calculate the instantaneous harvest mortality rate would require knowledge of both the early Paleoindian human population size or density and empirical evidence of exploitation efficiency (refered to in fisheries as the catchability coefficient, e.g., [130,131]). These are unlikely to ever be quantified precisely.

Because most scientists view the late Quaternary extinction in the New World as part of a single event (e.g., [19, 20, 113, 132]), we combine data for both continents in our analyses. When we examine the continents independently, we find some intriguing differences. While results for North America are indistinguishable from the results as a whole (Fig.4.4), South America is quantitatively different (Table 4.1). Not only is the fitted logistic slope nearly twice as steep as that for North America (1.23 versus 0.66; Table 4.1), but our model output lies outside the 95% confidence interval for the logistic regression. Indeed, to generate a theoretical curve consistent with the empirically derived one in South America required us to invoke some size bias for human harvest mortality (e.g., we set $\delta = 0.15$). This raises some interesting questions. Did early Paleoindian hunters "learn" to prefer large-bodied prey by the time they reached South America? While they may have hunted indiscriminately upon first reaching the New World, perhaps the naïve nature of the prey they encountered allowed them to begin concentrating on large-bodied, more cost-effective prey as they migrated southward. Alternatively, perhaps the difference in openness of habitats altered the susceptibility of prey in South America. It is also true that data for the late Quaternary of South America are less robust because of taphonomic and other issues [124].

Sensitivity analyses suggest that the adult mortality scaling relationship is the most important component influencing the magnitude of slope of our model. Although variation in all components of the model potentially influence the rate of change of the slope of the extinction probability curve, only adult mortality ($\theta = IM^{-0.25}$) determines the sign. The adult mortality scaling relationship is also important in terms of determining variation in the probability distribution of the extinction threshold, $g(x)$. Note that reduced variation about $g(x)$ implies that the extinction probability rises sharply with body mass; larger variation implies a slower rise in extinction probability with body mass. We have not implicitly included variation in human harvest (e.g., in I_1) because we have no *a priori* basis for characterizing

69

this. However, variation in the human harvest rate will increase the overall variation in $g(x)$, thus reducing the rate of change in the slope of the predicted extinction probability curve (Table 4.1).

Potentially our theory could be modified to reflect mortality due to other natural or human-mediated sources where a single added mortality pressure is imposed on the population. To adopt this model to a mass extinction where substantial environmental perturbations occur would require modification of many of the life history scaling relationships. However, it is straight forward to examine targeted human harvest of particular age stages. Currently, our theory (inequalities 4.1 and 4.3) assumes hunters harvest all age groups from independent juveniles to adults, but we could modify this to target only adults as is commonly done in conservational fisheries. Such a modification on Eq.4.2 gives an analytic solution for maximum recruitment compensation as simple as $C = \beta_{max} - 1$, which is independent of $\alpha \cdot \theta$. Therefore, the $g(x)$ curve (inequality 4.1 and Eq.4.5) is likewise very simple and depends upon the distributions of residuals of the adult mortality scaling relationship ($\ln I$) and the distributions of $\ln \beta_{max}^{-1}$.

Interestingly, human mediated Pleistocene extinctions in Australia are also reportedly highly size dependent, but with a much steeper slope than the other continents [31, 133]. At present, we cannot extend our model to this continent because our demographic data (e.g., Fig.4.5) are based on Eutherian mammals, which may vary in important ways from marsupials [133]. The steeper slope characteristic for Australia may suggest a smaller standard deviation of the $g(x)$ curve, which might suggest lower variation around the adult mortality scaling relationship. Alternatively, perhaps δ is even larger, which would imply a stronger size bias in hunting.

Finally, several important points arise from our theory. First, species with relatively low mortality rates (θ), and/or low maximum recruitment response (β_{max}) for any given body mass are more likely to have gone extinct. These would be species ly-

ing below the line in Fig.4.1 or have small x in Eq.4.4 and Fig.4.4. It is difficult to test this directly because of the unknown adult mortality rate, age of first reproduction and the recruitment response for these ancient species. Second, systematically analyzing variations around canonical curves or values can provide an insight to diverse behaviors or responses in the natural system, which helps to explore macro-patterns. Third, our model clearly indicates that extinction is inevitable if $R_{0max} < 1$. Early Paleoindian hunters did not have to find and kill all individuals of a population or species to drive them extinct. Rather, once sufficient pressure was imposed on a species to drive the maximum net reproductive rate less than one, the species was doomed to extinction.

4.6 Methods

4.6.1 Calculating the probability distribution of x, $g(x)$

By omitting the I_1 term, which merely positions the curve, Eq.4.4 gives

$$x \equiv \frac{\ln I + \ln \kappa + \ln (\ln \beta_{max})}{0.25 + \delta}. \tag{4.6}$$

Ignoring the multiplier $\frac{1}{0.25+\delta}$ for the moment, there are three main sources of variation, which contribute to variation in x. These are: a) the variation of the residuals around the adult mortality scaling relationship (the variation of $\ln I$); b) the variation among species of $\ln (\alpha \cdot \theta)$ (the variation of $\ln \kappa$); and c) the variation among species in the maximum recruitment response (the variation of $\ln (\ln \beta_{max})$). The variation among species in $\ln \kappa$ is captured by the distribution of $\ln (\alpha \cdot \theta)$, since numerically $\kappa \propto (\alpha \cdot \theta)^{-0.42}$(Fig.4.5B). The variation among species in $\ln (\ln \beta_{max})$ is less well defined, so we bracket likely values; these range from 2 to 3. This range for β_{max} values arises because the recruitment rate in mammals is constrained. The probability of surviving to reproductive adulthood, ζ_α, is already quite high (estimated to

be $0.3 \sim 0.4$ [120]).The number of daughters produced per mother per unit time, b, is expected to be highly dependent upon adult body mass, which is not expected to change much as population size, N, changes. If b is fixed, β_{max} can only reflect the increase in ζ_α at low N, and the maximum ζ_α is one. In reality, the value of maximum ζ_α is likely to be far below 1 (e.g., $0.6 \sim 0.8$), so β_{max} may be less than $2 \sim 3$. Here, we explore the effect of this variation. For Case I, we center β_{max} at 2 and allow species to vary following a distribution that constrains β_{max} to be not smaller than 1 and not larger than 3. A normal distribution for $\ln \beta_{max}$ with a mean of 0.69 (e.g., $\beta_{max} = 2$) and a standard deviation of 0.15 places 99% confidence interval at 0.30 to 1.09, which gives β_{max} from 1.35 to 2.97. In case II, we set $\beta_{max} = 2$, and hold it constant for all species. Supporting information (*SI text*) details our simulation/calculation which generates the distribution of $\ln \kappa + \ln I + \ln (\ln \beta_{max})$ numerically by combining the appropriate component distributions to produce a continuous distribution for the sum. With 10,000 random picks the distribution of $\ln \kappa + \ln I + \ln (\ln \beta_{max})$ is normal with a standard deviation of 0.60 (Case I: varied β_{max}). If we repeat this procedure allowing no variation in β_{max}, the resulting distribution is also normal with a standard deviation of 0.54 (Case II: fixed β_{max}). Substituting the distribution of $\ln \kappa + \ln I + \ln (\ln \beta_{max})$ into Eq.4.6 reveals that the probability distribution of the extinction threshold, $g(x)$, is normal with a standard deviation of $0.60/(0.25 + \delta)$ (Case I: varied β_{max}), and $0.54/(0.25 + \delta)$(Case II: fixed β_{max}).

4.6.2   Calibrating the Extinction Probability Curve

The additional harvest instantaneous mortality rate, F, may or may not depend on body mass. Consider a human population of density H, hunting on a landscape and harvesting prey in direct proportion to their abundance. Each mammal population will experience the same harvest mortality rate, which is $F = q \cdot H$, where q is the

exploitation efficiency or, as it is typically referred to in fisheries, the catchability coefficient [20, 130, 131]. If harvest mortality rate is dependent on prey body mass (M), the exploitation efficiency is proportional to M^δ, which would give $F \propto H \cdot M^\delta$ (or in our formulation, $F = I_1 \cdot M^\delta$). We apply this model to the mass extinction of Pleistocene mammals in the Americas about 13,000 BP, which is often attributed to newly arrived humans [19–21, 23]. We have no way to estimate the harvest mortality from $F = q \cdot H$. Without actually knowing harvest mortality, we cannot precisely know the position of the predicted extinction probability curve (P_{TH}) on the $\ln M$ axis. However, its steepness, the logistic regression slope, does not depend upon its position. Consequently, we use an inverse calculation to obtain the harvest mortality. By assuming $\alpha \cdot \theta = 0.6$ and $\beta_{max} = 2$, we obtain $F = 0.49 \cdot \theta$ (Fig.4.1). We combine the body mass at the 50% extinction probability from the fitted extinction probability curve (P_{LR}), $M|_{P_{LR}=0.5}$, and the adult mortality scaling relationship, $\theta = A \cdot M^{-0.25}$ derived from for living mammals, to estimate the adult mortality at this mid-risk-size $(\theta|_{P_{LR}=0.5})$. If the $g(x)$ curve is symmetric (Fig.4.3), the harvest mortality can be estimated by $0.49\theta|_{P_{LR}}$ at this mid-risk-size. We then place the predicted P_{TH} curve going through 0.5 at $M|_{P_{LR}=0.5}$ in Fig.4.4.

4.6.3 Datasets and Data Processing

We use an updated version of the global late Quaternary mammal database MOM (v 3.6) from Smith *et al.* [124]. Data are extracted for both North and South America and represent the entire terrestrial, nonvolant mammalian fauna for each continent. For the 150 species that are extirpated in the late Pleistocene, body mass estimates are derived from allometric regressions on molars or limb bones derived from studies of extant mammals; Body mass for modern species is empirically determined and represented an average across geographical range and gender (see [124] for details). Following the lead of Polishchuk [31], we exclude bats (Chiroptera) and pinipeds

(Odobenidae, Otariidae, and Phocidae) and fit the curve by logistic regression (see *SI text*).

4.7 Supporting Information (*SI*)

4.7.1 The Calculation of juvenile survivorship

The juvenile survivorship is a ratio, N_α/N_0, where N_α is the number of individuals who survive till age of first breeding, α, and N_0 is the number of cohorts born. In this paper, ζ_α is the juvenile survivorship of a stable population. If the additional human harvest mortality, F, is invariant with respect to age class, overall juvenile survivorship decreases. The number of individuals harvested per time is

$$\frac{dN}{dt} = -FN. \tag{4.7}$$

Thus, rewriting Eq.4.7 as $\frac{dN}{N} = -Fdt$ and integrating it from newborn to age α as $\int_{N_0}^{N_\alpha} \frac{dN}{N} = -\int_0^\alpha Fdt$ yields

$$\frac{N_\alpha}{N_0} = e^{-F\alpha}. \tag{4.8}$$

Equation 4.8 is the juvenile survivorship when human harvest of population occurs. Therefore, the overall juvenile survivorship is the product of the juvenile survivorship of a stable population and the juvenile survivorship associated with the human harvest, $\zeta_\alpha e^{-F\alpha}$.

4.7.2 The Calculation of Inequality 4.1

The maximum net reproductive rate is $R_{0max} = \frac{\beta_{max} \cdot \zeta_\alpha \cdot b \cdot e^{-F \cdot \alpha}}{\theta + F}$. If $R_{0max} < 1$, populations will go extinct. Thus, $\frac{\beta_{max} \cdot \zeta_\alpha \cdot b \cdot e^{-F \cdot \alpha}}{\theta + F} < 1$ can be rewritten as

$$\frac{\beta_{max} \cdot \zeta_\alpha \cdot b \cdot e^{-\frac{F}{\theta} \alpha \cdot \theta}}{\theta(1 + \frac{F}{\theta})} < 1. \tag{4.9}$$

We assume that for a human exploited population, all life history parameters remain the same as the stable population. This gives $\theta = \zeta_\alpha \cdot b$, and inequality 4.9 can be simplified as

$$\frac{\beta_{max} \cdot e^{-\frac{F}{\theta} \alpha \cdot \theta}}{1 + \frac{F}{\theta}} < 1, \tag{4.10}$$

which gives inequality 4.1.

4.7.3 The random process to generate the distribution of $x = \ln \kappa + \ln I + \ln (\ln \beta_{max})$, $g(x)$

The distribution of $x = \ln \kappa + \ln I + \ln (\ln \beta_{max})$, $g(x)$, is generated numerically by randomly picking 10,000 such sums that are combining the distributions of appropriate components, $\ln I$ and $\ln (\kappa \ln \beta_{max})$, to produce a continuous distribution for the sum.

The variation in $\ln I$ indicates variation of the residuals around the adult mortality (θ) allometry, which was obtained from Purvis and Harvey's dataset [121] (Fig.4.5A). The obtained variation is not significantly different from a normal distribution (Dagostino-Pearson-test: $df = 56$, $p = 0.332$ with alternative hypothesis: distribution is not normal).

The variation among species in $\ln (\kappa \ln \beta_{max})$ is uncertain, so we attempt to place bounds on it. The maximum recruitment response, β_{max}, is about 2∼3 and independent of body size [117–120]. β_{max} values are small because juvenile survivorship, ζ_α, cannot increase much in mammals and the number of daughters produced per mother per unit time, b, is more or less invariant. ζ_α is already quite high (estimated to be 0.3∼0.4 [120]) and b is expected to be highly dependent upon adult body size, which is not expected to change much as population size, N, changes. If b is fixed, β_{max} can only reflect the increase in ζ_α at low N, and the maximum ζ_α is, of course,

one. Probably, maximum ζ_α is far below 1 (maybe 0.6~0.8), rather limiting β_{max} to the range of 2~3. Consider case I where β_{max} is centered at 2 with a distribution that does not reach too close to $\beta_{max} = 1$. We assume that $\ln \beta_{max}$ is normal with a mean of 0.69 ($\beta_{max} = 2$) and a standard deviation (SD) of 0.15, which places 99% of the probability between $\beta_{max} = 1.35$ and 2.97. In case II we assume that $\beta_{max} = 2$ as a constant and the same for all species.

The between-species variation in $\ln (\kappa \ln \beta_{max})$ is more complicated than $\ln I$. Inequality 4.1, $\frac{e^{-\frac{F}{\theta} \alpha \cdot \theta}}{1 + \frac{F}{\theta}} < \frac{1}{\beta_{max}}$, is awkward to work with since F/θ does not have an analytical solution. The threshold rule is that species go extinct if $F/\theta > C$, where C is the maximum recruitment compensation. Though the maximum recruitment compensation is very well approximated as $C \approx \kappa \cdot \ln \beta_{max}$ for $\beta_{max} < 3.5$ (see Fig.4.1) and the appropriate κ value is well approximated by a power function: $\kappa \propto (\alpha \cdot \theta)^{-0.42}$ (for $\alpha \cdot \theta = 0.6$, $\kappa = 0.71$) (Fig.4.1). This rule is applied in numeric estimations for calculating threshold (F/θ). For a better accuracy of the final distribution a numerical calculation of C is conducted in R [125]. According to inequality 4.1, C is a function of $\alpha \cdot \theta$ and β_{max}, which can be calculated numerically. $\alpha \cdot \theta$ is obtained from Purvis and Harvey's dataset [121]. $\alpha \cdot \theta$ is significantly different from a normal distribution (Dagostino-Pearson-test: $df = 53$, $p < 0.001$ with alternative hypothesis: distribution is not normal), but $\ln (\alpha \cdot \theta)$ is not (Dagostino-Pearson-test: $df = 53$, $p = 0.370$ with alternative hypothesis: distribution is not normal). $\ln (\alpha \cdot \theta)$ has mean of -0.62 and SD of 0.41. To calculate any C, a random $\ln (\alpha \cdot \theta)$ is picked from its normal distribution, and so is a random $\ln \beta_{max}$ (picked from its normal distribution if Case I; equals to 0.69 if Case II.). Total 10,000 values of C are calculated to estimate the distribution of C. However, $\ln C$ is significantly different from a normal distribution (Dagostino-Pearson-test: $df = 999$, $p < 0.001$ with alternative hypothesis: distribution is not normal).

The final continuous distribution of $x = \ln \kappa + \ln I + \ln (\ln \beta_{max})$ is generated

numerically by randomly picking 10,000 such sums by combining the distributions of appropriate components, $\ln I$ and $\ln C$, where $\ln C$ is estimated by numerical as a function of $\alpha \cdot \theta$ and β_{max} in R instead of the approximation of $\ln C = \ln \kappa + \ln (\ln \beta_{max})$. However, $\ln I$ and $\alpha \cdot \theta$ are slightly covariant ($cov = 0.078$, Purvis and Harvey's dataset [121]). Therefore, for the final distribution of x has to be calculated from a multivariable normal distribution of $\ln I$ and $\alpha \cdot \theta$. Total 10,000 of x are calculated to estimate the distribution of x for each case respectively (Case I with varied β_{max} and Case II with fixed β_{max}). $g(x)$ is not significantly different from a normal distribution for both cases (Case I with mean of -0.70 and SD of 0.60, Dagostino-Pearson-test: $df = 999$, $p = 0.338$ with alternative hypothesis: distribution is not normal; Case II with mean of -0.67 and SD of 0.54, $p = 0.349$ with alternative hypothesis: distribution is not normal).
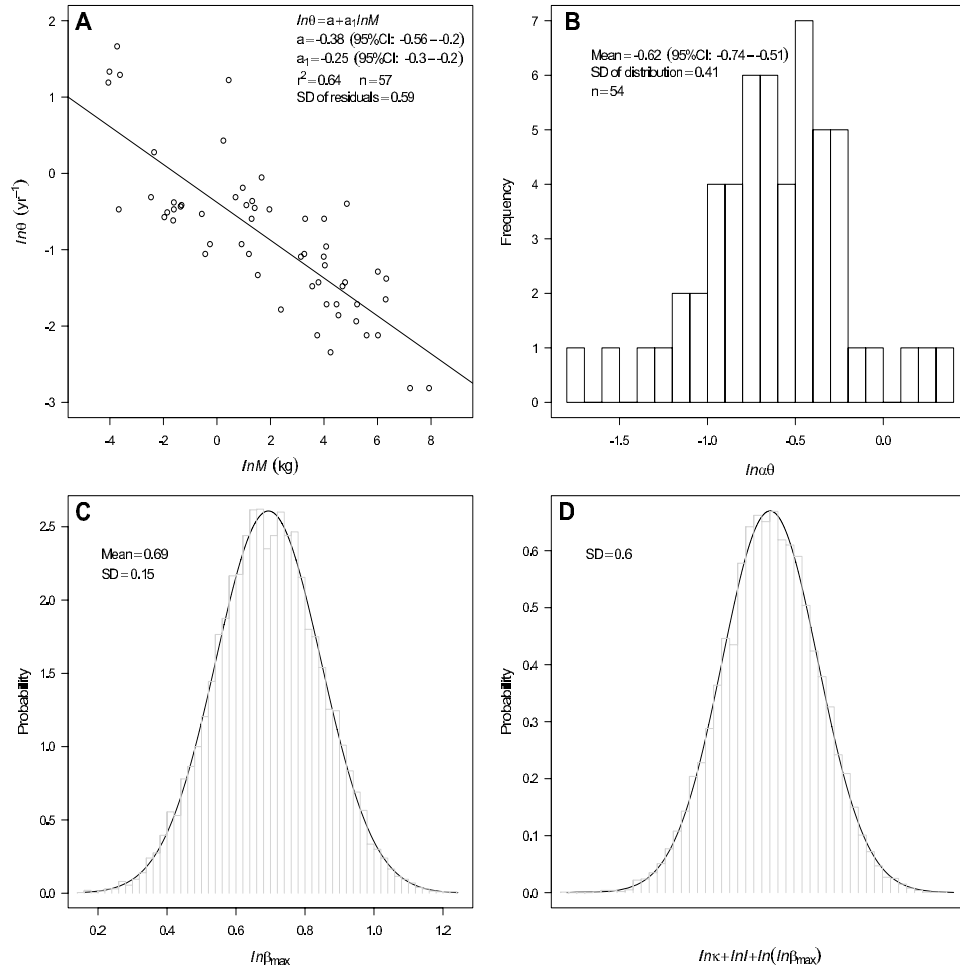
Figure 4.5: Distributions of different parameters. *(A)* Adult mortality (θ) scaling allometry from Purvis and Harvey's dataset [121] gives the standard deviation (SD) of residuals as 0.57, which is the SD of $\ln I$. *(B)* The empirical distribution of $\alpha \cdot \theta$ from Purvis and Harvey's dataset [121] gives the SD of 0.41. *(C)* The estimated distribution of $\ln \beta_{max}$ with SD of 0.15. *(D)* The distribution of $x = \ln \kappa + \ln I + \ln (\ln \beta_{max})$ with varied β_{max} (Case I) is estimated with SD of 0.60. We use the full standard deviation of the residuals (0.57) in our calculations, which assumes no error in the estimates of each $\ln \theta$. If we assume each $\ln \theta$ carries an error of plus or minus 25% for the 95% CI, it would reduce the standard deviation of the between species $\ln \theta$ by less than 5%, too small to affect our conclusions. A similar conclusion applies to $\ln (\alpha \cdot \theta)$ variance.

4.7.4 Datasets and Data Processing

Following the lead of Polishchuk [31], we estimate extinction probability, P, curve using logistic regression, which consists of fitting of the function $\ln\left(\frac{P}{1-P}\right) = D + slope \cdot \ln M$ to the 0, 1 data, where D is a constant, and the slope is of particular interest [31] as it shows the steepness of the curve. Fig.4.3 shows the resulting P versus $\ln M$ curve for North America; summary statistics are in Table 4.1. Fig.4.4 has all the species in the updated Lyons *et al.* data [23], except bats and marine mammals. From Fig.4.3, $P_{LR} = 0.5$ when $M \sim 60$kg for both continents. As first noted by Polishchuk [31] in Lyons *et al.* [23] data set, the continents differ in slope (Table 4.1). Since the P curve is a cumulative probability distribution, its steepness is also characterized by standard deviation (SD) of its probability density curve, $g(x)$ curve (Table 4.1). There is a standard mathematical formula,

$$SD = \frac{\pi}{\sqrt{3} \cdot slope}, \tag{4.11}$$

between these two parameters.

4.8 Acknowledgments

Chapter 5

Coda: The role of mechanistical models

As the discipline of ecology is developing, more and more modeling elements get involved. Existing approaches combine knowledge from statistics, mathematics, computer science, and physics to understand the flows of energy and materials within biotic systems and between biotic and abiotic systems. There are various kinds of models, which can be categorized approximately into four groups: descriptive models, predictive models, simulation models, and mechanistic models.

Descriptive models are pure statistical models. Statistics provides powerful tools to describe empirical data. With today's powerful computational ability, almost all data can be described by certain functions or combinations of functions. However, pure curve fitting is generally not informative, because there is hardly any biological or physical meaning to those parameters obtained from regression. Even though the model may "explain" most of the variation in the data set, there is no understanding of the system. Furthermore, the fitting is necessarily restricted to the ranges of the data, so that descriptive models have limited predictive power.

Chapter 5. Coda: The role of mechanistical models

Predictive models are generally based on partial mechanism for their model structure. To be able to make predictions, the model has to be extendable from original data ranges. This kind of model usually must be based on processes at lower levels of organization than the phenomenon being modeled, such as a family of "Pütter" growth models [7]. They are mathematic models that still use curve fitting to obtain their parameters, though they typically incorporate little or no mechanism. This is useful if prediction within a certain range is the goal of the modeling exercise.

Simulation models attempt to create a toy model of a particular system and provide numerical solutions to mathematic models where analytical solutions are difficult or impossible. With the rapid growth of computer science, concepts such as machine learning and network quickly influenced ecological studies. Simulation models may use some algorithms from purely statistical models, or combine simulations with mechanisms from idealized or actual systems. They provide graphical output or visualizations which can be useful to explore and gain new insights into the system.

Mechanistic models focus on the fundamental units and behaviors of the system based on first principles and natural laws. They always start with real world problems. According to the level and complexity of the solution wanted, they make assumptions and definitions of system parameters and functions. Following basic principles and natural laws, these models generally derive inspirations from various physical systems and are couched in rigorous mathematics. Parameters used in the models have physical meaning. It is preferred that these parameters be independently measurable. The intent of such models is often to predict a canonical pattern or behavior, which can then be evaluated by empirical data. If the model does not capture the major features of the system, a reconstruction from ground level is required. The mismatch between the model and data also provides a possibility to generate new questions.

All these kinds of models are used in scientific research. According to their different characteristics and goals, they contribute in different ways. However, they are not independent of each other. Both the predictive and simulation models are based upon a few known behaviors mechanisms of a specific system. They both need certain amount of input data in order to make meaningful predictions. Their goals are to explain most observed variation and make accurate predictions of system behavior within certain domain ranges. They generally do a very good job of capturing the important details for the given system. However, since mechanisms and input data are all from the given system, substantial information about the specific system is required in order to make accurate predictions. On the other hand, the mechanistic models are built from ground zero, based on natural laws and first principles. The goal is to characterize fundamental units and behaviors of the system and facilitate comparisons across systems. They make simplifying assumptions and use limited parameter values. Mechanism models sacrifice the ability to capture details of systems. They provide canonical solution of similar systems, but they do not aim to perfectly fit any of those systems. Their goal is to understand the essential mechanisms underlying systems. They can provide a basis for more detailed predictive and simulation models.

Current academic science, at least in ecology, most modeling activities focus on predictive and simulation models. These are very useful without a doubt, especially in applied sciences. However, those two kinds of models are both depend on having lots of information—meaning existing data—on the system. Without exploring the system more aggressively by mechanistic models, they are limited. Ideally, predictive and simulation models can be developed hand-in-hand with mechanistic models. Constructions of predictive and simulation models can benefit from theoretical platform built by mechanistic models, and output of predictive and simulation models can be used to prove or disprove assumptions and functions of mechanistic models. Science should be open minded to the roles and contributions of all kinds of mod-

els. In science, there is no absolute right or wrong, but the accumulated weight of evidence leading to increased understanding of mechanism and predictive power.

Appendices

Appendix A

Data sources for Chapter 2

Data of food assimilation rates for several mammals and birds over ontogeny are listed in Table A.5.

Data of resting metabolic rates for mammals are listed in Table A.6.

Data used to construct the growth rates for mammals and birds in Fig.2.3B are taken from the Supplementary Information of West *et al.* [11]. The growth rates, dm/dt, are calculated by numerically taking the derivative between adjacent points with respect to time of the growth curves and smoothing using the adjacent averaging method.

Table A.1: Parameters from Eq.2.5 (estimated using nonlinear least squares regression method based on the Levenberg-Marquardt algorithm).

	f_0	a	μ_d	$f(\mu = 1)$	$\bar{f}$	γ	R^2
Fox (male)	2.26	3.82	0.78	1.44	2.17	1.88	0.977
Fox (female)	2.25	5.09	0.84	1.42	2.18	1.75	0.979
Mink (male)	3.68	8.48	0.80	1.97	3.50	0.57	0.876

Appendix A. Data sources for Chapter 2

Table A.2: Empirical values of production efficiency (η), storage coefficient (γ), and quantity of energy to synthesize a gram of biomass (E_m); Details of calculation are in the text of *SI*.

Species	Production Efficiency η (%)	$\gamma = \frac{E_c}{E_m}$	E_m(J/gram dry mass)	Source
Theoretical results		10.2	2262	Data Compiling
Multiple species I	50 ~ 90	0.74 ~ 5	1400 ~ 9500	[38]
Multiple species II		1 ~ 9		[13]
Multiple species III	75	3		[50]
Chicken embryo	62	1.6		[12]
Gastropod embryo	62 ~ 67	1.8		[13]
Silkworm embryo	63	1.7		[12]
Frog embryo	51	1		[12]
Sea urchin embryo	59	1.4		[12]
Green iguana embryo	48	1		[12]
Herring embryo	70	2.3		[13]
Cow	45 ~ 63	0.8 ~ 1.7		[12]
Pig	52 ~ 88	1.1 ~ 7.3		[12]
Chicken	72 (38°C); 57 (21°C)	2.6 (38°C); 1.3 (21°C)		(S5)
Gilthead sea bream	65	1.9		[134]
European sea bass	68	2.1		[134]
Continued on Next Page...				

Table A.2 – Continued

Species	Production Efficiency η (%)	$\gamma = \frac{E_c}{E_m}$	E_m (J/gram dry mass)	Source
White grouper	69	2.2		[134]
Quail embryo		13.0	1774	[60]
Pheasant embryo		5.0	4583	[60]
Chicken embryo		4.1	5660	[60]
Mallard duck embryo		6.8	3388	[60]
Turkey embryo		6.4	3627	[60]

Table A.3: Resting metabolic rate ($B_{rest} = B_{0,rest}M^\psi$) for mammals and birds.

$B_{0,rest}$ (W/kg$^\psi$)	RMR scaling power, ψ	Method	Source	
Mammals (N = 49)	3.925	0.749	Data compiling	TableA.6
Passerine (N = 14)	$5.56 \sim 6.82$	$0.704 \sim 0.726$	Respirometry	[61]
Non passerine (N = 17)	$3.56 \sim 4.41$	$0.729 \sim 0.734$	Respirometry	[61]

Table A.4: Allometric equations ($B_{field} = B_{0,field}M^\psi$) for field metabolic rate (B_{field}) of free living and captive mammals and non passerine birds.

	$B_{0,field}$ (W/kg$^{3/4}$)	FMR Scaling power, ψ	f (B_{field}/B_{rest}) when $M = 1$kg	Method	Reference
All mammal (free living) (N = 79)	8.88	0.734	2.26	Doubly labeled water	[37]
Eutherians (free living) (N = 58)	10.09	0.772	2.57	Doubly labeled water	[37]
Free-living non passerine (N = 55)	13.39	0.673	2.96 ~ 3.76	Doubly labeled water	[37]
Caged non passerines (N = 9)	4.8	0.754	1.06 ~ 1.3	Metabolizable energy intake	[64]
Captive eutherian mammals (N = 120)	7.02	0.75	1.79	Metabolizable energy intake	[41]
Captive eutherian mammals	6.78	0.75	1.73	Metabolizable energy intake	[40]

Table A.5: Data of food assimilation rates for several mammals and birds over ontogeny.

Species	m (kg)	Metabolic Energy (W)	Adult M (kg)	Reference
Heifer	181	494.6627	454	[135]
Heifer	272	634.5328		
Heifer	363	743.6997		
Heifer	454	820.4577		
Pig I	4	39.73583	100	[136]
Pig I	7.5	78.5025		
Pig I	15	158.2165		
Pig I	35	293.1729		
Pig I	65	407.5346		
Pig I	100	486.0371		
Pig II	9.99999	82.32893	117	[137]
Pig II	19.99998	151.3715		
Pig II	29.99997	209.2718		
Pig II	40	257.828		
Pig II	50	298.5481		
Pig II	60	332.6968		
Pig II	70	361.3344		
Pig II	80	385.3505		
Pig II	90	405.4908		
Pig II	100	422.3808		
Pig II	110	436.5451		
Pig II	117	445.0768		

Continued on Next Page...

Table A.5 – Continued

Species	m (kg)	Metabolic Energy (W)	Adult M (kg)	Reference
Bull	25	85.28667	1000	[135]
Bull	150	434.962		
Bull	200	597.0067		
Bull	250	682.2933		
Bull	300	818.752		
Bull	400	989.3253		
Bull	500	1057.555		
Bull	600	1108.727		
Bull	700	1194.013		
Bull	800	1279.3		
Bull	900	1364.587		
Bull	1000	1449.873		
Sheep I	10	67.8287	50	[136]
Sheep I	20	140.5023		
Sheep I	30	174.4167		
Sheep I	40	203.4861		
Sheep I	50	203.4861		
Sheep II	10	82.36343	60	[136]
Sheep II	20	159.8819		
Sheep II	30	193.7963		
Sheep II	40	198.6412		
Sheep II	50	227.7107		
Sheep II	60	227.7107		

Continued on Next Page. . .

Table A.5 – Continued

Species	m (kg)	Metabolic Energy (W)	Adult M (kg)	Reference
Horse (M=700kg)	225	763.5574	700	[138]
Horse (M=700kg)	275	860.4556		
Horse (M=700kg)	420	1104.639		
Horse (M=700kg)	525	1395.333		
Horse (M=700kg)	600	1395.333		
Horse (M=600kg)	200	639.5278	600	[138])
Horse (M=600kg)	245	744.1778		
Horse (M=600kg)	375	972.8574		
Horse (M=600kg)	475	1240.296		
Horse (M=600kg)	540	1251.924		
Horse (M=500kg)	175	558.1333	500	[138]
Horse (M=500kg)	215	666.6593		
Horse (M=500kg)	325	825.5722		
Horse (M=500kg)	400	1027.12		
Horse (M=500kg)	450	1019.369		
Horse (M=400kg)	145	523.25	400	[138]
Horse (M=400kg)	180	562.0093		
Horse (M=400kg)	265	662.7833		
Horse (M=400kg)	330	837.2		
Horse (M=400kg)	365	833.3241		
Horse (M=200kg)	75	282.9426	200	[138]
Horse (M=200kg)	95	337.2056		

Continued on Next Page...

Table A.5 – Continued

Species	m (kg)	Metabolic Energy (W)	Adult M (kg)	Reference
Horse (M=200kg)	140	399.2204		
Horse (M=200kg)	170	449.6074		
Horse (M=200kg)	185	441.8556		
Duck (male)	0.27	4.41663	3.61	[139]
Duck (male)	0.78	15.45821		
Duck (male)	1.38	22.48467		
Duck (male)	1.96	25.69676		
Duck (male)	2.49	29.71188		
Duck (male)	2.96	32.72322		
Duck (male)	3.34	33.727		
Duck (male)	3.61	33.727		
Duck (female)	0.27	4.41579	3.29	[139]
Duck (female)	0.74	14.65238		
Duck (female)	1.28	22.27965		
Duck (female)	1.82	25.69185		
Duck (female)	2.3	28.70262		
Duck (female)	2.73	31.9141		
Duck (female)	3.06	32.71697		
Duck (female)	3.29	32.71697		
Chicken I	0.13	4.99219	2.1	[137]
Chicken I	0.32	7.5348		
Chicken I	0.56	10.29446		
Chicken I	0.86	13.56574		

Continued on Next Page...

Table A.5 – Continued

Species	m (kg)	Metabolic Energy (W)	Adult M (kg)	Reference
Chicken I	1.25	16.49594		
Chicken I	1.69	18.35639		
Chicken I	2.1	20.37187		
Chicken II	0.035	1.00378	1.475	[139]
Chicken II	0.1	2.81058		
Chicken II	0.26	5.21965		
Chicken II	0.45	6.8257		
Chicken II	0.66	7.22721		
Chicken II	0.75	7.62873		
Chicken II	0.98	8.03024		
Chicken II	1.1	8.43175		
Chicken II	1.22	8.63251		
Chicken II	1.375	9.03402		
Chicken II	1.475	10.0378		
Chicken III	0.037	1.40502	1.6	[139]
Chicken III	0.12	3.21148		
Chicken III	0.325	5.62009		
Chicken III	0.5	7.02512		
Chicken III	0.75	7.62727		
Chicken III	0.9	8.0287		
Chicken III	1.1	8.43014		
Chicken III	1.24	9.03229		
Chicken III	1.38	9.43373		
Chicken III	1.5	10.03588		

Continued on Next Page. . .

Table A.5 – Continued

Species	m (kg)	Metabolic Energy (W)	Adult M (kg)	Reference
Chicken III	1.6	11.03947		
Common Loon	0.46307	6.52112	3.354	[140]
Common Loon	0.67864	9.70216		
Common Loon	1.09381	13.92315		
Common Loon	1.40519	16.85949		
Common Loon	1.7006	19.42882		
Common Loon	2.02794	21.38634		
Common Loon	2.34731	22.79334		
Common Loon	2.77046	24.93437		
Common Loon	3.02595	25.60735		
Common Loon	3.27345	25.54618		
Rhesus Monkey	0.65	8.61981	6.5	[141]
Rhesus Monkey	1.71	18.15972		
Rhesus Monkey	1.76	18.69241		
Rhesus Monkey	2.37	26.10157		
Rhesus Monkey	4.5	29.29769		
Rhesus Monkey	6.5	36.22259		
Squirre Monkey	0.11	2.39708	0.788	[141]
Squirre Monkey	0.15	3.14769		
Squirre Monkey	0.2	3.9225		
Squirre Monkey	0.3	5.4237		
Squirre Monkey	0.4	5.95639		
Squirre Monkey	0.5	6.5375		

Continued on Next Page...

Table A.5 – Continued

Species	m (kg)	Metabolic Energy (W)	Adult M (kg)	Reference
Squirre Monkey	0.788	8.0387		
Fox (female)	1.35	12.45379	5.5	[142]
Fox (female)	2.3	20.06175		
Fox (female)	3.25	23.64767		
Fox (female)	3.95	26.79746		
Fox (female)	4.6	27.86354		
Fox (female)	5.1	24.71375		
Fox (female)	5.4	20.934		
Fox (female)	5.5	20.01329		
Fox (male)	1.45	13.3745	6.5	[142]
Fox (male)	2.5	21.80625		
Fox (male)	3.6	26.1675		
Fox (male)	4.4	29.85033		
Fox (male)	5.1	30.91642		
Fox (male)	5.75	27.86354		
Fox (male)	6.25	24.22917		
Fox (male)	6.5	23.64767		
Mink (female)	0.45	6.10575	1.325	[142]
Mink (female)	0.65	11.19388		
Mink (female)	0.81	13.76217		
Mink (female)	0.93	15.65204		
Mink (female)	1.03	14.00446		
Mink (female)	1.11	13.22913		

Continued on Next Page...

Table A.5 – Continued

Species	m (kg)	Metabolic Energy (W)	Adult M (kg)	Reference
Mink (female)	1.18	12.59917		
Mink (female)	1.24	12.88992		
Mink (female)	1.28	12.59917		
Mink (female)	1.32	11.19388		
Mink (female)	1.325	10.17625		
Mink (male)	0.63	8.38329	2.38	[142]
Mink (male)	0.93	14.87671		
Mink (male)	1.24	19.09258		
Mink (male)	1.52	21.56396		
Mink (male)	1.73	21.07937		
Mink (male)	1.9	21.27321		
Mink (male)	2.04	21.37013		
Mink (male)	2.16	21.12783		
Mink (male)	2.26	18.75338		
Mink (male)	2.33	16.282		
Mink (male)	2.35	15.65204		
Mink (male)	2.38	13.76217		

Table A.6: Data of resting metabolic rates for several mammals.

Common name	Conditions	M (kg)	RMR* (W)	Reference
Foxes	winter	3.79	9.398434	[143]
Foxes	summer	3.37	9.700342	[143]
Gapper's red -backed mouse		0.0206	0.396097	[144]
Rhoad's red -backed mouse		0.0256	0.519583	[144]
Meadow mouse		0.0312	0.549921	[144]
house mouse		0.017	0.317796	[144]
white mouse		0.0248	0.476854	[144]
deer mice		0.0223	0.428784	[144]
Nothern deer mouse		0.0197	0.31566	[144]
Pine mouse		0.0225	0.516753	[144]
California harvest mouse		0.0096	0.194844	[145]
Jumping mouse		0.022	0.493519	[144]

Continued on Next Page. . .

Table A.6 – Continued

Common name	Conditions	M (kg)	RMR* (W)	Reference
Beef cattle	male	500	512.8241	[146]
	female	400	408.3241	[146]
Dairy cattle	female	500	510.4051	[146]
Goat	male	70	142.2361	[146]
	female	70	115.1435	[146]
Guinea pig	male	0.8	2.438333	[146]
	female	0.8	2.631852	[146]
Horse	male	650	792.4583	[146]
	female	650	776.735	[146]
Mule	NA	600	766.3333	[146]
Rat	male	0.2	1.499769	[146]
	female	0.2	1.30625	[146]
Swine	male	250	286.6493	[146]
	female	250	215.2894	[146]
Cairo spiny mouse	Lactating (3 pups)	0.04	0.226852	[147]
Golden Spiny Mouse		0.051	0.218403	[147]

Continued on Next Page. . .

Table A.6 – Continued

Common name	Conditions	M (kg)	RMR* (W)	Reference
White-tailed		0.096	0.544444	[147]
Antelope Squirrels				
Yellow-necked Mouse	Cold (-10°C)	0.0284	0.371435	[147]
Field vole	Cold (5°C)	0.0237	0.641875	[147]
House Mouse	Lactating (14 pups)	0.0382	0.51287	[147]
white-footed mouse		0.021	0.184722	[147]
deer mouse	Cold frield measurements	0.0206	0.100139	[147]
Bushy-tailed Jird		0.041	0.175579	[147]
Golden-mantled	Lactating	0.232	1.15463	[147]
Ground Squirrel	(5 pups in the field)			
Botta's Pocket Gopher		0.143	0.662037	[147]
brown antechinus		0.037	0.196991	[147]
Leadbeater's Possum		0.166	0.557176	[147]
Tammar Wallaby		4.8	7.777778	[147]
Sugar Glider		0.128	0.474074	[147]
koala		4.77	11.04167	[147]
Common Ringtail Possum		0.86	1.592593	[147]

Continued on Next Page. . .

Table A.6 – Continued

Common name	Conditions	M (kg)	RMR* (W)	Reference
Quokka		2.51	4.357639	[147]
Fat Tailed Dunnart		0.014	0.103704	[147]
Mantled Howler Monkey		4.67	11.35069	[147]
Brown-throated		3.79	3.947917	[147]
Three-toed Sloth				
lesser hedgehog	Lactating (1 pup)	0.2626	0.334329	[147]
tenrec				
Modern humans	Tour de	68.5	79.28241	[147]
	France cyclist			

* RMR: Resting Metabolic Rate.

Appendix B

Data sources for Chapter 3

Table B.1: Data in Figs.3.2 and 3.3.

Species†	Sex	Temperature (°C)	Time (h)	Wet mass (mg)	Reference
C. elegans	NA	10	52.0	2.15×10^{-3}	[79]*
C. elegans	NA	10	140.5	3.46×10^{-2}	[79]*
C. elegans	NA	10	186.2	7.29×10^{-2}	[79]*
C. elegans	NA	10	239.1	0.29	[79]*
C. elegans	NA	10	334.2	0.90	[79]*
C. elegans	NA	10	382.8	1.10	[79]*
C. elegans	NA	10	478.9	1.26	[79]*
C. elegans	NA	10	578.3	1.34	[79]*
C. elegans	NA	10	647.2	1.32	[79]*
C. elegans	NA	15	137.5	0.53	[79]*
C. elegans	NA	15	187.0	1.05	[79]*

Continued on Next Page. . .

Table B.1 – Continued

Species[†]	Sex	Temperature (^oC)	Time (h)	Wet mass (mg)	Reference
C. elegans	NA	15	234. 2	1.19	[79]*
C. elegans	NA	15	306.2	1.14	[79]*
C. elegans	NA	15	358.1	1.23	[79]*
C. elegans	NA	15	401.1	1.14	[79]*
C. elegans	NA	15	474.5	1.17	[79]*
C. elegans	NA	25	1.52	2.81×10^{-4}	[79]*
C. elegans	NA	25	16.7	6.34×10^{-3}	[79]*
C. elegans	NA	25	24.3	1.97×10^{-2}	[79]*
C. elegans	NA	25	34.8	6.07×10^{-2}	[79]*
C. elegans	NA	25	41.8	0.25	[79]*
C. elegans	NA	25	52.3	0.32	[79]*
C. elegans	NA	25	70.0	0.58	[79]*
C. elegans	NA	25	95.5	0.83	[79]*
C. elegans	NA	25	118.6	0.79	[79]*
C. elegans	NA	25	190.2	0.93	[79]*
C. elegans	NA	25	139.7	0.95	[79]*
C. elegans	NA	25	165.2	1.01	[79]*
L. illustris	NA	26	22.5	2.60	[148]
L. illustris	NA	26	25.7	3.18	[148]
L. illustris	NA	26	26. 5	4.55	[148]
L. illustris	NA	26	33. 9	7.71	[148]
L. illustris	NA	26	45.8	32.1	[148]
L. illustris	NA	26	48.6	38.5	[148]

Table B.1 – Continued

Species[†]	Sex	Temperature (^oC)	Time (h)	Wet mass (mg)	Reference
L. illustris	NA	26	59.4	46.3	[148]
L. illustris	NA	26	76.0	47.4	[148]
L. illustris	NA	20	45.6	2.76	[148]
L. illustris	NA	20	46.6	3.43	[148]
L. illustris	NA	20	50.9	6.50	[148]
L. illustris	NA	20	69.0	22.1	[148]
L. illustris	NA	20	77.7	37.1	[148]
L. illustris	NA	20	88.6	35.7	[148]
L. illustris	NA	20	93.7	43.0	[148]
L. illustris	NA	20	102.6	45.0	[148]
L. illustris	NA	20	114.4	46.1	[148]
L. illustris	NA	15	51.0	0.67	[148]
L. illustris	NA	15	96.5	4.33	[148]
L. illustris	NA	15	122.5	12.4	[148]
L. illustris	NA	15	141.6	22.7	[148]
L. illustris	NA	15	164.6	33.3	[148]
L. illustris	NA	15	174.8	38.9	[148]
L. illustris	NA	15	193.4	43.6	[148]
L. illustris	NA	11	141.1	1.02	[148]
L. illustris	NA	11	164.4	1.49	[148]
L. illustris	NA	11	199.1	2.19	[148]
L. illustris	NA	11	221.2	4.55	[148]
L. illustris	NA	11	241.7	5.33	[148]

Continued on Next Page. . .

Table B.1 – Continued

Species[†]	Sex	Temperature (^{o}C)	Time (h)	Wet mass (mg)	Reference
L. illustris	NA	11	266.6	8.12	[148]
L. illustris	NA	11	287.7	9.91	[148]
L. illustris	NA	11	329.3	21.4	[148]
L. illustris	NA	11	361.6	28.9	[148]
L. illustris	NA	11	437.7	42.2	[148]
L. illustris	NA	11	466.5	44.6	[148]
A. viridis	female	5	1405.1	9.88×10^{-3}	[149][♭]
A. viridis	female	5	1896.8	1.82×10^{-2}	[149][♭]
A. viridis	female	5	1642.2	1.94×10^{-2}	[149][♭]
A. viridis	female	5	2168.8	6.45×10^{-2}	[149][♭]
A. viridis	female	5	2485.9	0.10	[149][♭]
A. viridis	female	5	3010.8	0.18	[149][♭]
A. viridis	female	8	826.5	5.60×10^{-3}	[149][♭]
A. viridis	female	8	978.8	1.10×10^{-2}	[149][♭]
A. viridis	female	8	1156.6	1.75×10^{-2}	[149][♭]
A. viridis	female	8	1323.5	5.49×10^{-2}	[149][♭]
A. viridis	female	8	1552.8	9.23×10^{-2}	[149][♭]
A. viridis	female	8	1976.2	0.17	[149][♭]
A. viridis	female	10	612.9	4.34×10^{-3}	[149][♭]
A. viridis	female	10	727.0	1.03×10^{-2}	[149][♭]
A. viridis	female	10	850.0	1.62×10^{-2}	[149][♭]
A. viridis	female	10	972.9	4.35×10^{-2}	[149][♭]
A. viridis	female	10	1167.9	8.62×10^{-2}	[149][♭]

Continued on Next Page...

Table B.1 – Continued

Species[†]	Sex	Temperature (^oC)	Time (h)	Wet mass (mg)	Reference
A. viridis	female	10	1545.0	0.15	[149][♭]
A. viridis	female	12	504.6	4.86×10^{-3}	[149][♭]
A. viridis	female	12	598.1	9.61×10^{-3}	[149][♭]
A. viridis	female	12	696.8	1.61×10^{-2}	[149][♭]
A. viridis	female	12	797.7	3.93×10^{-2}	[149][♭]
A. viridis	female	12	954.1	8.32×10^{-2}	[149][♭]
A. viridis	female	12	1291.4	0.14	[149][♭]
A. viridis	female	15	359.6	2.95×10^{-3}	[149][♭]
A. viridis	female	15	425.6	7.70×10^{-3}	[149][♭]
A. viridis	female	15	484.6	1.48×10^{-2}	[149][♭]
A. viridis	female	15	571.9	3.68×10^{-2}	[149][♭]
A. viridis	female	15	685.5	7.60×10^{-2}	[149][♭]
A. viridis	female	15	974.1	0.14	[149][♭]
A. viridis	female	20	235.0	1.56×10^{-3}	[149][♭]
A. viridis	female	20	283.4	5.72×10^{-3}	[149][♭]
A. viridis	female	20	326.4	1.34×10^{-2}	[149][♭]
A. viridis	female	20	399.9	3.12×10^{-2}	[149][♭]
A. viridis	female	20	457.8	7.04×10^{-2}	[149][♭]
A. viridis	female	20	679.9	0.14	[149][♭]
A. viridis	male	5	1405.1	9.88×10^{-3}	[149][♭]
A. viridis	male	5	1896.8	1.82×10^{-2}	[149][♭]
A. viridis	male	5	1642.2	1.94×10^{-2}	[149][♭]
A. viridis	male	5	2168.8	4.25×10^{-2}	[149][♭]

Continued on Next Page. . .

Table B.1 – Continued

Species[†]	Sex	Temperature (^oC)	Time (h)	Wet mass (mg)	Reference
A. viridis	male	5	2417.4	7.76×10^{-2}	[149][♭]
A. viridis	male	5	2661.7	9.30×10^{-2}	[149][♭]
A. viridis	male	8	826.5	5.60×10^{-3}	[149][♭]
A. viridis	male	8	978.8	1.10×10^{-2}	[149][♭]
A. viridis	male	8	1156.6	1.75×10^{-2}	[149][♭]
A. viridis	male	8	1323.5	3.65×10^{-2}	[149][♭]
A. viridis	male	8	1486.3	5.84×10^{-2}	[149][♭]
A. viridis	male	8	1679.8	7.80×10^{-2}	[149][♭]
A. viridis	male	10	612.9	4.34×10^{-3}	[149][♭]
A. viridis	male	10	727.0	1.03×10^{-2}	[149][♭]
A. viridis	male	10	850.0	1.62×10^{-2}	[149][♭]
A. viridis	male	10	972.9	3.46×10^{-2}	[149][♭]
A. viridis	male	10	1105.7	4.05×10^{-2}	[149][♭]
A. viridis	male	10	1274.8	7.32×10^{-2}	[149][♭]
A. viridis	male	12	504.6	4.86×10^{-3}	[149][♭]
A. viridis	male	12	598.1	9.61×10^{-3}	[149][♭]
A. viridis	male	12	696.8	1.61×10^{-2}	[149][♭]
A. viridis	male	12	797.7	3.33×10^{-2}	[149][♭]
A. viridis	male	12	900.5	3.75×10^{-2}	[149][♭]
A. viridis	male	12	1047.4	7.07×10^{-2}	[149][♭]
A. viridis	male	15	359.6	2.95×10^{-3}	[149][♭]
A. viridis	male	15	425.6	7.70×10^{-3}	[149][♭]
A. viridis	male	15	484.6	1.48×10^{-2}	[149][♭]

Continued on Next Page. . .

Table B.1 – Continued

Species[†]	Sex	Temperature (^oC)	Time (h)	Wet mass (mg)	Reference
A. viridis	male	15	571.9	2.85×10^{-2}	[149][♭]
A. viridis	male	15	638.3	3.50×10^{-2}	[149][♭]
A. viridis	male	15	758.4	6.82×10^{-2}	[149][♭]
A. viridis	male	20	235.0	1.56×10^{-3}	[149][♭]
A. viridis	male	20	283.4	5.72×10^{-3}	[149][♭]
A. viridis	male	20	326.4	1.34×10^{-2}	[149][♭]
A. viridis	male	20	399.9	2.47×10^{-2}	[149][♭]
A. viridis	male	20	421.4	3.48×10^{-2}	[149][♭]
A. viridis	male	20	516.4	6.69×10^{-2}	[149][♭]
M. albidus	female	5	1519.9	7.10×10^{-3}	[149][♭]
M. albidus	female	5	1763.6	1.18×10^{-2}	[149][♭]
M. albidus	female	5	2005.1	2.07×10^{-2}	[149][♭]
M. albidus	female	5	2285.8	5.03×10^{-2}	[149][♭]
M. albidus	female	5	2581.6	5.68×10^{-2}	[149][♭]
M. albidus	female	5	2926.7	0.15	[149][♭]
M. albidus	female	8	950.1	6.51×10^{-3}	[149][♭]
M. albidus	female	8	1111.3	1.12×10^{-2}	[149][♭]
M. albidus	female	8	1273.8	1.89×10^{-2}	[149][♭]
M. albidus	female	8	1453.8	4.73×10^{-2}	[149][♭]
M. albidus	female	8	1670.2	5.21×10^{-2}	[149][♭]
M. albidus	female	8	1933.8	0.14	[149][♭]
M. albidus	female	10	711.5	4.73×10^{-3}	[149][♭]
M. albidus	female	10	834.4	8.28×10^{-3}	[149][♭]

Continued on Next Page. . .

Table B.1 – Continued

Species[†]	Sex	Temperature (^oC)	Time (h)	Wet mass (mg)	Reference
M. albidus	female	10	981.4	1.83×10^{-2}	[149][♭]
M. albidus	female	10	1137.1	4.32×10^{-2}	[149][♭]
M. albidus	female	10	1314.9	4.97×10^{-2}	[149][♭]
M. albidus	female	10	1543.1	0.12	[149][♭]
M. albidus	female	12	424.5	3.55×10^{-3}	[149][♭]
M. albidus	female	12	529.1	8.28×10^{-3}	[149][♭]
M. albidus	female	12	634.3	1.72×10^{-2}	[149][♭]
M. albidus	female	12	743.9	3.73×10^{-2}	[149][♭]
M. albidus	female	12	889.6	4.62×10^{-2}	[149][♭]
M. albidus	female	12	1089.0	0.12	[149][♭]
M. albidus	female	15	332.1	2.96×10^{-3}	[149][♭]
M. albidus	female	15	404.7	6.51×10^{-3}	[149][♭]
M. albidus	female	15	498.6	1.18×10^{-2}	[149][♭]
M. albidus	female	15	607.7	2.90×10^{-2}	[149][♭]
M. albidus	female	15	702.0	4.32×10^{-2}	[149][♭]
M. albidus	female	15	863.7	0.11	[149][♭]
M. albidus	female	20	173.0	2.37×10^{-3}	[149][♭]
M. albidus	female	20	210.4	5.92×10^{-3}	[149][♭]
M. albidus	female	20	270.9	9.47×10^{-3}	[149][♭]
M. albidus	female	20	331.3	2.54×10^{-2}	[149][♭]
M. albidus	female	20	404.2	4.14×10^{-2}	[149][♭]
M. albidus	female	20	514.6	9.35×10^{-2}	[149][♭]
M. albidus	male	5	1519.9	7.10×10^{-3}	[149][♭]

Continued on Next Page. . .

Table B.1 – Continued

Species[†]	Sex	Temperature (^{o}C)	Time (h)	Wet mass (mg)	Reference
M. albidus	male	5	1763.6	1.18×10^{-2}	[149][♭]
M. albidus	male	5	2005.1	2.07×10^{-2}	[149][♭]
M. albidus	male	5	2285.8	3.55×10^{-2}	[149][♭]
M. albidus	male	5	2517.3	4.02×10^{-2}	[149][♭]
M. albidus	male	5	2720.1	4.73×10^{-2}	[149][♭]
M. albidus	male	8	950.1	6.51×10^{-3}	[149][♭]
M. albidus	male	8	1111.3	1.12×10^{-2}	[149][♭]
M. albidus	male	8	1273.8	1.89×10^{-2}	[149][♭]
M. albidus	male	8	1453.8	3.43×10^{-2}	[149][♭]
M. albidus	male	8	1627.4	3.79×10^{-2}	[149][♭]
M. albidus	male	8	1790.2	4.44×10^{-2}	[149][♭]
M. albidus	male	10	711.5	4.73×10^{-3}	[149][♭]
M. albidus	male	10	834.4	8.28×10^{-3}	[149][♭]
M. albidus	male	10	981.4	1.83×10^{-2}	[149][♭]
M. albidus	male	10	1137.1	3.20×10^{-2}	[149][♭]
M. albidus	male	10	1284.9	3.67×10^{-2}	[149][♭]
M. albidus	male	10	1427.7	4.02×10^{-2}	[149][♭]
M. albidus	male	12	424.5	3.55×10^{-3}	[149][♭]
M. albidus	male	12	529.1	8.28×10^{-3}	[149][♭]
M. albidus	male	12	634.3	1.72×10^{-2}	[149][♭]
M. albidus	male	12	743.9	2.90×10^{-2}	[149][♭]
M. albidus	male	12	868.2	3.37×10^{-2}	[149][♭]
M. albidus	male	12	997.5	3.97×10^{-2}	[149][♭]

Table B.1 – Continued

Species[†]	Sex	Temperature (^oC)	Time (h)	Wet mass (mg)	Reference
M. albidus	male	15	332.1	2.96×10^{-3}	[149][♭]
M. albidus	male	15	404.7	6.51×10^{-3}	[149][♭]
M. albidus	male	15	498.6	1.18×10^{-2}	[149][♭]
M. albidus	male	15	607.7	1.95×10^{-2}	[149][♭]
M. albidus	male	15	702.0	2.25×10^{-2}	[149][♭]
M. albidus	male	15	813.3	3.67×10^{-2}	[149][♭]
M. albidus	male	20	173.0	2.37×10^{-3}	[149][♭]
M. albidus	male	20	210.4	5.92×10^{-3}	[149][♭]
M. albidus	male	20	270.9	9.47×10^{-3}	[149][♭]
M. albidus	male	20	331.3	1.72×10^{-2}	[149][♭]
M. albidus	male	20	399.9	1.95×10^{-2}	[149][♭]
M. albidus	male	20	481.8	3.55×10^{-2}	[149][♭]
A. vernalis	female	5	1040.7	2.96×10^{-3}	[149][♭]
A. vernalis	female	5	1187.8	7.10×10^{-3}	[149][♭]
A. vernalis	female	5	1363.9	8.88×10^{-3}	[149][♭]
A. vernalis	female	5	1520.3	1.42×10^{-2}	[149][♭]
A. vernalis	female	5	1693.8	3.97×10^{-2}	[149][♭]
A. vernalis	female	5	1938.2	0.10	[149][♭]
A. vernalis	female	8	507.8	2.96×10^{-3}	[149][♭]
A. vernalis	female	8	631.6	6.51×10^{-3}	[149][♭]
A. vernalis	female	8	748.3	8.88×10^{-3}	[149][♭]
A. vernalis	female	8	878.1	1.30×10^{-2}	[149][♭]
A. vernalis	female	8	1006.7	3.73×10^{-2}	[149][♭]

Continued on Next Page. . .

Table B.1 – Continued

Species[†]	Sex	Temperature (^oC)	Time (h)	Wet mass (mg)	Reference
A. vernalis	female	8	1178.3	9.53×10^{-2}	[149][♭]
A. vernalis	female	10	413.4	2.37×10^{-3}	[149][♭]
A. vernalis	female	10	485.9	5.92×10^{-3}	[149][♭]
A. vernalis	female	10	571.8	8.28×10^{-3}	[149][♭]
A. vernalis	female	10	668.5	1.24×10^{-2}	[149][♭]
A. vernalis	female	10	777.8	3.55×10^{-2}	[149][♭]
A. vernalis	female	10	922.8	8.58×10^{-2}	[149][♭]
A. vernalis	female	12	321.3	2.37×10^{-3}	[149][♭]
A. vernalis	female	12	384.3	5.92×10^{-3}	[149][♭]
A. vernalis	female	12	463.3	7.69×10^{-3}	[149][♭]
A. vernalis	female	12	551.1	1.18×10^{-2}	[149][♭]
A. vernalis	female	12	645.4	3.20×10^{-2}	[149][♭]
A. vernalis	female	12	750.6	8.11×10^{-2}	[149][♭]
A. vernalis	female	15	231.3	2.37×10^{-3}	[149][♭]
A. vernalis	female	15	275.3	5.92×10^{-3}	[149][♭]
A. vernalis	female	15	321.2	7.69×10^{-3}	[149][♭]
A. vernalis	female	15	391.1	1.12×10^{-2}	[149][♭]
A. vernalis	female	15	468.2	2.96×10^{-2}	[149][♭]
A. vernalis	female	15	542.3	7.81×10^{-2}	[149][♭]
A. vernalis	female	20	108.8	2.37×10^{-3}	[149][♭]
A. vernalis	female	20	130.9	5.33×10^{-3}	[149][♭]
A. vernalis	female	20	154.3	7.10×10^{-3}	[149][♭]
A. vernalis	female	20	201.6	1.01×10^{-2}	[149][♭]

Continued on Next Page. . .

Table B.1 – Continued

Species[†]	Sex	Temperature (^oC)	Time (h)	Wet mass (mg)	Reference
A. vernalis	female	20	253.0	2.54×10^{-2}	[149][♭]
A. vernalis	female	20	284.6	7.57×10^{-2}	[149][♭]
A. vernalis	male	5	1040.7	2.96×10^{-3}	[149][♭]
A. vernalis	male	5	1187.8	7.10×10^{-3}	[149][♭]
A. vernalis	male	5	1363.9	8.88×10^{-3}	[149][♭]
A. vernalis	male	5	1520.3	1.12×10^{-2}	[149][♭]
A. vernalis	male	5	1648.8	1.72×10^{-2}	[149][♭]
A. vernalis	male	5	1801.3	2.96×10^{-2}	[149][♭]
A. vernalis	male	8	507.8	2.96×10^{-3}	[149][♭]
A. vernalis	male	8	631.6	6.51×10^{-3}	[149][♭]
A. vernalis	male	8	748.3	8.88×10^{-3}	[149][♭]
A. vernalis	male	8	878.1	1.07×10^{-2}	[149][♭]
A. vernalis	male	8	972.4	1.48×10^{-2}	[149][♭]
A. vernalis	male	8	1078.3	2.66×10^{-2}	[149][♭]
A. vernalis	male	10	413.4	2.37×10^{-3}	[149][♭]
A. vernalis	male	10	485.9	5.92×10^{-3}	[149][♭]
A. vernalis	male	10	571.8	8.28×10^{-3}	[149][♭]
A. vernalis	male	10	668.5	1.01×10^{-2}	[149][♭]
A. vernalis	male	10	741.4	1.42×10^{-2}	[149][♭]
A. vernalis	male	10	827.3	2.31×10^{-2}	[149][♭]
A. vernalis	male	12	321.3	2.37×10^{-3}	[149][♭]
A. vernalis	male	12	384.3	5.92×10^{-3}	[149][♭]
A. vernalis	male	12	463.3	7.69×10^{-3}	[149][♭]

Table B.1 – Continued

Species[†]	Sex	Temperature (^oC)	Time (h)	Wet mass (mg)	Reference
A. vernalis	male	12	551.1	1.01×10^{-2}	[149][♭]
A. vernalis	male	12	611.1	1.42×10^{-2}	[149][♭]
A. vernalis	male	12	676.9	2.19×10^{-2}	[149][♭]
A. vernalis	male	15	231.3	2.37×10^{-3}	[149][♭]
A. vernalis	male	15	275.3	5.92×10^{-3}	[149][♭]
A. vernalis	male	15	321.2	7.69×10^{-3}	[149][♭]
A. vernalis	male	15	391.1	8.88×10^{-3}	[149][♭]
A. vernalis	male	15	436.1	1.36×10^{-2}	[149][♭]
A. vernalis	male	15	483.8	1.95×10^{-2}	[149][♭]
A. vernalis	male	20	108.8	2.37×10^{-3}	[149][♭]
A. vernalis	male	20	130.9	5.33×10^{-3}	[149][♭]
A. vernalis	male	20	154.3	7.10×10^{-3}	[149][♭]
A. vernalis	male	20	201.6	8.28×10^{-3}	[149][♭]
A. vernalis	male	20	229.5	1.24×10^{-2}	[149][♭]
A. vernalis	male	20	247.9	1.78×10^{-2}	[149][♭]

† Latin name list: *Caenorhabditis elegans, Lucilia illustris, Acanthocyclops vernalis, Macrocyclops albidus,Acanthocyclops viridis.*

∗ To calculate the mass of *C. elegans*, we assume its density is the same as water density, $1000kg/m^3$. We do not analyze the data from 15^oC because its early stage data is not available.

♭ We assume dry mass is 30% of the wet mass. We eliminate *A. vernalis* because of the resolution of the figure in original paper is not fine to extract the precise data.

Table B.2: Parameters used in Figs.3.2 and 3.3. E_m here is smaller than the values published in our previous work [38] mainly on birds and mammals. Species studied here are invertebrates, such as insects, crustaceans and nematodes.

Species	Sex	E_m (g/J), for wet mass	C_1 (W/kg$^{0.75}$)	B_0 (W/kg$^{0.75}$)	B_0 at T_0 (^oC)	Group of B_0
C. elegans	NA	700	2.2×10^9	0.0236	20	Nematoda
L. illustris	NA	80	3.5×10^{10}	0.487	24	Beetles*
M. albidus	Male	350	7.99×10^{11}	0.361	29	Copepods
	Female	350	5.44×10^{11}	0.361	29	Copepods
A. viridis	Male	350	1.17×10^{11}	0.361	29	Copepods
	Female	350	1.17×10^{10}	0.361	29	Copepods

* Beetles are the closest organisms to *L. illustris* in the dataset [55]. However, it will potentially cause more deviation from the model prediction.

Table B.3: Data in Table 3.1.

Species[†]	Sex	Temperature (^oC)	Body mass or size[*]	Time (days)	Reference
D. willistoni	male	16	0.67♮	31	[150]
D. willistoni	male	19	0.63♮	16	[150]
D. willistoni	male	25	0.57♮	10	[150]
D. willistoni	male	29	0.41♮	10	[150]
D. willistoni	female	16	0.77♮	31	[150]
D. willistoni	female	19	0.8♮	16	[150]
D. willistoni	female	25	0.7♮	10	[150]
D. willistoni	female	29	0.6♮	10	[150]
D. equinoxialis	male	16	0.57♮	34	[150]
D. equinoxialis	male	19	0.58♮	19	[150]
D. equinoxialis	male	25	0.53♮	11	[150]
D. equinoxialis	male	29	0.46♮	10	[150]
D. equinoxialis	female	16	0.78♮	34	[150]
D. equinoxialis	female	19	0.8♮	19	[150]
D. equinoxialis	female	25	0.65♮	11	[150]
D. equinoxialis	female	29	0.61♮	10	[150]
D. pseudoobscura	male	13	1.28♮	45	[150]
D. pseudoobscura	male	16	1.27♮	32	[150]
D. pseudoobscura	male	19	1.08♮	22	[150]
D. pseudoobscura	male	24	0.84♮	18	[150]
D. pseudoobscura	female	13	1.52♮	45	[150]
D. pseudoobscura	female	16	1.54♮	32	[150]

Continued on Next Page. . .

Table B.3 – Continued

Species[†]	Sex	Temperature (^oC)	Body mass or size[*]	Time (days)	Reference
D. pseudoobscura	female	19	1.26$^\natural$	22	[150]
D. pseudoobscura	female	24	1.01$^\natural$	18	[150]
D. persimilis	male	13	1.24$^\natural$	42	[150]
D. persimilis	male	16	1.2$^\natural$	31	[150]
D. persimilis	male	19	1.13$^\natural$	18	[150]
D. persimilis	male	24	0.93$^\natural$	18	[150]
D. persimilis	female	13	1.56$^\natural$	42	[150]
D. persimilis	female	16	1.43$^\natural$	31	[150]
D. persimilis	female	19	1.42$^\natural$	18	[150]
D. persimilis	female	24	1.2$^\natural$	18	[150]
D. melanogaster	NA	12	0.95$^\natural$	NA	[151]
D. melanogaster	NA	14	1.02$^\natural$	NA	[151]
D. melanogaster	NA	17	1.04$^\natural$	NA	[151]
D. melanogaster	NA	21	0.98$^\natural$	NA	[151]
D. melanogaster	NA	25	0.89$^\natural$	NA	[151]
D. melanogaster	NA	28	0.82$^\natural$	NA	[151]
D. melanogaster	NA	31	0.73$^\natural$	NA	[151]
D. melanogaster	NA	12.9	NA	53.1	[152]
D. melanogaster	NA	13.7	NA	42.3	[152]
D. melanogaster	NA	14.6	NA	32.8	[152]
D. melanogaster	NA	16.5	NA	23.6	[152]
D. melanogaster	NA	18.3	NA	18.2	[152]
D. melanogaster	NA	21.1	NA	13.3	[152]

Continued on Next Page. . .

Table B.3 – Continued

Species[†]	Sex	Temperature (^oC)	Body mass or size*	Time (days)	Reference
D. melanogaster	NA	23.8	NA	10.2	[152]
D. melanogaster	NA	25.7	NA	8.62	[152]
D. melanogaster	NA	27.5	NA	7.34	[152]
D. melanogaster	NA	28.2	NA	7.36	[152]
D. melanogaster	NA	29.2	NA	7.78	[152]
D. melanogaster	NA	30.0	NA	8.72	[152]
D.simulans	NA	12.7	NA	49.2	[152]
D.simulans	NA	13.7	NA	39.5	[152]
D.simulans	NA	14.6	NA	30.7	[152]
D.simulans	NA	16.4	NA	22.4	[152]
D.simulans	NA	18.2	NA	17.3	[152]
D.simulans	NA	20.9	NA	12.3	[152]
D.simulans	NA	23.7	NA	9.50	[152]
D.simulans	NA	25.5	NA	7.96	[152]
D.simulans	NA	27.4	NA	7.08	[152]
D.simulans	NA	28.4	NA	7.36	[152]
D.simulans	NA	29.2	NA	8.70	[152]
R. sylvatica	NA	16.4	540♮	91	[150]
R. sylvatica	NA	20.6	330♮	51	[150]
L. illustris	NA	26	47.4♮	3.17	[148]
L. illustris	NA	20	46.1♮	4.77	[148]
L. illustris	NA	15	43.6♮	8.06	[148]
L. illustris	NA	11	44.6♮	19.4	[148]

Continued on Next Page. . .

Table B.3 – Continued

Species[†]	Sex	Temperature (^oC)	Body mass or size[*]	Time (days)	Reference
C. brunneus	female	25	82.1[♮]	17.2	[153][♭]
C. brunneus	female	30	121.8[♮]	10.9	[153][♭]
C. brunneus	female	35	138.5[♮]	6.8	[153][♭]
O. viridulus	female	25	95.4[♮]	NA	[153][♭]
O. viridulus	female	30	148.1[♮]	9.4	[153][♭]
O. viridulus	female	35	165.6[♮]	8.8	[153][♭]
M. maculatus	female	30	61.6[♮]	11	[153][♭]
M. maculatus	female	35	74.9[♮]	8.4	[153][♭]
S. lineatus	female	30	109.6[♮]	10	[153][♭]
S. lineatus	female	35	134.2[♮]	7	[153][♭]
A. viridis	female	5	53.53[♯]	125.5	[149]
A. viridis	female	8	49.58[♯]	82.3	[149]
A. viridis	female	10	45.99[♯]	64.4	[149]
A. viridis	female	12	42.05[♯]	53.8	[149]
A. viridis	female	15	40.95[♯]	40.6	[149]
A. viridis	female	20	40.53[♯]	28.3	[149]
A. viridis	male	5	27.89[♯]	110.9	[149]
A. viridis	male	8	23.40[♯]	70.0	[149]
A. viridis	male	10	21.96[♯]	53.1	[149]
A. viridis	male	12	21.22[♯]	43.6	[149]
A. viridis	male	15	20.47[♯]	31.6	[149]
A. viridis	male	20	20.05[♯]	21.5	[149]
M. albidu	female	5	44.38[♯]	121.9	[149]

Continued on Next Page. . .

Table B.3 – Continued

Species[†]	Sex	Temperature (^oC)	Body mass or size*	Time (days)	Reference
M. albidu	female	8	41.36[♯]	80.6	[149]
M. albidu	female	10	36.92[♯]	64.3	[149]
M. albidu	female	12	35.86[♯]	45.4	[149]
M. albidu	female	15	33.55[♯]	36.0	[149]
M. albidu	female	20	28.05[♯]	21.4	[149]
M. albidu	male	5	14.20[♯]	113.3	[149]
M. albidu	male	8	13.31[♯]	74.6	[149]
M. albidu	male	10	12.07[♯]	59.5	[149]
M. albidu	male	12	11.89[♯]	41.6	[149]
M. albidu	male	15	11.01[♯]	33.9	[149]
M. albidu	male	20	10.65[♯]	20.1	[149]
A. vernalis	female	5	30.53[♯]	80.8	[149]
A. vernalis	female	8	28.58[♯]	49.1	[149]
A. vernalis	female	10	25.74[♯]	38.4	[149]
A. vernalis	female	12	24.32[♯]	31.3	[149]
A. vernalis	female	15	23.43[♯]	22.6	[149]
A. vernalis	female	20	22.72[♯]	11.9	[149]
A. vernalis	male	5	8.88[♯]	75.1	[149]
A. vernalis	male	8	7.99[♯]	44.9	[149]
A. vernalis	male	10	6.92[♯]	34.5	[149]
A. vernalis	male	12	6.57[♯]	28.2	[149]
A. vernalis	male	15	5.86[♯]	20.2	[149]
A. vernalis	male	20	5.33[♯]	10.3	[149]

Continued on Next Page. . .

Table B.3 – Continued

Species[†]	Sex	Temperature (^{o}C)	Body mass or size*	Time (days)	Reference
H. azteca	NA	23.6	0.25[♯]	NA	[101]
H. azteca	NA	17.1	0.73[♯]	NA	[101]
H. azteca	NA	13.2	1.06[♯]	NA	[101]
H. azteca	NA	10.5	1.29[♯]	NA	[101]
H. azteca	NA	9.2	1.48[♯]	NA	[101]
H. azteca	NA	6.6	1.92[♯]	NA	[101]
A. aquaticus	NA	11.1	0.83[♯]	NA	[101]
A. aquaticus	NA	7.6	1.77[♯]	NA	[101]
A. aquaticus	NA	5.5	2.20[♯]	NA	[101]
A. aquaticus	NA	5.5	2.30[♯]	NA	[101]
A. aquaticus	NA	4.6	2.62[♯]	NA	[101]
A. aquaticus	NA	3.5	3.06[♯]	NA	[101]
A. aquaticus	NA	2.2	4.30[♯]	NA	[101]
I. baltica	NA	14.1	1.48[♯]	NA	[101]
I. baltica	NA	9.1	2.61[♯]	NA	[101]
I. baltica	NA	9.2	3.04[♯]	NA	[101]
P. sculpta	female	12.9	6.28[‡]	NA	[154]
P. sculpta	female	13.4	5.92[‡]	NA	[154]
P. sculpta	female	14.8	5.82[‡]	NA	[154]
P. sculpta	female	16.3	5.25[‡]	NA	[154]
P. sculpta	female	16.7	6.05[‡]	NA	[154]
P. sculpta	female	16.9	5.85[‡]	NA	[154]
P. sculpta	female	17.4	4.86[‡]	NA	[154]

Table B.3 – Continued

Species[†]	Sex	Temperature (^oC)	Body mass or size[*]	Time (days)	Reference
P. sculpta	female	18.4	4.62[‡]	NA	[154]
P. sculpta	female	20.2	5.61[‡]	NA	[154]
P. sculpta	female	20.8	5.66[‡]	NA	[154]
P. sculpta	female	21.6	4.88[‡]	NA	[154]
P. sculpta	female	23.6	4.68[‡]	NA	[154]
P. sculpta	female	23.9	4.86[‡]	NA	[154]
P. sculpta	female	24.2	5.06[‡]	NA	[154]
P. sculpta	female	25.6	4.59[‡]	NA	[154]
P. sculpta	female	26.0	4.66[‡]	NA	[154]
P. sculpta	female	26.3	4.81[‡]	NA	[154]
P. sculpta	female	27.2	4.94[‡]	NA	[154]
P. sculpta	female	27.3	4.59[‡]	NA	[154]
P. sculpta	female	29.0	4.64[‡]	NA	[154]
P. sculpta	female	29.4	4.67[‡]	NA	[154]
P. sculpta	female	30.3	4.68[‡]	NA	[154]
P. sculpta	female	30.4	4.55[‡]	NA	[154]
P. sculpta	male1	12.9	4.54[‡]	NA	[154]
P. sculpta	male1	13.4	5.38[‡]	NA	[154]
P. sculpta	male1	14.7	4.66[‡]	NA	[154]
P. sculpta	male1	16.7	4.96[‡]	NA	[154]
P. sculpta	male1	16.9	4.82[‡]	NA	[154]
P. sculpta	male1	17.4	4.33[‡]	NA	[154]
P. sculpta	male1	18.4	4.43[‡]	NA	[154]

Continued on Next Page. . .

Table B.3 – Continued

Species[†]	Sex	Temperature (^oC)	Body mass or size[*]	Time (days)	Reference
P. sculpta	male1	20.1	4.53[‡]	NA	[154]
P. sculpta	male1	20.9	4.50[‡]	NA	[154]
P. sculpta	male1	21.6	4.26[‡]	NA	[154]
P. sculpta	male1	21.5	4.66[‡]	NA	[154]
P. sculpta	male1	23.6	4.46[‡]	NA	[154]
P. sculpta	male1	24.3	4.53[‡]	NA	[154]
P. sculpta	male1	25.5	4.36[‡]	NA	[154]
P. sculpta	male1	26.0	4.37[‡]	NA	[154]
P. sculpta	male1	27.2	4.47[‡]	NA	[154]
P. sculpta	male1	27.3	3.96[‡]	NA	[154]
P. sculpta	male1	29.0	4.16[‡]	NA	[154]
P. sculpta	male1	29.4	4.16[‡]	NA	[154]
P. sculpta	male1	30.3	4.16[‡]	NA	[154]
P. sculpta	male1	30.3	4.06[‡]	NA	[154]
P. sculpta	male2	12.9	7.49[‡]	NA	[154]
P. sculpta	male2	13.3	7.49[‡]	NA	[154]
P. sculpta	male2	14.7	7.07[‡]	NA	[154]
P. sculpta	male2	16.3	6.95[‡]	NA	[154]
P. sculpta	male2	16.9	7.18[‡]	NA	[154]
P. sculpta	male2	16.7	7.33[‡]	NA	[154]
P. sculpta	male2	20.2	6.84[‡]	NA	[154]
P. sculpta	male2	17.4	6.19[‡]	NA	[154]
P. sculpta	male2	18.4	5.98[‡]	NA	[154]

Continued on Next Page. . .

Table B.3 – Continued

Species[†]	Sex	Temperature (^oC)	Body mass or size[*]	Time (days)	Reference
P. sculpta	male2	20.8	6.89[‡]	NA	[154]
P. sculpta	male2	21.5	6.28[‡]	NA	[154]
P. sculpta	male2	24.3	6.24[‡]	NA	[154]
P. sculpta	male2	23.8	6.08[‡]	NA	[154]
P. sculpta	male2	23.6	5.97[‡]	NA	[154]
P. sculpta	male2	25.6	5.92[‡]	NA	[154]
P. sculpta	male2	26.1	6.06[‡]	NA	[154]
P. sculpta	male2	26.3	6.04[‡]	NA	[154]
P. sculpta	male2	27.2	6.21[‡]	NA	[154]
P. sculpta	male2	27.3	6.02[‡]	NA	[154]
P. sculpta	male2	29.0	5.93[‡]	NA	[154]
P. sculpta	male2	29.3	6.03[‡]	NA	[154]
P. sculpta	male2	30.2	5.96[‡]	NA	[154]
P. sculpta	male2	30.4	5.86[‡]	NA	[154]
P. sculpta	male3	12.9	2.74[‡]	NA	[154]
P. sculpta	male3	13.3	2.72[‡]	NA	[154]
P. sculpta	male3	14.7	2.72[‡]	NA	[154]
P. sculpta	male3	16.7	2.94[‡]	NA	[154]
P. sculpta	male3	16.9	2.80[‡]	NA	[154]
P. sculpta	male3	16.3	2.52[‡]	NA	[154]
P. sculpta	male3	17.4	2.36[‡]	NA	[154]
P. sculpta	male3	18.4	2.31[‡]	NA	[154]
P. sculpta	male3	20.1	2.76[‡]	NA	[154]

Continued on Next Page. . .

Table B.3 – Continued

Species[†]	Sex	Temperature (^oC)	Body mass or size*	Time (days)	Reference
P. sculpta	male3	20.8	2.76[‡]	NA	[154]
P. sculpta	male3	21.6	2.47[‡]	NA	[154]
P. sculpta	male3	21.5	2.37[‡]	NA	[154]
P. sculpta	male3	23.8	2.76[‡]	NA	[154]
P. sculpta	male3	24.3	2.57[‡]	NA	[154]
P. sculpta	male3	23.7	2.32[‡]	NA	[154]
P. sculpta	male3	25.5	2.45[‡]	NA	[154]
P. sculpta	male3	26.3	2.30[‡]	NA	[154]
P. sculpta	male3	26.1	2.23[‡]	NA	[154]
P. sculpta	male3	27.2	2.48[‡]	NA	[154]
P. sculpta	male3	27.3	2.25[‡]	NA	[154]
P. sculpta	male3	29.0	2.29[‡]	NA	[154]
P. sculpta	male3	29.4	2.26[‡]	NA	[154]
P. sculpta	male3	30.2	2.31[‡]	NA	[154]
P. sculpta	male3	30.4	2.26[‡]	NA	[154]
C. plana	NA	20	1120.1[‡]	18.6	[155]
C. plana	NA	25	926.7[‡]	12.6	[155]
C. plana	NA	29	800.6[‡]	11	[155]
C. elegans	NA	10	0.122[§]	27.1	[79]
C. elegans	NA	15	0.115[§]	20	[79]
C. elegans	NA	20	0.101[§]	7.9	[79]
C. flavicans	NA	30	558[¶]	13.1	[156]
C. flavicans	NA	25	657[¶]	22.0	[156]

Continued on Next Page. . .

Table B.3 – Continued

Species[†]	Sex	Temperature (^oC)	Body mass or size[*]	Time (days)	Reference
C. flavicans	NA	20	905[¶]	26.7	[156]
C. flavicans	NA	15	1384[¶]	40.0	[156]

† Latin name list: *Drosophila willistoni, Drosophila equinoxialis, Drosophila pseudoobscura, Drosophila persimilis,Drosophila melanogaster, Drosophila simulans, Rana sylvatica, Paracerceis sculpta, Hyalella azteca, Asellus aquaticus, Idotea baltica, Crepidula plana, Chaoborus flavicans, Chorthippus brunneus, Omocestus viridulus, Myrmeleotettix maculatus, Stenobothrus lineatus.*

* Species have various entries for this parameter. Check table notes.

♮ Data are measured in wet mass (mg).

♭ The time here is not to adult. It is the time to first pod.

♯ Data are measured in dry mass (mg).

‡ Data are measured in length (mm).

§ Data are measured in area (mm^2).

¶ Data are measured in volume (mm^3).

References

[1] von Bertalanffy L (1938) A quantitative theory of organic growth. *Human Biology* 10:181–213.

[2] Kleiber M, Cole HH (1939) Body size and energy metabolism in growth hormone rats. *American Journal of Physiology – Legacy Content* 125:747–760.

[3] Brody S (1945) *Bioenergetics and Growth* (Reinhold, New York).

[4] Kleiber M (1947) Body size and metabolic rate. *Physiological Reviews* 27:511–541.

[5] von Bertalanffy L (1957) Quantitative laws in metabolism and growth. *The Quarterly Review of Biology* 32:pp. 217–231.

[6] Kleiber M (1961) *The Fire of Life an Introduction to Animal Energetics* (Wiley, New York).

[7] Ricklefs RE (2003) Is rate of ontogenetic growth constrained by resource supply or tissue growth potential? a comment on west *et al.*'s model. *Functional Ecology* 17:384–393.

[8] Zullinger EM, Ricklefs RE, Redford KH, Mace GM (1984) Fitting sigmoidal equations to mammalian growth curves. *Journal of Mammalogy* 65:pp. 607–636.

[9] West GB, Brown JH, Enquist BJ (2004) Growth models based on first principles or phenomenology? *Functional Ecology* 18:188–196.

[10] Kooijman SALM (1993) *Dynamic energy budgets in biological systems: theory and applications in ecotoxicology* (Cambridge Univ. Press, Cambridge).

References

[11] West GB, Brown JH, Enquist BJ (2001) A general model for ontogenetic growth. *Nature* 413:628–631.

[12] Brody S (1964) *Bioenergetics and Growth* (Hafner, Darien, CT).

[13] Withers PC (1992) *Comparative Animal Physiology* (Saunders College/Harcourt College, Fort Worth, TX).

[14] Kooijman SALM (2000) *Dynamic Energy and Mass Budgets in Biological Systems* (Cambridge Univ. Press, Cambridge).

[15] Makarieva AM, Gorshkov VG, Li. BL (2004) Iontogenetic growth: models and theory. *Ecological Modelling* 176:15–26.

[16] Gillooly JF, Brown JH, West GB, Savage VM, Charnov EL (2001) Effects of Size and Temperature on Metabolic Rate. *Science* 293:2248–2251.

[17] Atkinson D (1994) XXmissing booktitle & seriesXXAdvances in Ecological Research, eds Begon M, Fitter A (Academic Press) Vol. 25, pp 1 – 58.

[18] Arrhenius S (1889) Über die Reaktionsgeschwindigkeit bei der Inversion von Rohrzucker durch Säuren [On the rate of reaction of the inversion of sucrose by acids]. *Zeitschrift fuer physikalische Chemie* 4:226–248.

[19] Martin PS (1967) *Pleistocene Extinctions: The Search for a Cause* eds Martin PS, Wright, Jr. HE (Yale University Press, New Haven), pp 75–120.

[20] Alroy J (2001) A multispecies overkill simulation of the end-pleistocene megafauna mass extinction. *Science* 292:1893–1896.

[21] Barnosky AD, Koch PL, Feranec RS, Wing SL, Shabel AB (2004) Assessing the causes of late pleistocene extinctions on the continents. *Science* 306:70–75.

[22] Koch PL, Barnosky AD (2006) Late quaternary extinctions: State of the debate. *Annu Rev Ecol Evol Syst* 37:215–250.

[23] Lyons SK, Smith FA, Brown JH (2004) Of mice, mastodons and men: human-mediated extinctions on four continents. *Evolutionary Ecology Research* 6:339–358.

References

[24] Faith JT, Surovell TA (2009) Synchronous extinction of north america's pleistocene mammals. *Proceedings of the National Academy of Sciences* 106:20641–20645.

[25] Carrasco MA, Barnosky AD, Graham RW (2009) Quantifying the extent of north american mammal extinction relative to the pre-anthropogenic baseline. *PLoS ONE* 4:e8331.

[26] Grayson DK, Meltzer DJ (2003) A requiem for north american overkill. *Journal of Archaeological Science* 30:585–593.

[27] Grayson DK, Meltzer DJ (2004) North american overkill continued? *Journal of Archaeological Science* 31:133–136.

[28] Waguespack NM, Surovell TA (2003) Clovis hunting strategies, or how to make out on plentiful resources. *American Antiquity* 68:333–352.

[29] Surovell TA, Waguespack NM (2008) How many elephant kills are 14? clovis mammoth and mastodon kills in context. *Quaternary International* 191:82–97.

[30] Byers DA, Ugan A (2005) Should we expect large game specialization in the late pleistocene? an optimal foraging perspective on early paleoindian prey choice. *Journal of archaeological science* 32:1624–1640.

[31] Polishchuk LV (2010) The three-quarter-power scaling of extinction risk in late pleistocene mammals, and a new theory of the size selectivity of extinction. *Evolutionary Ecology Research* 12:1–22.

[32] Jobling M (1983) Effect of feeding frequency on food-intake and growth of arctic charr, salvelinus-alpinus l. *Journal of Fish Biology* 23:177–185.

[33] McCue MD (2006) Specific dynamic action: a century of investigation. *Comparative Biochemistry and Physiology* 144A:381–394.

[34] Ashworth A (1969) Metabolic rates during recovery from protein-calorie malnutrition: the need for a new concept of specific dynamic action. *Nature* 223:407–409.

[35] Krieger I (1978) Relation of specific dynamic action of food (SDA) to growth in rats. *The American Journal of Clinical Nutrition* 31:764–768.

[36] Blaxter KL (1989) *Energy Metabolism in Animals and Man* (Cambridge Univ. Press, Cambridge).

References

[37] Nagy KA, Girard IA, Brown TK (1999) Energetics of free-ranging mammals, reptiles, and birds. *Annual Review of Nutrition* 19:247–277.

[38] Moses ME, Hou C, Woodruff WH, West GB, Nekola JC, Zuo W, Brown JH (2008) Revisiting a model of ontogenetic growth: estimating model parameters from theory and data. *American Naturalist* 171:632–645.

[39] Cummins KW, Wuycheck JC (1971) Caloric equivalents for investigations in ecological energetics. *Mitt. Int. Ver. Theor. Angew. Limnol.* 18:1–151.

[40] Robbins CT (1983) *Wildlife Feeding and Nutrition* (Academic Press, New York).

[41] Evans E, Miller DS (1968) Comparative nutrition, growth and longevity. *Proceedings of the Nutrition Society* 27:121–129.

[42] Kirkwood JK (1991) Energy Requirements for Maintenance and Growth of Wild Mammals, Birds and Reptiles in Captivity. *The Journal of Nutrition* 121:S29–S34.

[43] Hou C, Zuo W, Moses ME, Woodruff WH, Brown JH, West GB (2008) Energy Uptake and Allocation During Ontogeny. *Science* 322:736–739.

[44] Makarieva AM, Gorshkov VG, Li BL (2009) Comment on "nergy Uptake and Allocation During Ontogeny". *Science* 325:1206.

[45] Sousa T, Marques GM, Domingos T (2009) Comment on "nergy Uptake and Allocation During Ontogeny". *Science* 325:1206.

[46] Poczopko P (1979) Metabolic rate and body size relationships in adult and growing homeotherms. *Acta theriol. (Warsz.)* 24:125–136.

[47] Wieser W (1984) A distribution must be made between the ontogeny the phylogeny of metabolism in order to understand the mass exponent of energy metabolism. *Respiration Physiology* 55:1–9.

[48] Sousa T, Domingos T, Kooijman S (2008) From empirical patterns to theory: a formal metabolic theory of life. *Philosophical Transactions of the Royal Society B: Biological Sciences* 363:2453–2464.

[49] van der Meer J (2006) Metabolic theories in ecology. *Trends in Ecology & Evolution* 21:136 – 140.

References

[50] Ricklefs RE (1974) *Avian Energetics* ed Paynter Jr. RA (Nuttall Ornithological Club Publication Number 15, Cambridge, MA).

[51] Morowitz HJ (1978) *Foundations of Bioenergetics* (Academic Press, New York).

[52] Calow P (1977) Conversion efficiencies in heterotrophic organisms. *Biological Reviews* 52:385–409.

[53] Morowitz HJ (1968) *Energy flow in Biology* (Academic Press, New York and London).

[54] Lehninger AL, Nelson DL, Cox MM (1993) *Principles of Biochemistry* (Worth Publishers, New York), 2 edition.

[55] Peters RH (1983) *The ecological implications of body size* (Cambridge Univ. Press, Cambridge).

[56] Kleiber M, Dougherty JE (1934) The influence of environmental temperature on the utilization of food energy in baby chicks. *The Journal of General Physiology* 17:701–726.

[57] Klaassen M (1994) Growth and energetics of tern chicks from temperate and polar environments. *The Auk* 111:pp. 525–544.

[58] Ørskov ER (1970) *Energy Metabolism of Farm Animals* (Juris Verlag, Zurich) No. 13, p 65.

[59] Kielanowski J (1972) *Pig Production* ed Cole DJA (Butterworths, London), pp 183–201.

[60] Hoyt DF (1987) A new model of avian embryonic metabolism. *Journal of Experimental Zoology. Supplement* 1:127–138.

[61] Aschoff J, Pohl H (1970) Rhythmic variations in energy metabolism. *Federation Proceedings* 29:1541–1552.

[62] Hulbert AJ, Else PL (2000) Mechanisms underlying the cost of living in animals. *Annual Review of Physiology* 62:207–235.

[63] Nagy KA (1987) Field metabolic rate and food requirement scaling in mammals and birds. *Ecological Monographs* 57:111–128.

[64] Kendeigh SC (1970) Energy requirements for existence in relation to size of bird. *The Condor* 72:pp. 60–65.

References

[65] Calder WA (1984) *Size, Function and Life History* (Harvard University Press, Cambridge, MA).

[66] Schmidt-Nielsen K (1984) *Scaling: Why is Animal Size so Important?* (Cambridge University Press, Cambridge).

[67] Brown JH, Gillooly JF, Allen AP, Savage VM, West GB (2004) Toward a metabolic theory of ecology. *Ecology* 85:1771–1789.

[68] Savage VM, et al. (2004) The predominance of quarter-power scaling in biology. *Functional Ecology* 18:257–282.

[69] Glazier DS (2005) Beyond the 3/4-power law: variation in the intra- and interspecific scaling of metabolic rate in animals. *Biological Reviews* 80:611–662.

[70] Froese R, Pauly D, eds (2006) Fishbase. (http://www.fishbase.org/).

[71] Webster AJF, Smith JS, Crabtree RM, Mollison GS (1976) Prediction of the energy requirements for growth in beef cattle. 2. hereford british friesian steers given dried grass or barley. *Animal Science* 23:329–340.

[72] Agricultural Research Council (1980) *The Nutrient Requirements of Ruminant Livestock* (Commonwealth Agricultural Bureaus, Gresham Press, Surrey), 2 edition.

[73] Garrett WN, Johnson DE (1983) Nutritional energetics of ruminants. *J. Anim Sci.* 57:478–497.

[74] Subcommittee on Beef Cattle Nutrition, Committee on Animal Nutrition, National Research Council (2000) *Nutrient Requirements of Beef Cattle* (The National Academy Press, Washington, DC), 7 edition.

[75] Blaxter KL, Fowler VR, Gill JC (1982) A study of the growth of sheep to maturity. *The Journal of Agricultural Science* 98:405–420.

[76] Lofgreen GP, Garrett WN (1968) A system for expressing net energy requirements and feed values for growing and finishing beef cattle. *J. Anim Sci.* 27:793–806.

[77] Knies JL, Kingsolver JG (2010) Erroneous arrhenius: Modified arrhenius model best explains the temperature dependence of ectotherm fitness. *The American Naturalist* 176:pp. 227–233.

References

[78] Irlich UM, Terblanche JS, Blackburn TM, Chown SL (2009) Insect rate - temperature relationships: Environmental variation and the metabolic theory of ecology. *The American Naturalist* 174:pp. 819–835.

[79] Voorhies WAV (1996) Bergmann size clines: A simple explanation for their occurrence in ectotherms. *Evolution* 50:pp. 1259–1264.

[80] Nijhout H, Davidowitz G, Roff D (2006) A quantitative analysis of the mechanism that controls body size in *Manduca sexta*. *Journal of Biology* 5:16.

[81] de Jong G, van der Have TM (2009) in *Phenotypic Plasticity of Insects: Mechanisms and Consequences*, eds Whitman DW, Ananthakrishnan TN (Science Publishers, Inc., Plymouth, UK), pp 461–526.

[82] de Jong G (2010) A biophysical interpretation of temperature-dependent body size in *Drosophila aldrichi* and *D. buzzatii*. *Journal of Thermal Biology* 35:85 – 99.

[83] Partridge L, Barrie B, Fowler K, French V (1994) Evolution and development of body size and cell size in drosophila melanogaster in response to temperature. *Evolution* 48:pp. 1269–1276.

[84] French V, Feast M, Partridge L (1998) Body size and cell size in drosophila: the developmental response to temperature. *Journal of Insect Physiology* 44:1081 – 1089.

[85] van der Have TM, de Jong G (1996) Adult size in ectotherms: Temperature effects on growth and differentiation. *Journal of Theoretical Biology* 183:329 – 340.

[86] Davidowitz G, Nijhout HF (2004) The Physiological Basis of Reaction Norms: The Interaction Among Growth Rate, the Duration of Growth and Body Size. *Integrative and Comparative Biology* 44:443–449.

[87] Davidowitz G, D'Amico, L. J.and Nijhout HF (2004) The effects of environmental variation on a mechanism that controls insect body size. *Evolutionary Ecology Research* 6:49–62.

[88] Azevedo RBR, French V, Partridge L (1996) Thermal evolution of egg size in drosophila melanogaster. *Evolution* 50:pp. 2338–2345.

[89] Atkinson D, Morley SA, Weetman D, Hughes RN (2001) in *Environment and Animal Development: Genes, Life Histories and Plasticity*, eds Atkinson D, Thorndyke M (BIOS Scientific, Oxford), pp 269–286.

References

[90] Booth DT, Kiddell K (2007) Temperature and the energetics of development in the house cricket (*Acheta domesticus*). *Journal of Insect Physiology* 53:950 – 953.

[91] Carey C, Rahn H, Parisi P (1980) Calories, water, lipid and yolk in avian eggs. *The Condor* 82:pp. 335–343.

[92] Ar A, Rahn H (1980) Water in the avian egg: Overall budget of incubation. *American Zoologist* 20:pp. 373–384.

[93] Perrin N (1988) Why are offspring born larger when it is colder? phenotypic plasticity for offspring size in the cladoceran *Simocephalus vetulus* (müller). *Functional Ecology* 2:pp. 283–288.

[94] Sibly RM, Atkinson D (1994) How rearing temperature affects optimal adult size in ectotherms. *Functional Ecology* 8:pp. 486–493.

[95] Nunney L (1996) The response to selection for fast larval development in *Drosophila melanogaster* and its effect on adult weight: An example of a fitness trade-off. *Evolution* 50:pp. 1193–1204.

[96] Partridge L, French V (1996) in *Animals and temperature: Phenotypic and evolutionary adaptation*, eds Johnston IA, Bennett AF (Cambridge University Press, Cambridge, UK), pp 265–292.

[97] Yampolsky LY, Scheiner SM (1996) Why larger offspring at lower temperatures? a demographic approach. *The American Naturalist* 147:pp. 86–100.

[98] Atkinson D, Sibly RM (1997) Why are organisms usually bigger in colder environments? making sense of a life history puzzle. *Trends in Ecology & Evolution* 12:235 – 239.

[99] Nunney L, Cheung W (1997) The effect of temperature on body size and fecundity in female drosophila melanogaster: Evidence for adaptive plasticity. *Evolution* 51:pp. 1529–1535.

[100] Angilletta, Jr. MJ, Dunham AE (2003) The temperature-size rule in ectotherms: Simple evolutionary explanations may not be general. *The American Naturalist* 162:pp. 332–342.

[101] Angilletta MJ, Steury TD, Sears MW (2004) Temperature, Growth Rate, and Body Size in Ectotherms: Fitting Pieces of a Life-History Puzzle. *Integrative and Comparative Biology* 44:498–509.

References

[102] Gilchrist GW, Huey RB (2004) Plastic and Genetic Variation in Wing Loading as a Function of Temperature Within and Among Parallel Clines in *Drosophila subobscura*. *Integrative and Comparative Biology* 44:461–470.

[103] Walters RJ, Hassall M (2006) The temperature-size rule in ectotherms: May a general explanation exist after all? *The American Naturalist* 167:pp. 510–523.

[104] Frazier MR, Huey RB, Berrigan D (2006) Thermodynamics constrains the evolution of insect population growth rates: warmer is better.. *The American Naturalist* 168:pp. 512–520.

[105] Atkinson D (1995) Effects of temperature on the size of aquatic ectotherms: Exceptions to the general rule. *Journal of Thermal Biology* 20:61 – 74 Effects of Rising Temperature on the Ecology and Physiology of Aquatic Organisms.

[106] Gillooly JF, Dodson SI (2000) Latitudinal patterns in the size distribution and seasonal dynamics of new world, freshwater cladocerans. *Limnology and Oceanography* 45:pp. 22–30.

[107] Bull JJ (1980) Sex determination in reptiles. *The Quarterly Review of Biology* 55:pp. 3–21.

[108] Göth A, Booth DT (2005) Temperature-dependent sex ratio in a bird. *Biology Letters* 1:31–33.

[109] Crews D, Bull JJ (2008) Sex determination: Some like it hot (and some don't). *Nature* 451:527–528.

[110] Ospina-Álvarez N, Piferrer F (2008) Temperature-dependent sex determination in fish revisited: Prevalence, a single sex ratio response pattern, and possible effects of climate change. *PLoS ONE* 3:e2837.

[111] Working Group I (2007) *IPCC Fourth Assessment Report, Climate Change 2007 (AR4)* (Cambridge Univ. Press, UK).

[112] Fiedel S (2009) *American Megafaunal Extinctions at the End of the Pleistocene* ed Haynes G (Springer, New York), pp 21–37.

[113] Alroy J (1999) The fossil record of north american mammals: evidence for a paleocene evolutionary radiation. *Systematic Biology* 48:107–118.

References

[114] Cannon MD, Meltzer DJ (2004) Early paleoindian foraging: examining the faunal evidence for large mammal specialization and regional variability in prey choice. *Quaternary Science Reviews* 23:1955–1987.

[115] Cannon MD, Meltzer DJ (2008) Explaining variability in early paleoindian foraging. *Quaternary International* 191:5–17.

[116] Myers RA, Bowen KG, Barrowman NJ (1999) Maximum reproductive rate of fish at low population sizes. *Can J Fish Aquat Sci* 56:2404–2419.

[117] Fowler CW (1981) Density dependence as related to life history strategy. *Ecology* 62:602–610.

[118] Fowler CW (1987) *Current Mammalogy* ed Genoways H (Plenum Press, New York), pp 401–441.

[119] Fowler CW (1988) Population dynamics as related to rate of increase per generation. *Evolutionary Ecology* 2:197–204.

[120] Charnov EL (1993) *Life History Invariants* (Oxford University Press, New York).

[121] Purvis A, Harvey PH (1995) Mammal life-history evolution: a comparative test of charnov's model. *J Zool, Lond* 237:259–283.

[122] Charnov EL (2001) Evolution of mammal life histories. *Evolutionary Ecology Research* 3:521–535.

[123] Brook BW, Bowman DMJS (2005) One equation fits overkill: why allometry underpins both prehistoric and modern body size-biased extinctions. *Population Ecology* 47:137–141.

[124] Smith FA, et al. (2003) Body mass of late quaternary mammals. *Ecology* 84:3403.

[125] R Development Core Team (2009) R: A language and environment for statistical computing. (http://www.R-project.org/).

[126] Ricker WE (1958) Maximum sustained yields from fluctuating environments and mixed stocks. *Jour Fish Res Bd Can* 15:991–1006.

[127] Paulik GJ, Hourston AS, Larkin PA (1967) Exploitation of multiple stocks by a common fishery. *Jour Fish Res Bd Can* 24:2527–2540.

[128] Myers RA, Mertz G (1998) The limits of exploitation: a precautionary approach. *Ecol App* 8:S165–S169.

References

[129] Myers RA, Worm R (2005) Extinction, survival or recovery of large predatory fishes. *Phil Trans R Soc B* 360:13–20.

[130] Quinn TJ, Deriso RB (1999) *Quantitative Fish Dynamics* (Oxford University Press, New York).

[131] Hilborn R, Walters CJ (1992) *Quantitative Fisheries Stock Assessment: Choice, dynamics and Uncertanity* (Chapman and Hall, New York).

[132] Martin PS, Klein RG (1989) *Quaternary Extinctions: A Prehistoric Revolution* (University of Arizona Press, Tucson, AZ).

[133] Hamilton MJ, Davidson AD, Sibly RM, Brown JH (2011) Universal scaling of production rates across mammalian lineages. *Proc R Soc B* 278:560–566.

[134] Lupatsch I, Kissil GW, Sklan D (2003) Comparison of energy and protein efficiency among three fish species gilthead sea bream (*Sparus aurata*), european sea bass (*Dicentrarchus labrax*) and white grouper (*Epinephelus aeneus*): energy expenditure for protein and lipid deposition. *Aquaculture* 225:175 – 189.

[135] Altman PL, Dittmer DS, eds (1968) *Metabolism. Biological Handbooks* (Federation of American Societies for Experimental Biology, Bethesda, MD).

[136] Committee on Animal Nutrition, National Research Council (1985) *Nutrient Requirements of Sheep* (The National Academy Press, Washington, DC), 6 edition.

[137] Subcommittee on Feed Intake, Committee on Animal Nutrition, National Research Council (1987) *Predicting Feed Intake of Food-Producing Animals* ed National Research Council (The National Academy Press, Washington, DC).

[138] Committee on Animal Nutrition, National Research Council (1989) *Nutrient Requirements of Horses* (The National Academy Press, Washington, DC), 5 edition.

[139] Committee on Animal Nutrition, National Research Council (1994) *Nutrient Requirements of Poultry* (The National Academy Press, Washington, DC), 9 edition.

References

[140] Karasov WH, Kenow KP, Meyer MW, Fournier F (2007) Bioenergetic and pharmacokinetic model for exposure of common loon (*Gavia Immer*) chicks to methylmercury. *Environmental Toxicology and Chemistry* 26:677–685.

[141] Committee on Animal Nutrition, Ad Hoc Committee on Nonhuman Primate Nutrition, National Research Council (2003) *Nutrient Requirements of Nonhuman Primates* (The National Academy Press, Washington, DC), 2 edition.

[142] Committee on Animal Nutrition, National Research Council (1982) *Nutrient Requirements of Mink and Foxes* (The National Academy Press, Washington, DC), 2 edition.

[143] Fuglei E, Øitsland NA (1999) Seasonal trends in body mass, food intake and resting metabolic rate, and induction of metabolic depression in arctic foxes (alopex lagopus) at svalbard. *Journal of Comparative Physiology B: Biochemical, Systemic, and Environmental Physiology* 169:361–369 10.1007/s003600050232.

[144] Pearson OP (1947) The rate of metabolism of some small mammals. *Ecology* 28:pp. 127–145.

[145] Pearson OP (1948) Metabolism of Small Mammals, With Remarks on the Lower Limit of Mammalian Size. *Science* 108:44.

[146] Spector WS, ed (1956) *Handbook of Biological Data* (W. B. Saunders Company, Philadelphia and London).

[147] Hammond KA, Diamond J (1997) Maximal sustained energy budgets in humans and animals. *Nature* 386:457–462 10.1038/386457a0.

[148] Hanski I (1976) Assimilation by *Lucilia illustris* (diptera) larvae in constant and changing temperatures. *Oikos* 27:pp. 288–299.

[149] Abdullahi BA, Laybourn-Parry J (1985) The effect of temperature on size and development in three species of benthic copepod. *Oecologia* 67:295–297 10.1007/BF00384303.

[150] Ray C (1960) The application of bergmann's and allen's rules to the poikilotherms. *Journal of Morphology* 106:85–108.

[151] Karan D, Morin JP, Moreteau B, David JR (1998) Body size and developmental temperature in *Drosophila melanogaster*: analysis of body weight reaction norm. *Journal of Thermal Biology* 23:301 – 309.

References

[152] Petavy G, David JR, Gibert P, Moreteau B (2001) Viability and rate of development at different temperatures in *Drosophila*: a comparison of constant and alternating thermal regimes. *Journal of Thermal Biology* 26:29–39.

[153] Willott SJ, Hassall M (1998) Life-history responses of british grasshoppers (orthoptera: Acrididae) to temperature change. *Functional Ecology* 12:pp. 232–241.

[154] Shuster SM, Guthrie EE (1999) Effects of temperature and food availability on adult body length in natural and laboratory populations of *Paracerceis sculpta* (holmes), a gulf of california isopod. *Journal of Experimental Marine Biology and Ecology* 233:269 – 284.

[155] Zimmerman KM, Pechenik JA (1991) How do temperature and salinity affect relative rates of growth, morphological differentiation, and time to metamorphic competence in larvae of the marine gastropod *Crepidula plana*? *Biol Bull* 180:372–386.

[156] Hanazato T, Yasuno M (1989) Effect of temperature in laboratory studies on growth of *Chaoborus flavicans* (diptera: Chaoboridae). *Archiv. Hydrobiol.* 114:497–504.